WHEN INTERNEURONS GET EXCITED -

HOW CHANGES IN CHLORIDE CONCENTRATIONS OF PARVALBUMINERGIC INTERNEURONS CAN INFLUENCE BRAIN WORK AND EXCITABILITY

Dissertation

zur Erlangung des akademischen Grades

doctor rerum naturalium (Dr. rer. nat)

vorgelegt dem Rat der Medizinischen Fakultät

der Friedrich-Schiller-Universität Jena

von Diplom-Biologin Melanie Gerth

geboren am 04.12.1988 in Altenburg

Gutachter:

1. Prof. Dr. med. Christian Hübner, Universitätsklinikum Jena, Institut für Humangenetik

2. Prof. Dr. rer. nat. Aria Baniahmad, Universitätsklinikum Jena , Institut für Humangenetik

3. Prof. Dr. Claudio Rivera Baeza, Institut de Neurobiologie de la Méditerranée, Marseille, Frankreich

Tag der öffentlichen Verteidigung: 16.10.2018.....

CONTENT

LIST OF ABBREVIATIONS

5HT3aR	5-hydroxytryptamine (serotonin) receptor
ACTH	adrenocorticotropic hormone
AIS	axon initial segment
ALS	amyotrophic lateral sclerosis
BLA	basolateral amygdaloid nucleus
CBP	calcium-binding protein
CCC	cation-chloride cotransporter
CeA	central nucleus of amygdala
CNS	central nervous system
CORT	corticosterone
CRH	corticotropin-releasing hormone
Ctx	cortex
EPSP	excitatory postsynaptic potential
fEPSP	field EPSP
GABA	gamma-aminobutyric acid
GABAR	gamma-aminobutyric acid receptor
HFS	high frequency stimulus
HPA axis	hypothalamic pituitary adrenal axis
I	current
IHC	immunohistochemistry
IPSC	inhibitory postsynaptic current
IPSP	inhibitory postsynaptic potential
KCC2	potassium-chloride cotransporter 2
KCC3	potassium-chloride cotransporter 3
KO	knock out
LTP	long term potentiation
NKCC1	sodium-potassium-chloride cotransporter 1
OLM cells	oriens-lacunosum moleculare neurons

PBGN	parabigeminal nucleus
PPR	paired pulse ratio
PTZ	pentylenetetrazole
PV	parvalbumin
PVN	paraventricular nucleus
R	resistance
SC	superior colliculus
SLC12	soluble carrier 12
V	voltage
Vm	resting membrane potential
WT	wild-type

ABSTRACT

Ion homeostasis is essential for proper neuronal function, since changes in intra- or extracellular ion concentrations can cause neuropathological conditions including seizures and neuropathic pain. The Cl^- gradient determines the strength and polarity of GABAergic neurotransmission. It is established by the activity of cation-chloride cotransporters (CCCs), the K^+-Cl^- co-transporter 2 (KCC2) and the Na^+-K^+-$2Cl^-$ co-transporter 1 (NKCC1).

To investigate how changes in Cl^- concentration in inhibitory neurons affect GABAergic neurotransmission and overall excitability, KCC2 expression was inhibited in parvalbuminergic (PV^+) interneurons of C57BL/6 mice.

KO mice showed an ataxic gait, spontaneous epileptic seizures and a shortened life span. Immunohistochemistry revealed a loss of PV^+ neurons in the hippocampus and the layer V/VI of the somatosensory cortex without detectable morphological changes. Field potential recordings showed altered short and long-term plasticity and a switch from increased inhibition at 8 weeks to enhanced excitation at 21 weeks. *In vivo* studies suggested increased anxiety and a significant delay of PTZ induced seizures in KO mice.

This study suggests a role of KCC2 for proper Cl^- homeostasis in PV^+ interneurons and impressively showed how impairment in GABAergic inhibition contributes to balanced brain activity. Furthermore, our results demonstrate a role of PV+ interneurons for the stress axis, neuronal excitability and higher brain functions like learning and memory.

ZUSAMMENFASSUNG

Die Ionenhomöostase spielt bei der Regulation physiologischer neuronaler Prozesse eine herausragende Rolle. Sowohl intra- als auch extrazelluläre Ionenkonzentrationsänderungen können zu neurologischen Störungen führen. In Neuronen ist die Chloridionen (Cl^-)-Konzentration von besonderem Interesse, da diese die Stärke und Polarität der GABAergen Transmission bestimmt. Die Konzentration wird dabei hauptsächlich durch die Aktivität von Kationen-Chlorid-Kotransportern (CCCs) eingestellt. Dabei kommt sowohl dem Kalium-Chlorid-Kotransporter 2 (KCC2) als auch dem Natrium-Kalium-Chlorid-Kotransporter 1 (NKCC1) eine besondere Bedeutung zu.

In parvalbuminergen (PV^+) Interneuronen von C57BL/6-Mäusen erfolgte die gezielte Hemmung der KCC2-Expression, um den Einfluss einer veränderten Cl^--Konzentration in inhibitorischen Neuronen auf die GABAerge Neurotransmission und die Erregbarkeit des neuronalen Gewebes zu untersuchen.

Interessanterweise zeigten diese konditionalen KO-Mäuse einen sehr auffälligen Phänotyp, gekennzeichnet durch Gangstörung, spontane epileptische Anfälle sowie eine verkürzte Lebensspanne. In immunhistochemischen Untersuchungen stellte sich ein Verlust parvalbuminerger Interneurone sowohl im Hippokampus als auch in der Schicht V/VI des somatosensorischen Kortex heraus. Weitere morphologische Veränderungen waren nicht zu beobachten. Extrazelluläre Ableitungen an akuten Hirnschnitten offenbarten eine veränderte Kurz- und Langzeitplastizität und eine Verschiebung von erhöhter Inhibition im Alter von 8 Wochen zu verstärkter neuronaler Erregbarkeit mit 21 Wochen im konditionalen KO. Die durchgeführten *in vivo*-Versuche

deuten auf eine Angststörung hin und demonstrieren eine signifikante Verzögerung PTZ-induzierter Krampfanfälle.

Diese Arbeit weist auf eine herausragende Rolle von KCC2 bei der Regulation der intrazellulären Chloridkonzentration parvalbuminerger Neurone hin. Sie zeigt, wie eine gestörte Chloridhomöostase parvalbuminerger Interneurone die GABAerge Inhibition verändert und somit die neuronale Erregbarkeit beeinflusst. Darüber hinaus unterstreichen die gewonnenen Resultate die besondere Wichtigkeit dieser Interneurone für die hormonelle Feinregulation der Stressachse.

INTRODUCTION

EPILEPSY

According to a report of the U.S. Institute of Medicine (England et al., 2012) epilepsy is the fourth most common neurological disorder that affects 1 in 26 people at some point in their lifetime.

Clinically it comprises a broad spectrum of disorders with various seizure types and causes, a range of severities and an array of coexisting conditions that affects people of all ages, with onset most often occurring in childhood or older adulthood (Hauser, 1995). More than 25 epilepsy syndromes can be distinguished (Berg et al., 2010) with epilepsy defined as the occurrence of two or more unprovoked seizures separated by at least 24 hours (ILAE, 1993).

During the last decade classification and characterisation of the subtypes improved, making a successful treatment more likely. The epilepsies can be broadly grouped into three classes: generalised epilepsy; focal epilepsy; and epileptic encephalopathy. Within each class, several specific syndromes are defined by differences in specific seizure types, electroencephalogram (EEG) patterns, age of onset and disease progression.

The genetic contribution to epilepsies is known since the antiques and well established through family and twin studies. 20-30 % of epilepsies are caused by acquired conditions such as stroke, tumour or head injury. The other 70–80 % are thought to be due to genetic risk factors (Hildebrand et al., 2013). Since whole genome sequencing

became affordable and exome sequencing is well established as a standard technology, many genes associated with specific types of epilepsies were discovered (Helbig and Lowenstein, 2013, McTague et al., 2016, Oliver et al., 2014). The spectrum includes genes of chromatin remodelling, ion channels and neurotransmitter receptors, intracellular signalling, metabolism and synaptic vesicle cycle (Myers and Mefford, 2015).

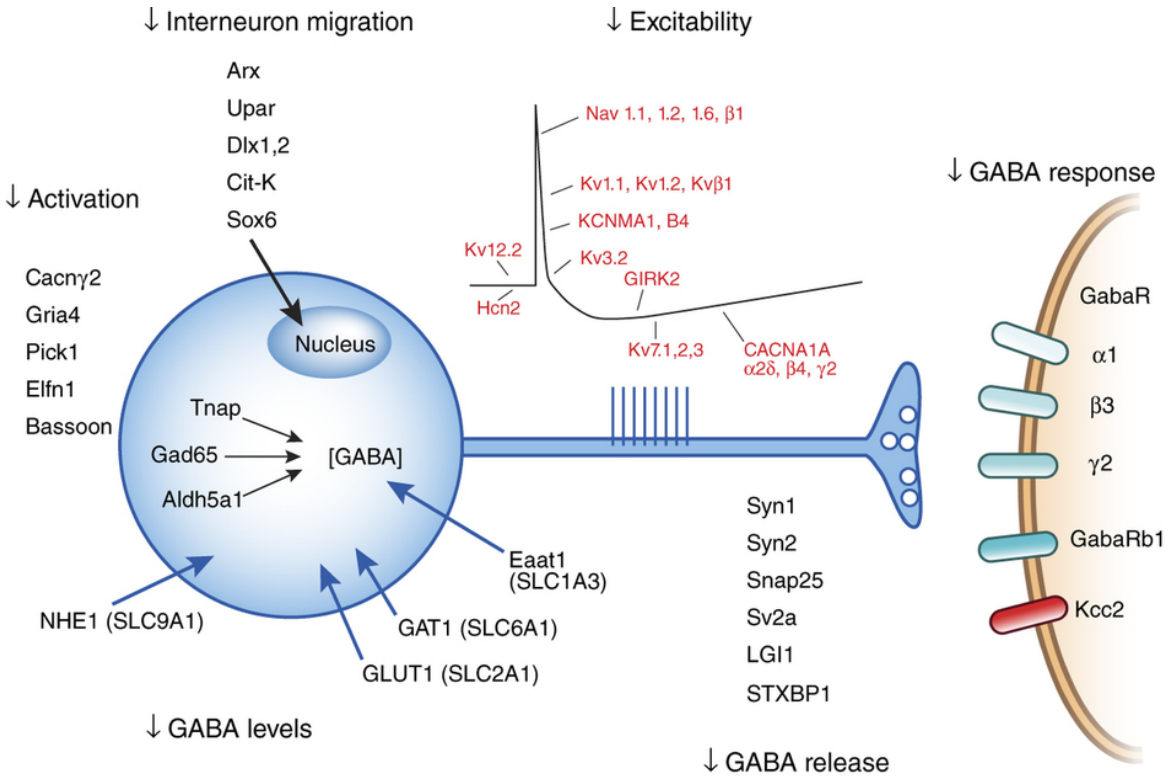

FIGURE 1: LIST OF SELECTED GENES INVOLVED IN THE CONTROL OF EXCITATION/INHIBITION BALANCE. Mutations in the displayed genes impair synaptic inhibitory transmission from early development through maturation of adult GABA neurotransmission. Many others genes remain to be functionally assigned to their target location and impact on excitation and inhibition balance in epileptic microcircuits (adapted from Noebels 2015). The list of genes is displayed in the appendix.

This diversity shows the large number of molecular pathways involved. Many of these genes identified by whole genome or exome sequencing have been further

investigated in mouse models and a major fraction of those regulate the birth, development, or function of inhibitory interneurons (figure 1; (Noebels, 2015)). During the last years publications speculate on the importance of GABAergic inhibition to trigger or maintain epileptic seizures (Avoli et al., 2016, Campbell et al., 2015, de Curtis and Avoli, 2016, Ellender et al., 2014, Kahle et al., 2016, Kaila et al., 2014b).

INTERNEURONS AND INHIBITION

Although glutamatergic excitatory synapses account for the vast majority of synapses in the brain, inhibitory synapses play an essential role in the nervous system. They are not only controlling excitation but also coordinating activity among networks of neurons. The coordination of activity is important for neuronal processing of information. Recent studies in animals and humans indicate that subtle perturbations in inhibition lead to epilepsy and psychiatric disorders like schizophrenia, autism or contributes to the phenotype of Angelman syndrome (Marín, 2012, Lewis et al., 2005).

INTERNEURON SUBTYPES

Inhibitory interneurons are a heterogeneous group of GABAergic or glycinergic neurons that constitute approximately 20% of cortical neurons and 10% of hippocampal neurons (Marín, 2012, Olbrich and Braak, 1985). They mediate the precise gating of information through specific signalling pathways by controlling the amounts of excitatory and inhibitory inputs that individual neurons receive both spatially and temporally (Vogels and Abbott, 2009).

Various subpopulations can be distinguished by a combination of morphological, physiological and molecular attributes. Classification occurs according to the spatial localisation of the synapse, expression of specific calcium-binding proteins (CBPs) or the firing pattern (figure 2B). For example, Martinotti cells form synapses onto the dendrites of pyramidal cells, whereas basket cells and chandelier cells primarily contact the soma and axon initial segment (AIS) of pyramidal cells (Marín, 2012).

As the spatial location of synapses is one of the features that determine the effect of interneurons on a postsynaptic target (Somogyi and Klausberger, 2005), each class of interneurons modulates pyramidal cell function in a specific manner. Based on histochemical markers, inhibitory cells can be divided into three non-overlapping categories in mice: those that express parvalbumin (PV), somatostatin (SST), and 5-hydroxytryptamine (serotonin) receptor 3a (5HT3aR), and one overlapping class of SST and calretinin (CR) positive cells (figure 2A) (Somogyi and Klausberger, 2005, Freund and Buzsaki, 1996, Ascoli et al., 2008, Rudy et al., 2011). 5HT3aR is the only known murine serotonergic ionotropic receptor and is present exclusively in GABAergic neurons (Ferezou et al., 2002, Morales and Bloom, 1997, Puig et al., 2004). Although these classes don't account for all inhibitory interneurons - a small number of interneurons express other less common markers like vasoactive intestinal peptide (VIP), Calbindin (CB) or neuropeptide Y (NPY) - they represent the vast majority (80–90 %) of all inhibitory cells (Rudy et al., 2011, Pfeffer et al., 2013).

The interneuron subpopulations also display different electrophysiological properties as e.g. their spiking pattern.

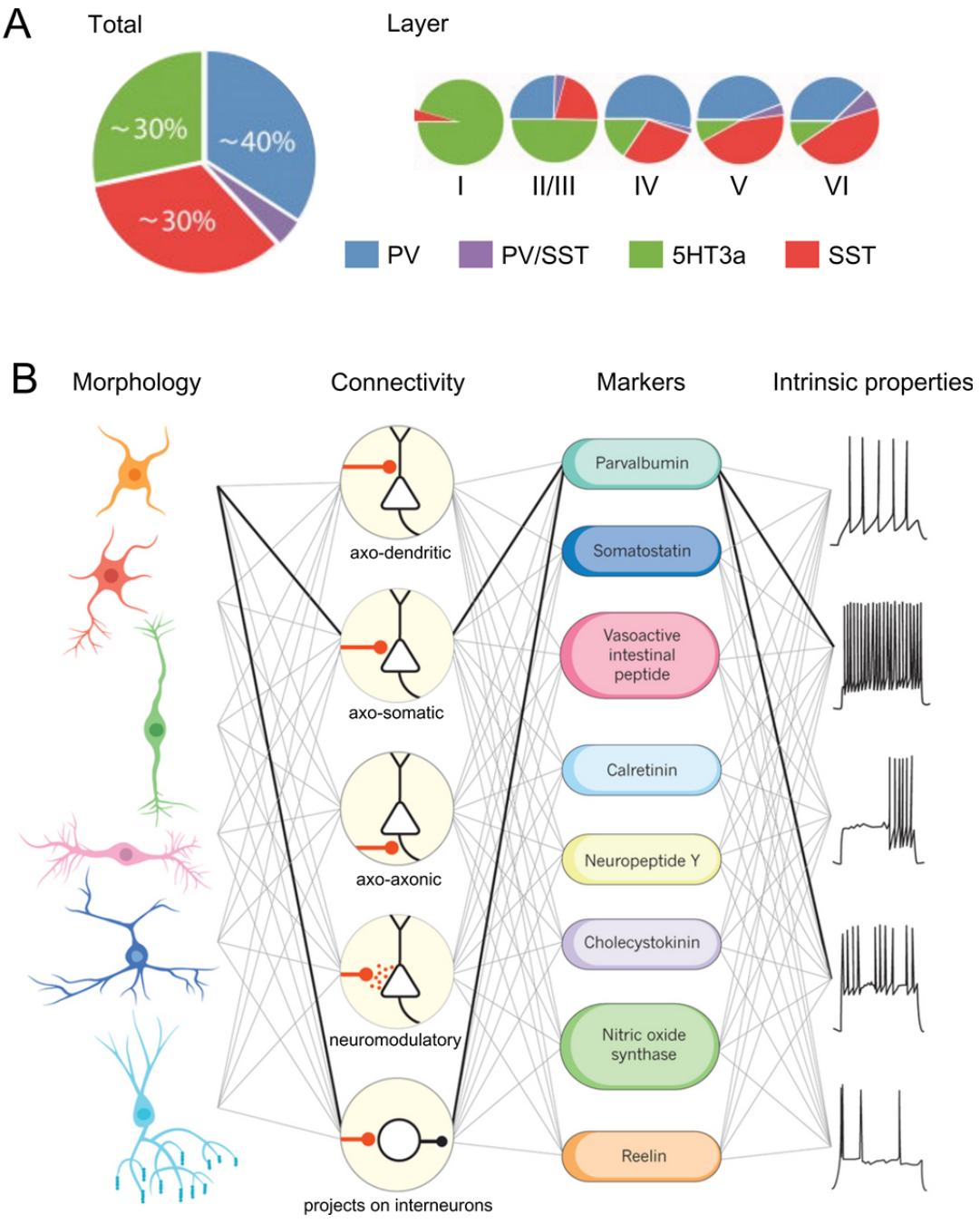

FIGURE 2: SUBPOPULATIONS OF GABAERGIC NEURONS. A| Classification of GABAergic interneurons in adult neocortex. The majority belongs to one of three groups defined by the expression of parvalbumin (PV), somatostatin (SST), and the ionotropic serotonin receptor 5ht3a (5HT3aR). In turn, each subgroup consists of several functionally distinct types or classes of interneurons (adapted and modified from Rudy et al. 2011). B| Interneuron cell types are defined using a combination of criteria based on morphology, connectivity pattern, synaptic properties, marker expression and firing pattern. The highlighted connections define fast-spiking cortical basket cells (modified from Kepecs and Rudy 2014).

A correlation between spiking pattern and the already mentioned histochemical markers was reported by several publications. In the majority of cases CR positive interneurons are referred to as accommodating or irregular-spiking neurons (Porter et al., 1998); CB positive ones represent bursting interneurons (Kawaguchi and Kubota, 1993) and PV positive ones are fast-spiking interneurons (Ascoli et al., 2008, Kawaguchi and Kubota, 1993, Chow et al., 1999). This correlation does not seem to be distinct and ideally the characterisation of a neuron will consider all three sets of criteria - morphology, molecular biology, and physiology (Ascoli et al., 2008).

PV^+ NEURONS

PV is a calcium-binding protein that is involved in Ca^{2+} signalling and many physiological processes. PV is expressed in fast-contracting muscles as well as in the brain and some endocrine tissues. In the cerebral cortex PV is found in subsets of GABAergic neurons, which are present in all areas of the neocortex and in all layers except layer I (Celio and Heizmann, 1981). Morphologically they can be divided into at least two categories of GABAergic local circuit neurons: basket cells and chandelier cells (figure 3) (Hendry et al., 1989, Jones and Hendry, 1986, Lewis and Lund, 1990), but some also display other morphological features like bi-stratisfied cells or oriens-lacunosum-moleculare neurons (OLM cells). In basket cells, the axon forms a basket-like arrangement around the principal cell somata and proximal dendrites. In axo-axonic cells, the axon of the interneuron follows the axon initial segment (AIS) of the principal cell, resulting in a chandelier-like configuration (figure 3). By controlling a large set of principal cells at the site of action potential initiation and electrical coupling of

dendrites over gap junctions, PV+ interneurons can mediate powerful inhibition (Bartos et al., 2001, Gibson et al., 1999, Galarreta and Hestrin, 1999a). This inhibition influences rhythmic synchrony and facilitates information processing during cognitive tasks. They are involved in both feedforward and feedback inhibition (figure 3) (Pouille and Scanziani, 2001, Buzsàki and Eidelberg, 1981, Pouille and Scanziani, 2004). Feedforward inhibition is regulated primarily by fast-spiking PV+ cells, because these interneurons fire early after stimulation, before pyramidal cells and regularly spiking interneurons (Pouille et al., 2009).

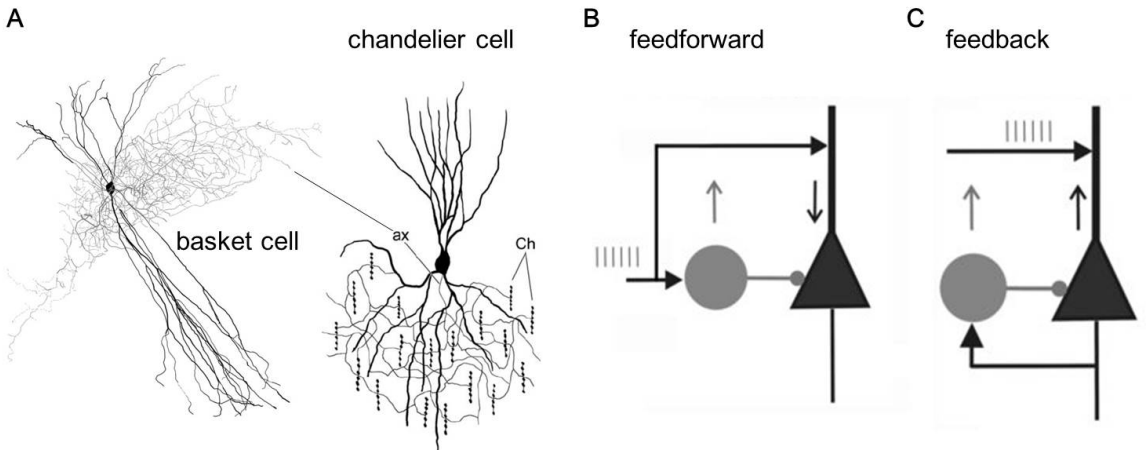

FIGURE 3: MORPHOLOGY OF PV+ INTERNEURONS AND MECHANISMS OF INHIBITION. **A|** Morphology of a PV+ basket or chandelier cell. Both types have multiple dendrites (black) that often cross layers. Axons (ax, grey) show extensive arborisation. Ch – terminal portion of the axon, which forms a short vertical row of boutons resembling candlesticks. Each Ch terminal innervates a single initial segment of a pyramidal cell (DeFelipe, 1999). Basket cell adapted from http://www.people.vcu.edu/~amcquiston/photogallery. **B|** Feed-forward inhibition dampens ("filters") the effect of afferent excitation. The interneuron (grey circle) is activated by upstream pyramidal cells, which results in a decreased activity of the downstream principal cell (black triangle). **C|** Increased firing of the principal cell elevates the discharge frequency of the interneuron. This may decrease the principal cell output, providing a regulatory mechanism by limiting the own activity. B and C adapted from (Buzsaki and Jonas, 2007).

Feedback inhibition implements the “winner takes all” network mechanism: principal cells with the strongest input fire and action potential initiation in the remaining cells are inhibited. Feedback inhibition, both recurrent and lateral, has been demonstrated to rely on the activation of PV^+ interneurons. (Pouille and Scanziani, 2004, de Almeida et al., 2009b, de Almeida et al., 2009a).

Several optogenetic manipulations of PV^+ interneuron activity showed that they are necessary and sufficient for the generation of network oscillations in both the hippocampus and neocortex. Activation of PV^+ cells at theta frequency (4-10 Hz) triggers theta spike resonance in CA1 pyramidal cells (Stark et al., 2013), and stimulation of PV^+ cells at gamma frequency (32-100 Hz) induced gamma oscillations in the local field potential in the somatosensory cortex (Cardin et al., 2009, Sohal et al., 2009). This major role of PV^+ interneurons for network oscillations, which are the hallmark of neuronal network function in several brain areas, determines the role of PV^+ interneurons for complex animal behaviour (Murray et al., 2011, Fuchs et al., 2007, Korotkova et al., 2010).

Additionally to this diverse population of inhibitory PV^+ interneurons a small subgroup of excitatory PV^+ interneurons are distributed throughout the brain (Markram et al., 2004). In 2015 an excitatory PV^+ visual pathway from the superior colliculus (SC) to the parabigeminal nucleus (PBGN) and amygdala has been identified which triggers fear responses, induces conditioned aversion, and causes depression-related behaviour (Shang et al., 2015). Moreover, the majority of PV^+ corticostriatal projection neurons are glutamatergic (Lewis et al., 2001, Jinno and Kosaka, 2004).

GABAERGIC SIGNALLING

GABA (gamma-aminobutyric acid) is the main inhibitory neurotransmitter in the mature mammalian central nervous system and thereby the main regulator of excitation via inhibition. In inhibitory synapses, GABA is synthesised from glutamate by the enzyme glutamate decarboxylase (GAD) and stored in vesicles until released. If interneurons in the adult brain are activated by upstream excitatory neurons, the resulting action potentials lead to activation of signalling cascades leading to GABA release into the synaptic cleft. At the synapse GABA will activate GABA receptors, either the fast ionotropic chloride ion-selective $GABA_A$ receptors or the metabotropic G-protein coupled $GABA_B$ receptors. A third class of GABA receptor, the $GABA_C$ receptor, is found predominantly in the vertebrate retina (Bormann and Feigenspan, 1995). The three classes differ in localisation, electrophysiological, biochemical and pharmacological properties.

$GABA_A$ RECEPTOR ($GABA_AR$)

The $GABA_A$ receptor, which is the principal mediator of synaptic inhibition, belongs to the superfamily of Cys-loop receptors and is a hetero-oligomeric protein that consists of five membrane spanning subunits around a central pore (figure 4A) (Campagna-Slater and Weaver, 2007). At least 19 mammalian genes encode for different $GABA_A$ receptor subunits (α1–6, β1–3, γ1–3, δ, ε, φ, π and ρ1–3) with additional diversity arising from alternative splicing (Macdonald and Olsen, 1994). The individual subunits exhibit specific expression patterns in certain brain regions, and a distinct subcellular localisation (Korpi et al., 2002, McKernan and Whiting, 1996). However, most

$GABA_ARs$ are composed of two α subunits, two β subunits and one other (γ, δ, ε, φ, or π) subunit (Rudolph and Mohler, 2004). In addition, receptors with different subunit compositions mediate primarily synaptic or primarily extrasynaptic signalling (figure 4B) in dependence of the respective subcellular localisation.

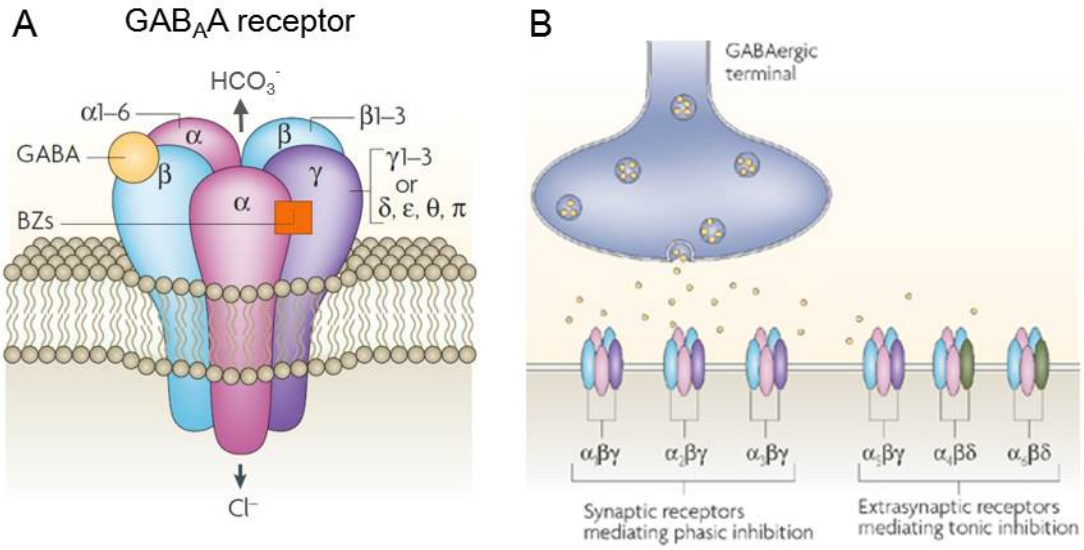

FIGURE 4: COMPOSITION OF $GABA_AR$. **A|** Five subunits from seven subunit subfamilies (α, β, γ, δ, ε, φ, π) form a heteropentameric channel that is permeable for Cl^- and HCO_3^-. Binding of the neurotransmitter GABA occurs at the interface between the α and β subunits and triggers the opening of the channel, allowing the rapid flux of Cl^- and HCO_3^-. Benzodiazepines (BZ) bind at the interface between α (1, 2, 3 or 5) and γ subunits and potentiate GABA-induced Cl^- flux. **B|** $GABA_ARs$ composed of α (1–3) subunits together with β and γ subunits primarily localise synaptically, whereas α5βγ and α(4 or 6)βδ receptors are located largely at extrasynaptic sites. Modified from (Jacob et al., 2008).

Upon binding of GABA, allosteric movements in the channel result in an opening of the ion pore allowing Cl^- and bicarbonate (HCO_3^-) ions to cross the membrane (Bormann et al., 1987, Kash et al., 2004, Kaila, 1994). The direction of the ion flow, inward or outward, depends on the electrochemical gradient of distribution of these two anions

across the plasma membrane and the membrane potential of the cell. In mature neurons the chloride equilibrium potential (E_{Cl^-}) is more negative than the resting membrane potential (V_m). The equilibrium potential for bicarbonate is more positive than V_m, but KCC2 is much less permeable for bicarbonate than for chloride. Therefore, activation of $GABA_A$ receptors mediates a net inward flow of anions and a hyperpolarising postsynaptic response - the inhibitory postsynaptic potential (IPSP). This leads to a reduction in the probability of action potential generation, causing neuronal inhibition (Cherubini, 2012).

Afterwards, GABA diffuses in the extracellular space before being taken up by selective plasma membrane transporters, which regulate the clearance of the neurotransmitter and shape synaptic currents (Cherubini and Conti, 2001).

GABAERGIC INHIBITION

The short-lasting inhibition, called phasic inhibition, typically generated by synaptic $GABA_AR$ activation following action potentials in a presynaptic interneurons is just one mechanism of inhibition (Cherubini, 2012).

Additionally, spill over of GABA in the extracellular space can stimulate molecularly and functionally specialised $GABA_A$ receptors that localise extrasynaptically and have a higher affinity to GABA (Farrant and Nusser, 2005), a process termed tonic inhibition. Moreover, they are more resistant to desensitisation and submicromolar concentrations of ambient GABA lead to a permanent increased membrane conductance, dampening the voltage change of synaptic input (Farrant and Kaila, 2007, Glykys and Mody, 2007).

Opening the chloride channel not only allows free flow of chloride ions across the membrane but also reduces the transmembrane resistance. If E_{Cl^-} equals V_m, no net ion flow occurs through an open $GABA_AR$. Due to the channel opening the membrane conductance increases and the membrane resistance falls. According to Ohm's law (V=I*R) the smaller membrane resistance causes a decrease of voltage (Mitchell and Silver, 2003) and thereby inhibits the neuron via reduction of excitatory currents. These reduced excitatory currents diminish the excitatory postsynaptic potentials (EPSP) locally. This process is termed shunting inhibition and effectively suppresses excitation from distal sources that must pass through that region on the way to the soma, whereas it has less influence on proximal EPSPs that influence the soma directly (Paulus and Rothwell, 2016).

Since this effect also takes place simultaneously with 'classical' hyperpolarising inhibition, the result is a dual inhibitory effect on ongoing excitatory inputs (Furman, 1965).

GABAERGIC EXCITATION

In embryonic neurons the intracellular Cl^- concentration $[Cl^-]_i$ is around 25mM due to a different ion channel expression pattern than in adult neurons (Ben-Ari, 2002). This shifts E_{Cl^-} from more negative than V_m to more positive than V_m, causing efflux of Cl^- across $GABA_AR$ channels and thus GABA-mediated depolarisation. The depolarizing action of GABA in immature neurons can generate action potentials by activating voltage-gated sodium channels, promote glutamate signalling by removing the magnesium block of N-methyl-D-aspartate receptors (NMDARs), and increase

intracellular Ca^{2+} by activating voltage-gated calcium channels. In addition, the depolarising response may be enhanced non-synaptically by the extracellular accumulation of potassium (K^+) ions (Kaila et al., 1997, Smirnov et al., 1999). Through these mechanisms, depolarising GABA promotes synchronous network oscillations and modulates activity-dependent processes such as neuronal maturation and synaptogenesis (Ben-Ari, 2002). Essential to switch from depolarising to hyperpolarising seems to be the change of Cl^- ion transporter expression, with sodium-potassium-chloride cotransporter 1 (NKCC1) and potassium-chloride cotransporter 2 (KCC2) being the most important.

Besides the role in development, the role of GABAergic excitation in mature neuronal function, network regulation and disease has been discussed intensively (Avoli and de Curtis, 2011, Ben-Ari et al., 2012, Cherubini and Conti, 2001, Cossart et al., 2005, Ellender et al., 2014, MacKenzie and Maguire, 2015, Nabekura et al., 2002, Staley et al., 1995, Staley and Mody, 1992, Viitanen et al., 2010, van den Pol et al., 1996, Chavas and Marty, 2003). There is growing evidence that GABAergic depolarisation occurs naturally and functionally in the CNS of adult animals. In some brain regions, GABA acts both excitatory and inhibitory (Wagner et al., 1997, Bazhenov et al., 1999, Chavas and Marty, 2003), suggesting that dynamic excitatory GABAergic transmission plays a critical role in controlling normal brain function. Interestingly, excitatory GABA actions have also been reported in seizure generation (Cohen et al., 2002, Fujiwara-Tsukamoto et al., 2003, Ben-Ari et al., 2012).

CATION-CHLORIDE COTRANSPORTERS (CCCS)

Electroneutral chloride transporters are often referred to as cation-chloride cotransporters (CCCs) and belong to the superfamily of solute carrier transporters (SLC). These transporters can be subdivided into four groups with (1) the NKCC symporters which transport sodium (Na^+), K^+ and Cl^-, (2) the NCC symporters, which move Na^+ and Cl^-, (3) the KCC cotransporter which carries K^+ and Cl^- and (4) Cl^--cation cotransporters (Knoflach et al., 2016). These latter transporters have a structure with 12 putative transmembrane domains with both the N- and C-termini facing the intracellular compartment. They are thought to form dimers in the membrane allowing the formation of the anion–cation binding pocket enabling the translocation of ions. As symporters, they cover the energy requirements passively from transmembrane differences in ion concentrations. The CCCs utilize the K^+ or Na^+ gradients built up by the Na^+/K^+-ATPase to translocate Cl^- across the membrane. NKCC1 and KCC2, two members of SLC12 family, are known to have cell-autonomous functions in central neurons especially in creating the reversal potential and driving force of anion currents utilised by $GABA_A$Rs and glycin receptors (GlyRs) (Blaesse et al., 2009).

NKCC1

Na^+-K^+-Cl^- cotransporters (NKCC) belong to the cation dependent chloride cotransporter family (CCCs; figure 5) and mediate the transport of Na^+, K^+ and Cl^- ions into the cell.

The Na^+-K^+-Cl^- cotransporter 1 (NKCC1), encoded by the gene *Slc12A2*, is widely expressed in different tissues and cell types.

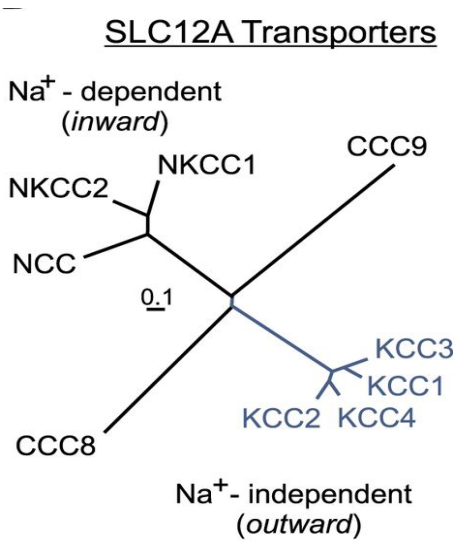

FIGURE 5: THE SLC12A GENE FAMILY.

Cluster dendrogram of human Slc12a cotransporters. The two major branches of cation-chloride cotransporters (CCC) separated early during evolution. The functionally not yet characterized CCC9 separated early from the Na^+-dependent branch of cation-Cl^- cotransporters. In a similar fashion, CCC8 separated early from Na^+-independent K^+-Cl^- cotransporters. The length of tree branches can be compared with the reference bar, which represents 0.1 amino acid substitutions per site. Adapted from (Gagnon and Delpire, 2013).

Two alternative splicing variants have been reported in humans and mice (Vibat et al., 2001, Bailey et al., 2013), *NKCC1a* and *NKCC1b*. In mice *Nkcc1b* lacks exon 21, which encodes a 16-amino acid peptide located in the COOH-terminal tail of the protein. The absence of this exon causes the loss of the single protein kinase A (PKA) consensus site of the cotransport protein (Bailey et al., 2013). In neurons the NKCC1 mediated flux of ions is directed inward, creating a high Cl^- ion concentration.

Even though it has been shown by several studies that NKCC1 is important for establishing the Cl^- concentration in neurons, it is controversially discussed whether a decreased expression of NKCC1 is responsible for the switch from high to low Cl^- in adult neurons (figure 6B) (Dzhala et al., 2005, Zhang et al., 2007). While some studies suggest a postnatal downregulation of NKCC1 (Dzhala et al., 2005, Liu and Wong-Riley, 2012, Hübner et al., 2001a), others indicate an upregulation of NKCC1 expression in the CNS during development (Mikawa et al., 2002, Hyde et al., 2011,

Morita et al., 2014). In 2009 Blaesse et al. concluded that the use of antibodies and probes insensitive to *NKCC1b*, the splice variant that constitutes up to ~80 % of the total *NKCC1* transcript in the human CNS (Vibat et al., 2001) confounds those results. On the basis of microarray data analysis with probes spanning both major human *NKCC1* splice variants *NKCC1a* and *NKCC1b* (Vibat et al., 2001, Morita et al., 2014), Sedmak et al. found that NKCC1 expression in all of the examined human brain regions undergoes developmental upregulation (Sedmak et al., 2015).

NKCC1 is kinetically regulated through a Cl^--sensing cascade involving with no lysine kinase (WNK), STE20-related proline/alanine-rich kinase (SPAK) and oxidative stress–responsive kinase 1 (OSR1). SPAK-mediated phosphorylation of key N-terminal threonine residues (for example, T212 and T217) of NKCC1 results in its activation and Cl^- accumulation. In contrast, dephosphorylation of these residues by protein phosphatase 1 (PP1) inactivates NKCC1 (figure 6A). Reciprocal regulation of transport activities of NKCC1 and KCC2 by the WNK–SPAK and WNK–OSR1 cascade has been demonstrated in heterologous expression systems and may also take place in neurons (Medina et al., 2014).

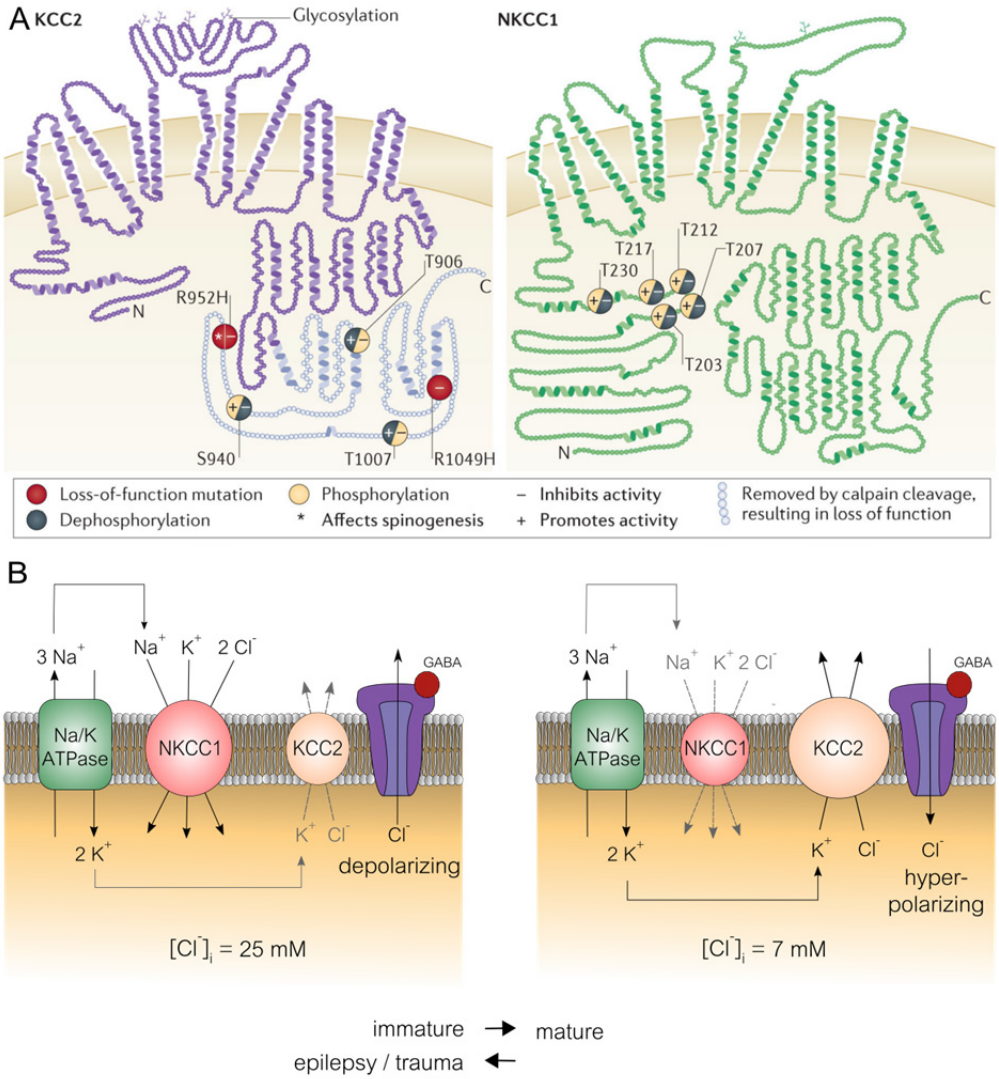

FIGURE 6: NKCC1 AND KCC2. **AI** Secondary structures of human KCC2b and NKCC1b splice isoforms. KCC2: Dephosphorylation sites at threonine T906 and T1007 and phosphorylation at serine S940 are associated with functional activation. Phosphorylation by protein kinase C (PKC) at S940 promotes membrane stability. An arginine-to-histidine mutation at residue 952 (R952H) results in loss of both transport activity and spinogenesis. NKCC1: Phosphorylation of NKCC1 by SPAK and OSR1 at the depicted N-terminal residues leads to functional activation. Dephosphorylation of NKCC1 by PP1 at threonine residues renders it transport-deficient. Putative glycosylation sites in KCC2 and NKCC1 are highlighted. Adapted from Kaila et al 2014. **BI** Regulation of intracellular chloride concentration by NKCC1 and KCC2. In immature neurons NKCC1 dominates over KCC2 expression resulting in high intracellular chloride concentrations of around 25 mM. Activation of $GABA_A$ results in outward directed Cl^- flow and depolarization. In adult neurons KCC2 expression increases and $[Cl^-]_i$ is lowered to 7 mM. Opening of $GABA_A$ receptor leads to Cl^- influx and hyperpolarization. Epilepsy/trauma may reverse the channel composition.

KCC2

The neuron-type and brain region-specific expression patterns of KCC2 have been studied extensively in different species (Kaila et al., 2014a). In mammals, the sodium-potassium cotransporter 2 (KCC2), encoded by the gene *SLC12A5,* is abundantly expressed in neuronal cells, with very little or no expression in peripheral neurons, neuronal progenitors, and non-neuronal cell types, including glia (Blaesse et al., 2009, Gagnon et al., 2013, Kanaka et al., 2001). KCC2 is located in the plasma membrane of somata and dendrites of neurons throughout the CNS including all layers of the cortex, neurons of the brainstem, thalamus, olfactory bulb, and spinal cord, CA1–CA4 pyramidal neurons of the hippocampus, granular layer, and Purkinje neurons (Payne et al., 1996, Uvarov et al., 2007). The CNS neuron specific expression depends on various mechanisms, including binding sites for neuron-enriched transcription factors such as Egr4 and neuron-restrictive silencing elements (Uvarov et al., 2006, Uvarov et al., 2005).

Alternative splicing of the *Kcc2* gene results in two *Kcc2* isoforms, *Kcc2a* and *Kcc2b*. They differ in 40 amino acids in the N terminus encoded by an alternatively spliced exon (called exon 1a and 1b). *Kcc2a* contributes 20–50 % of the total *Kcc2* mRNA expression in the neonatal mouse brain stem and spinal cord but only 5–10 % in the mature cortex. During postnatal development, the KCC2a expression remains relatively constant whereas Kcc2b expression increases and prevails. Since mice that lack only KCC2b but retain an apparently normal level of KCC2a expression survive for up to 2 weeks, absence of KCC2b is presumably sufficient to support vital neuronal functions in the brain stem and spinal cord but not in the cortex (Uvarov et al., 2007). Mice

lacking both KCC2 isoforms die immediately after birth due to severe motor defects, including respiration failure (Hübner et al., 2001b). Since the investigated mouse model affects both isoforms in what is discussed below, ‘‘KCC2’’ will refer to both splice variants.

The already mentioned upregulation of KCC2 expression seems to be part of neuronal differentiation and maturation. It takes place around time of birth and is both brain region- and species-specific. Cortical neurons of new born rats show very low KCC2 expression with depolarizing $GABA_AR$-mediated responses, whereas cortical neurons of the guinea pig increase KCC2 expression *in utero* and show hyperpolarising $GABA_AR$ responses at birth (Rivera et al., 1999). In human cortical neurons KCC2 expression was detected from the 25^{th} postconceptional week onwards indicating that, unlike in rodents, upregulation of KCC2 begins prenatally (Robinson et al., 2010, Sedmak et al., 2015).

ROLE OF KCC2 IN MORPHOLOGY OF NEURONS

In addition to the ion transport function of KCC2, it has been reported to be essential for spine formation in excitatory neurons. Essential for this shaping function seems to be the interaction of the KCC2 C-terminus with the cytoskeleton-associated protein 4.1N (figure 7) (Chamma et al., 2012). 4.1N possesses a 4.1 Ezrin Radixin Moesin (FERM) domain that binds a variety of transmembrane proteins and a spectrin/actin interaction domain (Baines et al., 2009). Therefore, KCC2 is expected to interact with the sub-membrane actin cytoskeleton. Such interactions may have multiple implications like e.g. (1) regulation of KCC2 clustering and thereby its membrane

stability/activity, (2) restriction of KCC2 localisation to specific membrane domains, (3) control of the local organisation of actin filaments with effects on subcellular morphology of synapses (Li et al., 2007, Mohandas et al., 1992, Cancedda et al., 2007, Gauvain et al., 2011), and (4) regulation of cell migration (Wei et al., 2011) (Mills et al., 1994).

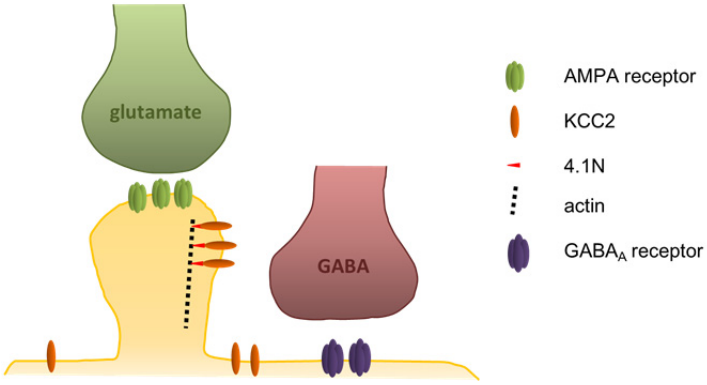

FIGURE 7: KCC2 LOCALISATION AT DENDRITIC SPINES. KCC2 interacts with the cytoskeleton-associated protein 4.1N and thereby regulates correct AMPA receptor localization at glutamatergic synapses (Gauvain et al., 2011). GABAergic synapses do not form on spines, but on dendrites. Here ion transport function of KCC2 is important for polarity of GABAergic currents (Chamma et al., 2012).

REGULATION OF KCC2 EXPRESSION

Many signalling molecules are important in controlling KCC2 function. Brain derived neurotrophic factor (BDNF), Insulin-like growth factor 1 (IGF-1) and Neurturin (NRTN, which belongs to the glial cell-line derived neurotrophic factor (GDNF) family of neurotrophic factors) have been identified as efficient modulators of the expression (Rivera et al., 2004), but only the regulatory effects of BDNF are well characterized. By binding to its receptor tropomyosin-related kinase B (TrkB), BDNF promotes the up-regulation of KCC2 expression by activating extracellular signal-regulated kinase 1/2

(ERK1/2)-dependent expression of Early Growth Response Protein 4 (EGR4) (Uvarov et al., 2006). Additionally the transcription is controlled by upstream stimulating factors 1 (USF1) and 2 (USF2) (Markkanen et al. (2008) and steroid hormones (Galanopoulou, 2008, Kight and McCarthy, 2014). Fast functional regulation of CCCs is mediated by post translational mechanisms, including phosphorylation of key residues in the intracellular domains and calpain-mediated cleavage (figure 5A) (Puskarjov et al., 2012). Phosphorylation of C-terminal serine residue S940 by protein kinase C (PKC) limits clathrin-mediated endocytosis of KCC2 and PP1-dependent dephosphorylation of S940 leads to internalisation of KCC2 and a reduction in neuronal Cl^- extrusion capacity. Intense activation of N-methyl-D-aspartate receptors (NMDARs) and the consequent

increase in $[Ca^{2+}]_i$ also induce cleavage of KCC2 C-terminally by the Ca^{2+}- and BDNF-activated protease calpain, which results in irreversible inactivation of KCC2 (Zhou et al., 2012). KCC2 activity is limited by phosphorylation of two C-terminal threonines, Thr(906) and Thr(1007), which depends on WNK1 and downstream SPAK/OSR1 (Friedel et al., 2015, Inoue et al., 2012).

PRELIMINARY WORK

The importance of KCC2 in chloride homeostasis and inhibition has been investigated in many studies and constitutive and conditional knockout mouse models for KCC2 are well established. Our lab created a constitutive knockout model for total KCC2 that dies immediately after birth due to severe motor deficits that also impair respiration (Hübner et al., 2001b) and a conditional knockout mouse model (Seja et al., 2012). Notably the

specific disruption of *Kcc2* in cerebellar granule cells (GCs) and Purkinje cells (PCs), did not change synapse density nor spine morphology, but increased $[E_{Cl^-}]_i$ roughly two-fold and nearly abolished GABA-induced hyperpolarization in PCs. Interestingly, these mice did not show an obvious motoric phenotype, but deficits in motor learning.

To study the role of KCC2 in interneurons and the subsequent effects to the neuronal network, KCC2 has been deleted in the largest subpopulation of interneurons by crossing the conditional KCC2 knockout mouse with a PV^+ - Cre line. The resulting knockout animals show a severe phenotype with decreased weight (figure 8A), motor deficits, a shortened life span (figure 8B) and spontaneous epilepsy.

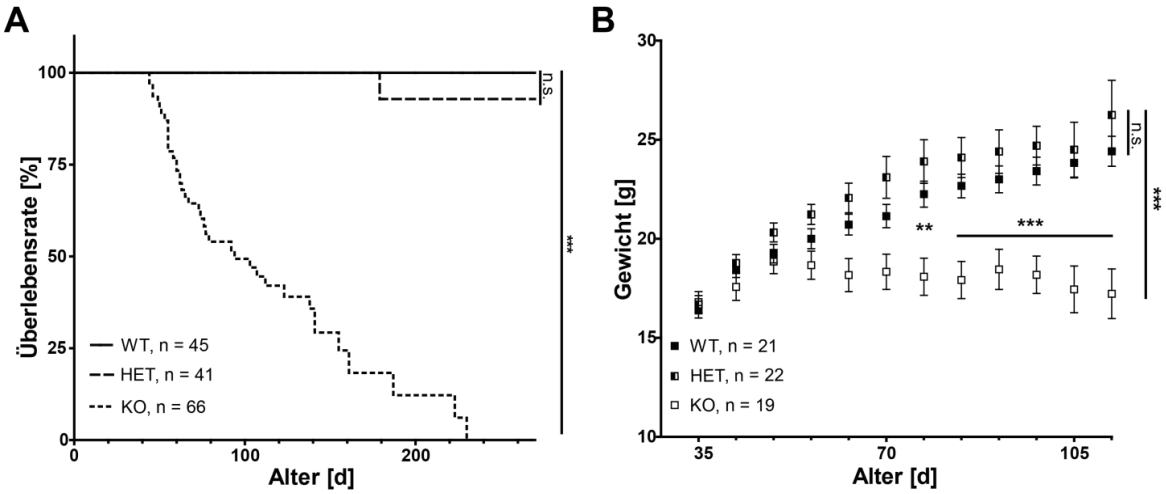

FIGURE 8: SURVIVAL AND DEVELOPMENT OF WEIGHT IN PV+-KCC2 KNOCKOUT MICE. A| Kaplan-Meier survival curve of wild type (WT), heterozygous knockout (HET) and homozygous knockout (KO) mice. KO animals present a shortened life span with an average life time of 94 days (Mantel-Cox-Test $p < 0{,}0001$). B| Weight development of KCC2 mice. WT and HET mice show a normal development whereas PV-KO animals demonstrate a decrease of body weight (two-way ANOVA $p < 0{,}0001$). Unpublished data from Ralf Dittmann.

AIM OF THE STUDY

During the last decades, the published data more and more suggest a dynamic role of GABAergic inhibition in early brain development and microcircuit formation. Since the GABA response critically depends on chloride gradients, which are mainly established via cation chloride cotransporters KCC2 and NKCC1, the latter have been the focus of many studies. However, because of the high diversity of interneurons, their role in interneurons has not been properly addressed so far. Our aim was to study whether KCC2 plays a role for the regulation of the parvalbuminergic interneurons and their activity. To address, how changes in chloride concentrations of PV^+ interneurons affect network excitability and brain function we disrupted *Kcc2* in parvalbuminergic interneurons.

MATERIAL AND METHODS

MICE

The mice were bread and housed in our animal facility. All experiments were officially approved by the Thüringer Landesamt für Lebensmittelsicherheit und Verbraucherschutz (Tierversuchsantrag Reg.-Nr. 22-2684-04-02-066/11).

The two mouse strains involved in this study are conditional KCC2 knock out mouse models that lack KCC2 expression in parvalbuminergic neurons. Both express a *Kcc2* allele with exons 2-5 flanked by loxP sites (described in (Seja et al., 2012); figure 9A) resulting in a non-functional protein if recombined by Cre recombinase. Those mice were bread with B6;129P2-Pvalb$^{tm1(cre)Arbr}$/J mice that express the Cre recombinase under the parvalbumin promoter (Hippenmeyer et al., 2005) (PV^{cre+}, 9B), leading to a specific knock out of KCC2 in parvalbuminergic cells. The specificity of this Cre line was proven by Ralf Dittmann. For all experiments, mice with the following genotypes were used: (WT) = KCC2$^{flox/flox}$, PVcre^{-}; (HET) = KCC2$^{flox/+,}$ PVcre^{+} and (KO) = KCC2$^{flox/flox}$, PVcre^{+}.

For the second mouse line the described mice were bread with B6.Cg-Gt(ROSA)26Sor$^{tm14(CAG-tdTomato)Hze}$/J reporter mice (figure 9C) that express *tdTomato* if activated by Cre recombinase (Madisen et al., 2010). In our mouse model this results in fluorescent dye labelled parvalbuminergic cells with the following genotypes: homozygous knockout (KO) = KCC2$^{flox/flox}$ resepctively wildtype (WT) = KCC2$^{+/+}$, PVcre^{+}, tdTomato$^{flox/flox}$ and heterozygous KO (HET) = KCC2$^{flox/+}$, PVcre+,

tdTomato$^{flox/flox}$. WT animals had to be PV cre+ to induce tdTomato expression and therefore only animals with two wildtype *Kcc2* alleles (KCC2$^{+/+}$) were suitable as controls.

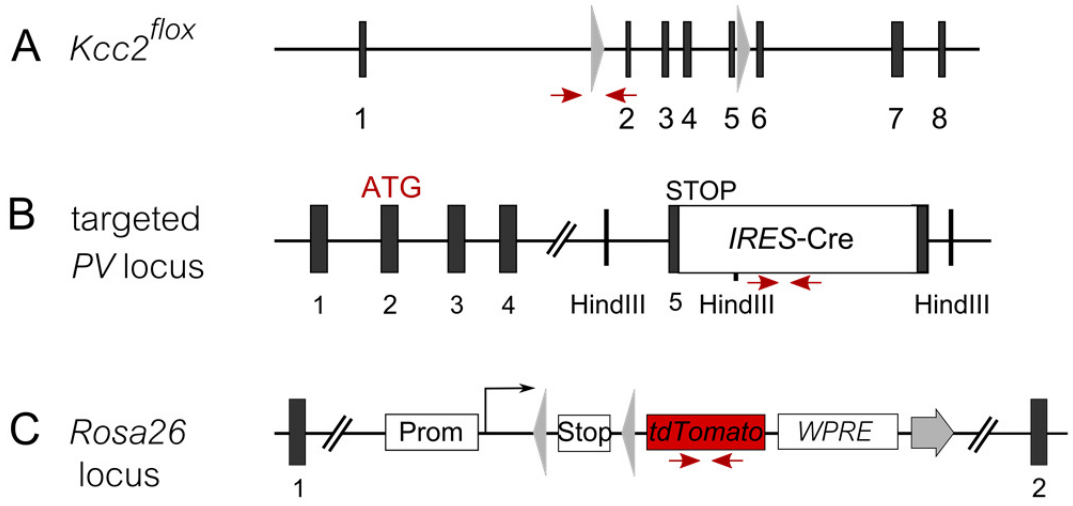

FIGURE 9: GENETIC MODIFICATIONS OF MICE. **A|** Strategy for generation of cell type specific KCC2 knockout mice. Exons 2–5 were flanked by loxP sites, which are recognised by Cre recombinase. **B|** *PV* genomic locus. Expression of Cre was realised by integration of an *IRES*-Cre cassette 3′ to the translational stop codon of *PV*. **C|** Schematic diagram of the gene targeting strategy with a Cre reporter cassette inserted into the *Rosa26* locus into intron 1. The construct contains a strong and ubiquitously expressed CAG promoter and the loxP-flanked ('floxed') stop cassette–controlled *tdTomato* gene. The woodchuck hepatitis virus posttranscriptional regulatory element (*WPRE*) was added to enhance mRNA transcript stability (Madisen et al., 2010). Grey arrowheads mark the loxP sites and red arrows mark the primer binding sites.

GENOTYPING

For genotyping of mice, the DNA was isolated from tail biopsies by adding alkaline lysis buffer (25 mM NaOH, 0.2 mM EDTA; 30 min; 95°C) and the reaction was neutralized

using 40 mM Tris-HCl for 2 min at 4°C. The DNA was stored at 4°C until used for genotyping by polymerase chain reaction (PCR).

Therefore, a PCR reaction master mix (20 µl) with 14.6 µl ddH_2O, 2 µl reaction buffer (10x), 0.8 µl $MgCl_2$, 0.5 µl dNTP-Mix (dATP, dCTP, dGTP, dTTP 8 mM), 0.5 µl *sense* primer (100 nM, table 1), 0.5 µl *antisense* primer (100 nM, table 1), 0.08 µl Taq-Polymerase (Invitrogen) was prepared, added to 1.5 µl DNA and then placed into a thermo cycler (T3000, Biometra). The primers for genotyping were designed by screening of the MGI-data base (http://www.informatics.jax.org/), NCBI-data base (http://www.ncbi.nlm.nih.gov) and with the online tool of LabLife (https://www.lablife.org/ll). Specificity was verified with „Primer-Blast" (http://www.ncbi.nlm.nih.gov/tools/primer-blast). PCR programs were set up according to the melting temperatures of primers.

Primer	Sequence (5'-3')
Kcc2 loxP forward	TCT GCC TGG AAC ACT CTC CTG C
Kcc2 loxP reverse	CAA CCT GAA CTC CCA AGG ATA CC
mKA1 forw	AAC AGC GAG CCC GAG TAG TG
mKA1 rev	TAA GAA CTA GAC CCA GGG TAC AAT G
Cre forw	AAA CGT TGA TGC CGG TGA ACG TGC
Cre rev	TAA CAT TCT CCC ACC GTC AGT ACG
tdTomato wt forw	AAG GGA GCT GCA GTG GAG TA
tdTomato wt rev	CCG AAA ATC TGT GGG AAG TC
tdTomato mutant rev	GGC ATT AAA GCA GCG TAT CC
tdTomato mutant forw	CTG TTC CTG TAC GGC ATG G

TABLE 1: PRIMER FOR GENOTYPING.

Horizontal gel electrophoresis (2 % agarose in running buffer, containing 40 mM Tris, 0.11 % acetic acid and 1 mM EDTA) was done to separate PCR products. DNA

fragments were visualised by addition of ethidium bromide to the gel (0.05 ng/ml). Samples with loading dye (25 % ficoll 400, 100 mM EDTA, 0.25 % bromphenolblue) and gels were loaded in tris acetate EDTA buffer. Fragment sizes were determined by comparison with bands of a 100kb-ladder (Gene graft). Depending on the expected fragment sizes, bands were separated at a constant voltage of 120 V for 30-60 min and evaluated under ultraviolet light. Genotyping for KCC2 resulted in a 490 bp band for floxed *Kcc2*-allels or a 291 bp band for WT *Kcc2*-alleles. Genotyping for *PV* showed a 388 bp band for the internal control gene KA1 and a 214 bp band for *Cre*. The *tdTomato* PCR resulted in a wildtype band of 297 bp and a mutant band of 196 bp.

IMMUNOHISTOCHEMISTRY

To obtain brain sections for staining mice were anesthetised (67 % v/v NaCl-Lösung 0.9 %, 28 % w/v Ketamin, 0.17 % v/v Rompun) via intraperitoneal injection of anaesthesia (ketamine 80 mg/kg bodyweight, xylazin 10 mg/kg bodyweight). To assure effective anesthesia the mice were pinched in the foot several times painfully with forceps to trigger nociceptive reflexes. When no reflexes could be observed after painful stimulation, the mice were placed on a preparation surface and transcardially perfused with phosphate buffered saline (PBS: pH 7.4, 140 mM NaCl, 2.7 mM KCl, 10 mM Na_2HPO_4, 1.8 mM KH_2HPO_4) and 4 % paraformaldehyde in PBS (PFA: 20 g paraformaldehyde in 500 ml PBS, filtered, pH 7.4). The ventral skin was cut with scissors, just below the xiphoid process. The ventral skin opening was expanded by manually pulling the opposing skin segments rostrally and caudally. Thoracic and peritoneal muscles and muscle fasciae were exposed, cut with scissors, just below the

xiphoid process and the diaphragm and visceral organs were exposed. The thoracic cavity was opened by cutting the diaphragm and both lateral aspects of the rib cage. Using blunt forceps, the right ventricular free-wall of the heart was gently grasped and a hypodermic needle (0.40x20 mm, B.Braun) was carefully inserted in the brighter coloured left ventricle. After opening of right atrial-chamber with scissors, the blood was removed by perfusion with saline for 5 min (flow 2-3 ml/min). Fixation was performed with 4 % PFA for 10 min (flow 2-3 ml/min). Brains were removed and further processed.

QUANTIFICATION

Quantifications of PV^+ interneurons in cortices and in hippocampi of WT, HET and KO mice were performed at the age of 4 weeks, 8 weeks and 23 weeks as previously described (Gerstmann et al., 2015). The dissected brain was post fixed in 4 % PFA over night at 4°C and afterwards incubated in sucrose (15 % and 30 % consecutively) for cryoprotection. For free-floating stainings cryosections (40µm) were cut with a sliding microtome (Leica) and stored in anti-freezing medium (150 g glucose, 300 ml ethylenglycol, 200 mg sodium acid, 0.24 ml NaH_2PO_4 x H_2O, 0.425 ml Na_2HPO_2 anhydr., filled up to 1000 ml with aqua dest.) at -20°C.

After three times washing with PBS for 5 min, the slices were permeabilised in PBS-T (PBS with 0.25 % Triton X-100, Sigma-Aldrich) for 20 min at room temperature, incubated for 1 hour in blocking solution (PBS with 0.25 % Triton X-100 and 5 % goat serum, Millipore) to avoid unspecific staining and transferred to wells containing primary antibodies diluted in blocking solution overnight at 4°C. The primary antibodies

were diluted as indicated in table 2. After three times washing with PBS for 5 min, the slices were incubated in secondary antibodies diluted in blocking solution (table 2) for 3 hours at room temperature. Washing with PBS was followed by incubation with 4',6-diamidino-2-phenylindole (DAPI; 1 µg/mL; Sigma-Aldrich) for 5 min, another wash step and mounting of slices to glass slides (HistoBond® adhesive microscope slides, Marienfeld) with a brush. Fluoromount® (Calbiochem) was applied with a Pasteur pipette for mounting. Cover slips (Marienfeld) were fixed to the slides by transparent nail polish (p2 cosmetics). Until analysis by confocal laser microscopy (TCS SP5, Leica) or Cell Observer (Carl Zeiss), slides were kept at 4°C.

Antibody	Company	Dilution
Mouse Anti-Parvalbumin	Svant (235)	1:5000
Rabbit anit-KCC2	Millipore (07-432)	1:1000
Rabbit anti-GABA	Sigma (A2052)	1:2000
Alexa Fluor® 555 goat anti–mouse IgG	Invitrogen (A21424)	1:2000
Alexa Fluor® 488 goat anti–rabbit IgG	Invitrogen (A11008)	1:2000

TABLE 2: DILUTION OF PRIMARY AND SECONDARY ANTIBODIES

Quantification of hippocampal PV^+ interneurons was performed by counting of PV^+ cells in the whole hippocampus of three consecutive slices (coronal, bregma -2.30, according to mouse brain atlas (Paxinos and Franklin, 2004)) at the cell observer.

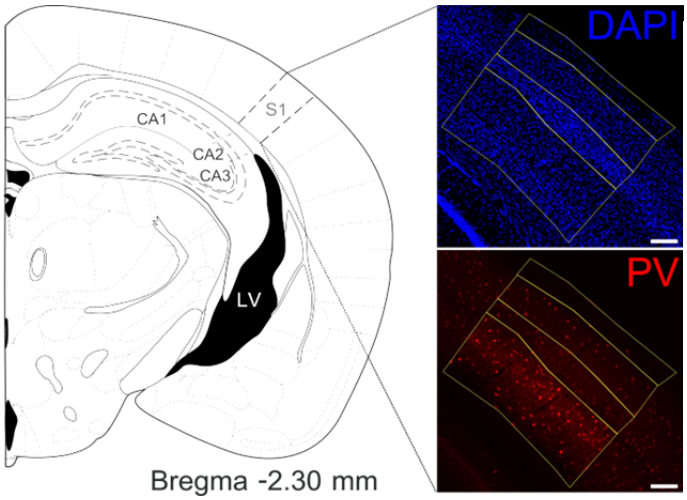

FIGURE 10: QUANTIFICATION OF PV⁺ NEURONS. Coronal slices were taken at position - 2.30 from the bregma and stained with anti-parvalbumin antibody (PV, red) and DAPI (blue). Identification and mapping of single cortical layers was accomplished in the DAPI channel of every image. Scale bar 75 µm.

To calculate the number in the cortex, images of somatosensory cortex were taken at the confocal laser-scanning microscope from the same slices used for quantification of hippocampal interneurons. The settings at the confocal laser-scanning microscope were optimized by taking the WT pictures first and then saved to be reused for all other pictures. The pictures were processed in ImageJ and cells were counted according to cortical layers. Therefore, the cortical regions of interest (ROI) were mapped in the DAPI channel, saved to the ROI manager and displayed in the parvalbumin channel (figure 10). The cells were counted in the different ROIs and cell number per 100000 µm² was calculated:

$$\text{cell number per } 100000\ \mu m^2 = \frac{(\text{cell number ROI})}{\text{ROI area in } \mu m^2} * 100000\ \mu m^2$$

MORPHOLOGY

Acute brain slices (100 µm) from PV-tomato-KCC2 mice were cut at a vibratome (VT 1000S, Leica Instruments), placed in 4 % PFA overnight and mounted on glass slides (HistoBond® adhesive microscope slides, Marienfeld, Germany) in Fluoromount® (Calbiochem) and stored at 4°C. Pictures were taken at the LSM and analysed with LAS AF Lite (Leica) and Axio Vision Rel4.8 (Zeiss) to identify possible changes in interneuron morphology.

The number of dendrites emerging from the soma of investigated interneurons (referred to as basal dendrites) was counted by scrolling through the Z-Stacks and visualising the 3D structure of interneurons. The size of cell body was measured with the Axio Vision software.

CORTICOSTERONE LEVEL

ANIMAL HANDLING AND BLOOD PROCESSING

To minimise stress, 10 days prior to blood collection the animals were housed in sets of two and handling of the mice was avoided. At the day of blood collection, the animals were placed in a quiet environment and left undisturbed. In a separate room, mice were rapidly decapitated and trunk blood collected 2 to 3 hours before the end of the light cycle, when the corticosterone (CORT) levels reach its peak (Atkinson and Waddell, 1997). The blood was then centrifuged at 5000 rpm for 5 min; the serum was collected and stored at −80 °C until CORT analysis was performed.

ELISA

Serum CORT was measured using an enzyme immunoassay kit (# 900-097; Enzo Life Sciences) according to the manufacturer's instructions. The sensitivity of the assay was 27 pg/ml; all samples were run in the same assay to avoid interassay variability. Sample size was 8–9 mice/group. The samples were diluted 1:40 in ELISA buffer and run in duplicates. Every plate included wells with negative controls (Blank, NSB), positive controls (Total Activity TA, Maximum binding Bo) and standards #1 - #5 (#1: 20000 pg/mL; #2: 4000 pg/mL; #3: 800 pg/mL; #4: 160 pg/mL; #5 32 pg/mL). The ELISA plate reader was normalised against the Blank wells and optical density read at 405 nm, with correction at 580 nm.

Average net Optical Density (OD) bound for each standard and sample was calculated by subtracting the average NSB OD from the average OD bound:

$$\text{Average net OD} = \text{average bound OD} - \text{average NSB OD}.$$

The binding was calculated as a percentage of the maximum binding wells (Bo):

$$\text{Percent bound} = \text{net OD} / \text{net Bo OD} * 100.$$

Plotting a graph with the standard absorbance value as the dependent variable (Y-axis) and CORT concentration as the independent variable (X-axis) results in a standard curve. The standard curve was fitted with the exponential regression function:

$$y = a*x^2 + b*x + c.$$

Solving for x determines the protein concentration of the sample.

ELECTROPHYSIOLOGY

SLICE PREPARATION

After decapitation of mice (8-10 weeks or 23 weeks of age) the brain was quickly removed, placed in ice cold artificial cerebrospinal fluid (aCSF: 120 mM NaCl, 3.5 mM KCl, 1.3 mM $MgSO_4$ x 7 H_2O, 12.5 mM NaH_2PO_4 x H_2O, 2.5 mM $CaCl_2$ x 2 H_2O, 10 mM Glucose, 25 mM $NaHCO_3$; bubbled with 5 % CO_2, 95 % O_2) and cut into coronal slices with a vibroslicer (VT 1000S, Leica Instruments) as described previously (Liebmann et al., 2009). Slices (350 µm) were stored at RT in aCSF for at least 1 hour until use.

FIELD POTENTENTIAL RECORDINGS

After equilibration, the slices were transferred to an interface-recording chamber. Slices were allowed to adapt onto recording conditions for 1 hour (oxygenated aCSF, 32°C, flow 2–3 mL/min). Bipolar stimulating electrodes with a tip diameter of 100 µm (SNE-200X, Science-Products) were placed onto the glutamatergic Schaffer collaterals of the hippocampus CA3 region to stimulate CA1 pyramidal neurons. Upon stimulation (pulse duration 50 µs), field excitatory postsynaptic potentials (fEPSPs) were recorded using glass microelectrodes (2–5 MΩ, filled with aCSF) impaled into the stratum pyramidale or the stratum radiatum of hippocampal CA1 region. Slopes of fEPSPs and amplitudes of population spikes (PS) were analysed (figure 11). Data of field potential recordings were collected with an extracellular amplifier (EXT-02, NPI, Germany), low pass filtered at 4 kHz and digitally stored with a sample frequency of 10 kHz. Data acquisition and

analysis of population spike amplitudes were performed using the software Signal (Cambridge Electronic Design).

To determine the maximal population spike amplitude or the maximal slope of fEPSP the stimulus intensity was increased in steps of 10 Volt (range 0-100 V) for each experiment (interstimulus interval 30 s). The relationship between stimulus intensity and the evoked response was fitted by a sigmoid function: $R_{(i)}=R_{max}/1+\exp(i-i_h)$, where $R_{(i)}$ is the response at intensity (i), R_{max} is the maximal response and i_h is the intensity at which half-maximal response was observed.

LONG-TERM POTENTIATION (LTP)

For investigation of changes in LTP the following protocol was applied: Stimuli with half-maximal intensity were applied (interstimulus interval 20 s) for 30 min to record the baseline. The high frequency stimulus (HFS, 5 x 100 pulses a 100 Hz) induced increasing PS amplitudes and slopes of fEPSPs, which were recorded over 1 hour (interstimulus interval 20 s). The amount of potentiation was analysed by comparing baseline values (normalised and averaged 20 min before induction) with those values collected within 60 min after HFS application.

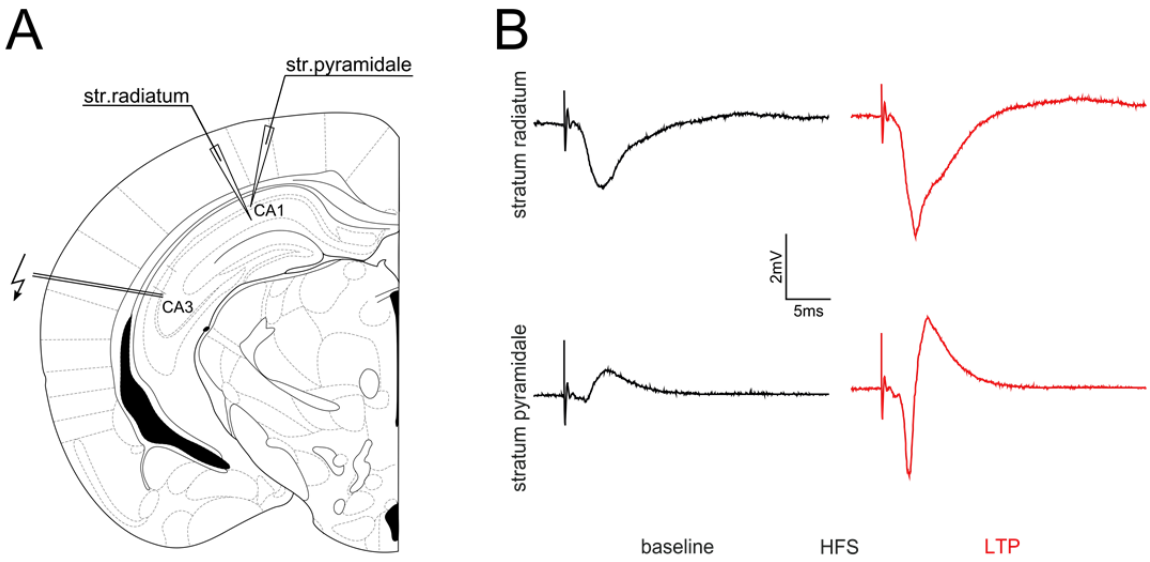

FIGURE 11: RECORDINGS OF FIELD POTENTIALS. **A|** Placement of electrodes for electrophysiological recordings in the hippocampus of acute coronal brain slices. The stimulation electrode is located in the stratum radiatum at the border of the CA2/3 area, while recording electrodes were placed in the stratum radiatum of the CA1. **B|** Exemplary baseline and post-HFS traces recorded from the stratum radiatum and the stratum pyramidale.

FEPSP – TO – SPIKE COUPLING

The fEPSP - to - spike ratio (also called E-S coupling) was recorded at the age of 8 and 23 weeks. A stimulating electrode was placed into the stratum radiatum while recording electrodes were placed in the stratum radiatum and stratum pyramidale in the CA1 to measure fEPSPs generated by glutamatergic CA1 synapses between the fibres of Schaffer collaterals and CA1 pyramidal neurons and population spikes of CA1 neurons on the other hand, resulting from EPSP-driven action potential discharges. The stimulus intensity was increased in steps of 10 V (range 0-100 V) and the recorded slopes of fEPSPs with associated PS were grouped in the following classes: 0.5 mV/ms, 1.0 mV/ms and 1.5 mV/ms

IN VIVO EXPERIMENTS

FEAR CONDITIONING

Fear conditioning is a form of Pavlovian conditioning in which an initially neutral stimulus (conditioned stimulus; CS), usually a tone, is paired with the presentation of an aversive event (unconditioned stimulus; US), usually a footshock, to elicit fearful behaviour characterized by robust autonomic responses and a cessation of movement or freezing (Fanselow and Poulos, 2005, Smith et al., 2007).

The experimental setup (Ugo Basile) consisted of 4 identical sound-attenuating chambers (d 55 x w 60 x h 57 cm) equipped with door switch, electrified grid floor, fan, camera, speaker, infrared and LED light. Animals were recorded the whole time for automatic detection of freezing by ANY-maze software (Stoelting).

For delayed fear conditioning, a protocol was established similar as previously described (Langwieser et al., 2010, Kamprath and Wotjak, 2004). Adult animals (age 8-13 weeks) were placed in the animal enclosure (d 17 x w 17 x h 25 cm) inside the chamber and allowed to explore the surrounding area for 180 s. A tone (CS) was played for the following 20 s (9 kHz, volume 20 %, 80 dB) paired with a foot shock (US, 0.7 mA for 2 s) in the last 2 s administered via the metal grid. Mice remained in the chamber for additional 60 s after the shock before they were returned to their home cages.

After 24 h, tone-shock association was analysed first. This was followed by test of context-shock association 2 h later. Animals were placed in a differently shaped animal

enclosure with altered colour (striped wall, white floor), lightening (2 lux), odour (3 % acetic acid) and fan speed (50 %). They were allowed to explore the new area for 180s before the conditioned stimulus (tone) was applied for 180 s. Mice remained in the chamber for additional 60 s before they were transferred back to their home cages. After 2 h they were placed in the same context as during acquisition (plexiglas walls, metal grid floor, lightening 5 lux, odour 70 % ethanol, fan speed 100 %) and observed for 180 s.

For automatic freezing detection, the minimal freezing detection was set to 250 ms and the threshold (min: 33 a.u., max: 44 a.u.) defined. To verify the results of automatic detection all videos were assessed off-line from video tapes by an experienced observer who quantified the freezing response to the tone (Kamprath and Wotjak, 2004). Freezing time was presented as percentage of the investigated 60 s intervals:

$$\text{freezing time (\%)} = \left(\frac{\text{freezing time (s)}}{\text{60 (s)}}\right) * 100$$

To assess the increase in freezing time (Δt_f (%)) induced by application of CS during the cued fear test, the change in freezing time was calculated as described:

$$\Delta t_f \text{ (\%)} = \frac{\text{freezing pretone (\%)}}{\text{freezing time CS (\%)}}$$

SEIZURE THRESHOLD

To analyse the susceptibility to seizure inducing substances pentylentetrazole (PTZ) was injected (Sigma, 5 mg/ml in PBS) as described previously (Jacobs et al., 2008).

Therefore, the mice were weighed and the according amount of PTZ was calculated (60 mg per kg body weight). After injection, the mice were placed in a glass cylinder and the video camera was started. The latencies of the different stages (table 3) described as myoclonic jerks (focal seizure), clonic and tonic-clonic (generalized) seizures were analysed off-line. Onset of the epileptic seizure was defined by the following criteria:

Phase	Characteristic criteria
myoclonic	ear twitching, shaking
clonic	clonic seizures without loss of righting reflexes, clamping of the forefeet, rearing
tonic-clonic	loss of posture, tonic forelimb or hindlimb extrusion, generalized seizure

TABLE 3: CRITERIA FOR SEIZURE PHASES

STATISTICS

Data are presented as mean ± standard error of mean (SEM). N defines the number of animals per experiment (biological replicate) and n defines the number of slices or cells (technical replicate) analysed. Statistical analysis was performed with GraphPad prism software. The unpaired, parametric two-tailed Student's t-test was applied for results of experiments with two experimental groups. If more than two groups were compared, one-way analysis of variance (ANOVA) and subsequent Tukey's test for post-hoc analysis were performed. In experiments, which included repeated measurements,

differences between groups were tested by repeated measures ANOVA. Two-way ANOVA was applied in a subset of experiments with subsequent Bonferroni's multiple comparison tests. Significance was considered at p-values < 0.05 (* indicates p < 0.05; ** indicates p < 0.01; *** indicates p < 0.001; **** indicates p < 0.0001).

NOMENCLATURE

The names of genes and proteins in this thesis are written according to the Mouse Genome Informatics Database (MGI) nomenclature (http://www.informatics.jax.org/mgihome/nomen/). The names are italicised when referring to the gene but nonitalic when referring to the protein.

Symbols for human genes use all uppercase letters and symbols for mouse genes generally are written with only the first letter in uppercase and the remaining letters in lowercase.

If referring to the protein, the symbols use all uppercase letters independent of the species.

RESULTS

GENERAL OBSERVATIONS

Compared to WT the PV^{+}-KCC2 KO mice showed an abnormal gait starting around 6-8 weeks of age, which progresses over time. Their hind limbs appear spastic and an abnormal spreading of the legs was observed, when lifted up. HET animals could not be distinguished from WT.

The difficulties to move properly also affected food uptake, since the KO animals were not able to climb to the food at the top of the cage. After onset of the described phenotype, the food was placed into the cage. Additionally; the bodyweight of KO mice was slightly reduced.

Spontaneous seizures in KO animals were the most striking observation. The seizures were described by animal caretakers and emerged around 15 and 20 weeks of age. The age of onset was not quantified.

MEMORY AND STRESS

LTP

LTP is considered as an electrophysiological correlate of learning and since PV-KCC2 KO mice showed a decreased memory in the Morris water maze (Herrmann, 2015) long term plasticity was analysed in the stratum radiatum and stratum pyramidale of the hippocampus. As shown in figure 12A the fEPSP potentials of WT animals showed a

potentiation of 20 % after HFS and both HET and KO animals presented with slightly increased potentials. During the whole recording time no significant difference were observed between genotypes (WT 121 ± 8.17%; HET 133 ± 4.65%; KO 132 ± 6.55%; two-way ANOVA F = 0.70; p = 0.51; n = 12/12/11; N = 6/6/6).

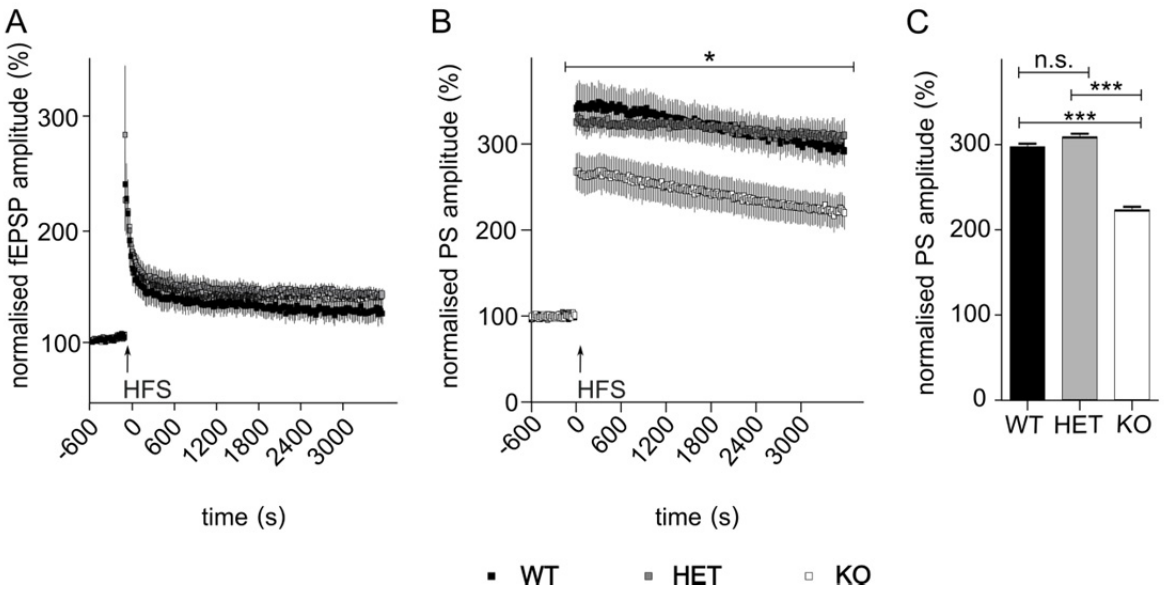

FIGURE 12: LTP RECORDINGS OF PV-KCC2 MICE. **A|** fEPSP amplitudes did not differ between WT, HET and KO during LTP recordings in the str.radiatum; two-way ANOVA p = 0.5083. **B|** Slices from PV-KCC2 KO animals showed decreased population spike amplitudes after HFS; two-way ANOVA p = 0.01; n = 12/12/11; N = 6/6/6 **C|** Mean of PS amplitudes recorded during the last 5 min of LTP. KO slices presented smaller amplitudes than WT and HET slices; Bonferroni's multiple comparison test WT vs. HET $p > 0.05$; WT vs. KO $p < 0.0001$; HET vs. KO $p < 0.0001$. n= 8/8/8; N = 4/4/4.

The PS amplitudes recorded in the pyramidal layer of WT and HET mice showed a potentiation of around 340 % after high frequency stimulation (figure 12B; WT = 341.0 ± 26.6%; HET = 331.0 ± 13.1%). There was no significant difference between these two genotypes for the whole recording time and after one hour both showed a similar potentiation (figure 12B; WT = 292.0 ± 18 %; HET = 305.0 ± 20.3 %). Recordings of

KO mice showed a decreased potentiation after HFS (KO = 220.0 ± 19.2 %) and analysis with two-way ANOVA showed a significant difference over the complete recording time ($F = 5.516$; $p = 0.01$; n = 8/8/8; N = 4/4/4).

The mean of PS amplitudes - normalised to the baseline - during the last 5 min was determined (figure 12C). One-way ANOVA revealed a significant difference ($F = 119.8$; $p < 0.0001$). Bonferroni's multiple comparison test calculated no difference between WT and HET (WT = 297.0 ± 4.1 %; HET = 308.5 ± 4.3 %; $p > 0.05$), but confirmed the decrease PS amplitude potentiation in KO (KO = 223.0 ± 4.4 %; WT vs. KO $p < 0.0001$; HET vs. KO $p < 0.0001$).

FEAR CONDITIONING

Fear conditioning is a form of one-trial learning (Fanselow, 1990). Only one conditioning session is necessary to induce a robust and long-term behavioural change; thus, fear conditioning serves as a model to clarify the electrophysiological and molecular mechanisms underlying learning. To determine whether the KO of KCC2 in parvalbuminergic neurons regulates additional forms of hippocampus-dependent memory, aversive contextual fear conditioning (Phillips and LeDoux, 1992) was studied. In figure 13 the applied protocol (figure 13A-C) and corresponding results (figure 13D-F) are illustrated. The tables with the detailed results for every time point are present in the appendix. During acquisition, all groups showed progressively increasing levels of freezing after application of the auditory cue and foot shock (figure 13D), indicating that they successfully acquired the task. There was no difference in acquisition between WT and HET mice, but KO mice showed an increase in freezing

time (two-way ANOVA F=9.484; p=0.0005; N = 12/12/12) that became significant before the neutral auditory cue (CS) was presented after 180 s (WT = 5.085 %, KO = 16.48 %, Bonferroni's multiple comparison test $p < 0.05$).

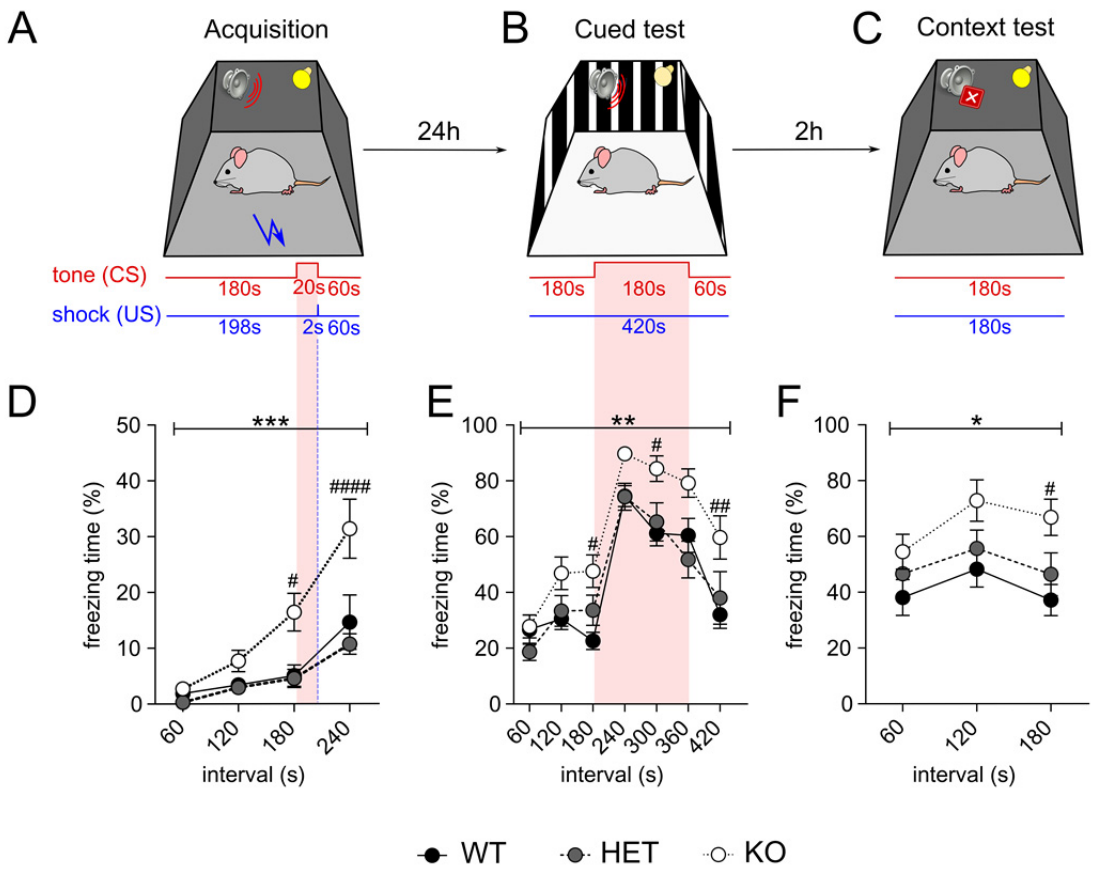

FIGURE 13: CUED AND CONTEXTUAL FEAR CONDITIONING. **A|** Acquisition protocol at day 1. The period of the tone is illustrated in red, time point of the foot shock in blue. **B|** 24 hours after the acquisition, the cued test was carried out followed by **C|,** the context test. The corresponding results of fear conditioning of PV-KCC2 mice are shown in the lower panel. **D|** During acquisition PV-KCC2 KO mice showed an increased freezing behaviour already before application of CS or US. **E|** 24 h after acquisition the mice were placed in a new context and the CS was applied after 180 s (red). All genotypes show a similar waveform, but PV-KCC2 KO mice demonstrated an upward shift, * two-way ANOVA p = 0.003. **F|** When returned to the acquisition context, all genotypes showed elevated freezing levels compared to the acquisition trial and KO mice showed a significant increase in the freezing behaviour compared to WT and HET animals, * two-way ANOVA p = 0.03, N = 12/12/12, # Bonferroni's post-test.

To assess the cued fear memory the mice were placed in a new context 24 h after fear acquisition and were allowed to explore this new context for 180 s. During this time, period baseline freezing was determined in the new environment. WT and HET mice showed freezing between 20 and 30 % of the time assessed (WT 26.6 ± 3.4 %; HET = 28.6 ± 3.8 %), whereas KO animals were more anxious in the new context (KO = 39.7 ± 4.3 %). The rise in freezing time after application of CS was analysed separately and revealed a similar increase of around 50 % in all genotypes (figure 14: Δt_f (%): WT = 38.8 ± 4.3 %; HET = 34.2 ± 4.6 %; KO = 41.9 ± 4.9 %; one-way ANOVA F = 0.079; p = 0.92; N = 12/12/12). This increase in freezing time was followed by a slow recovery to baseline. WT and HET displayed a comparable curve shape whereas KO mice show significantly elevated levels of freezing time at nearly all investigated time points (two-way ANOVA F = 67.00; p = 0.003; figure 13E).

FIGURE 14: RISE OF FREEZING TIME DURING CUED TEST. Analysis of the rise in freezing time after application of CS during cued test. No significant difference was detected between genotypes, p=0.92.

Δt_f change of freezing time.

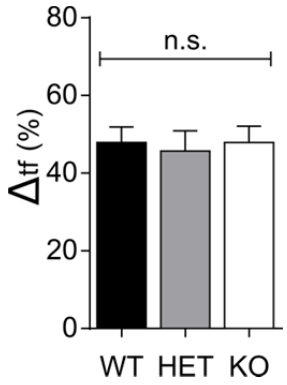

To measure contextual fear memory, mice were put back to the training context 2 h after completion of the cued testing. The memory of the foot shock related context was intact in all genotypes which was evident by an increase of the freezing time compared to the freezing time during acquisition. WT and HET animals showed freezing during 40–60 %

of the time period analysed, which is comparable with results from other studies with a similar protocol (Ikegami et al. 2014). In contrast, KO mice spent around 50–80 % of the time freezing in the context test, which was significantly increased compared to WT and HET (figure 13F; two-way ANOVA $F = 3.87$ $p = 0.031$).

PARVALBUMINERGIC NEURONS IN THE SUPERIOR COLLICULUS

Shang et al. reported in 2015 that PV^+ neurons in the superior colliculus (SC) contribute to a subcortical visual pathway that transmits threat-relevant visual information to the amygdala to trigger fear responses. These PV^+ neurons are predominantly glutamatergic projection neurons. To verify whether the PV^+ neurons in the SC are GABAergic and whether the KCC2 knockout was effective, sagittal brain slices were stained with antibodies against KCC2, parvalbumin and GABA.

As shown in figure 15 A the adjacent cortical area (retrosplenial granular cortex) of the SC was used as an internal control. In the retrosplenial granular cortex neurons stained for parvalbumin (green) were also positive for GABA (red) as expected for parvalbuminergic interneurons (figure 15C). In addition, some neurons were found that were positive for GABA but not for PV, representing other subgroups of inhibitory neurons in this area. In the superior colliculus the parvalbumin and the GABA signal did not overlap; there were either PV^+ neurons or GABAergic neurons. These observations are consistent with published data (Shang et al., 2015). Slices from the same mice were taken to verify the knockout of KCC2 in these neurons.

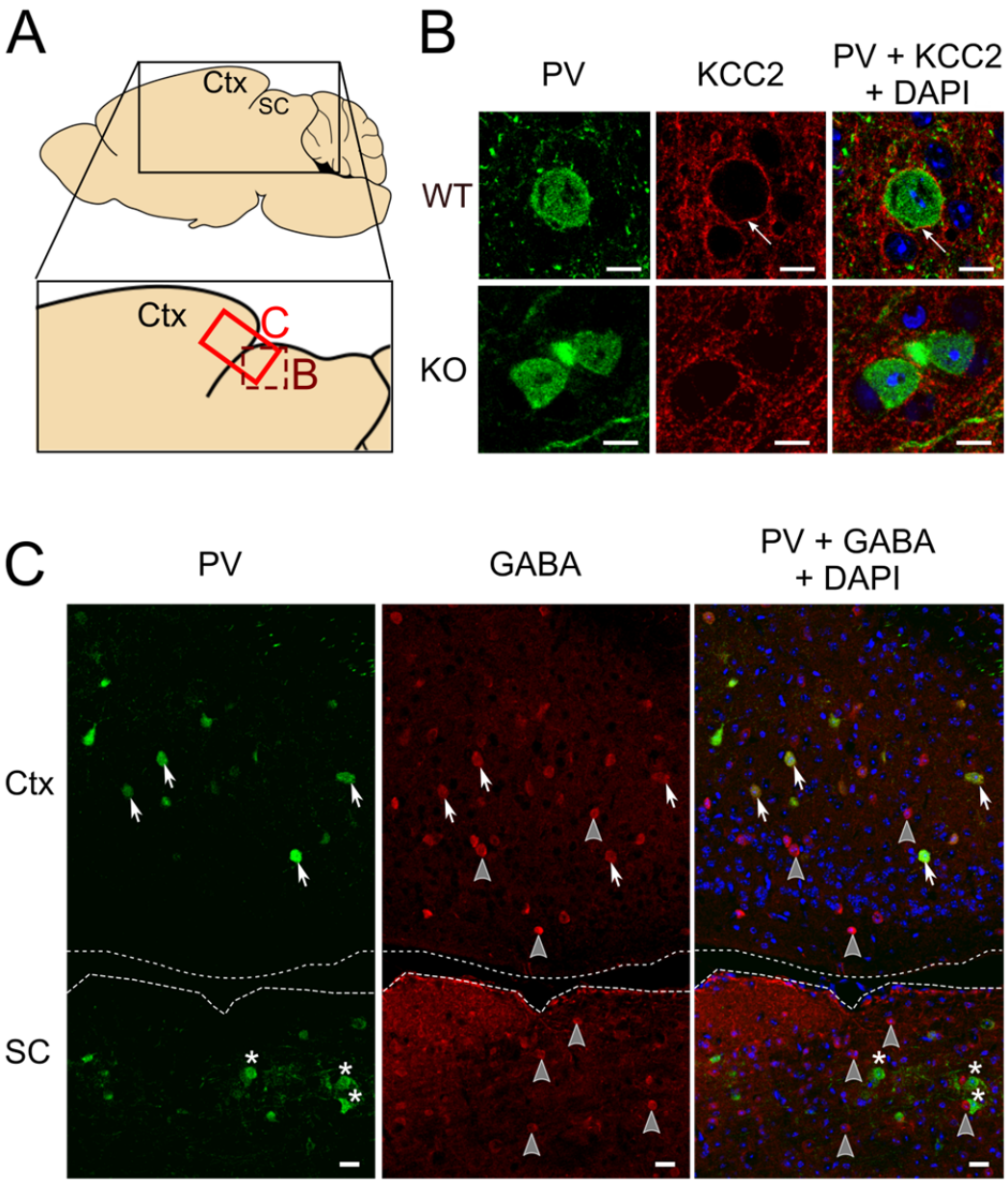

FIGURE 15: STAINING OF PV+ INTERNEURONS IN THE SUPERIOR COLLICULUS AND ADJACENT CORTICAL AREAS. **A|** Scheme of sagittal brain section with detailed positions of the pictures displayed in B and C. **BI** Co-staining of PV and KCC2 in neurons of SC. In WT mice neurons show KCC2 staining at the plasma membrane (arrow) and in KO animals this signal was absent. Scale bar 10 µm. **C|** Sagittal sections were stained with anti-PV and anti-GABA antibodies. In cortical areas there is a colocalisation, all PV positive cells are GABAergic representing parvalbuminergic interneurons (arrows). Some GABA positive neurons (grey arrow heads) did not stain for parvalbumin. In the SC PV positive cells are negative for GABA (stars). Scale bar 20 µm. Ctx cortex; GABA γ-Aminobutyric acid; KCC2 potassium chloride cotransporter 2; PV parvalbumin; SC superior colliculus.

As shown in figure 15B, parvalbuminergic neurons of the SC express KCC2 at the plasma membrane in WT whereas neurons of KO tissue lack KCC2. Ralf Dittmann already quantified the knock out efficiency. His calculation revealed an ablation of KCC2 expression in around 60% of all cortical PV^+ neurons (WT = 77.9 ± 1.5 %; KO = 18.1 ± 1.3 %; Students t-test $p < 0.0001$; n = 6/6: N = 3/3) and a 50 % decrease of KCC2 mRNA expressing PV^+ neurons (WT = 84,7 ± 1,9 %; KO = 42,2 ± 4,6 %; Students t-test $p < 0,0001$; n=9/6; N = 1/1).

SERUM CORTICOSTERONE LEVELS

Since KO mice showed increased freezing levels even at baseline conditions serum corticosterone levels were analysed by ELISA.

The measurement of the supplied standards resulted in a standard curve that was fitted by exponential regression analysis (figure 16A). The formula of the regression line ($y=76631*e^{-0.087*x}$) was used to determine sample concentrations.

As shown in figure 16B, WT animals had low CORT concentrations (WT=1748.1pg/mL ± 286.4; N=8), in agreement with a resting, quiescent state. Serum CORT levels of KO mice were significantly higher during this resting state (KO = 4806.5 pg/mL ±1037.0; N=9; students t-test p = 0.016).

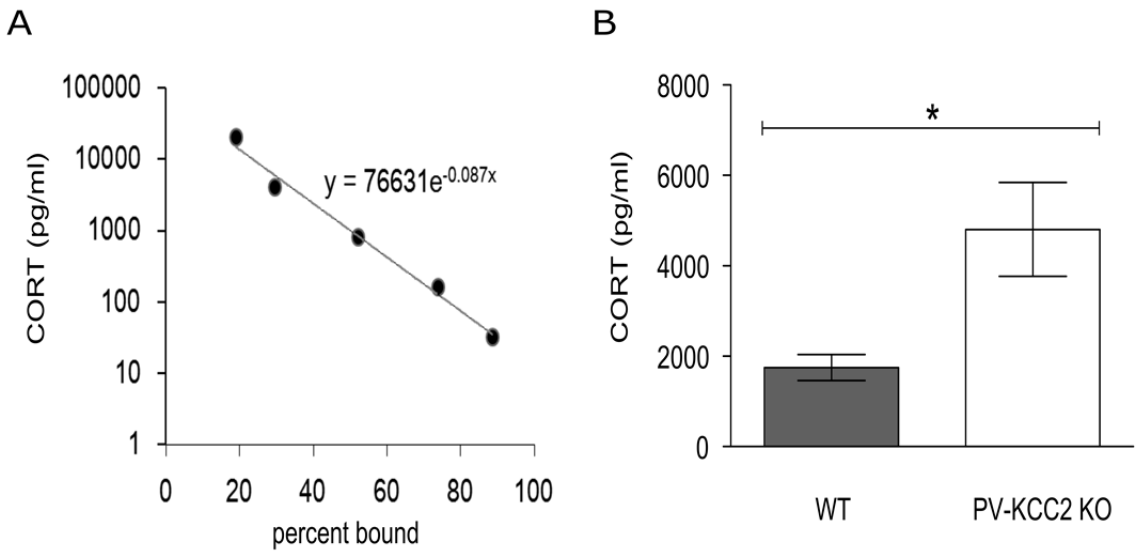

FIGURE 16: SERUM CORTICOSTERONE LEVELS. **A|** Standard curve of the corticosterone (CORT) ELISA. The exponential regression line (y= 76631*e-0.087*x) was used to calculate the CORT levels from serum samples. **B|** Serum CORT levels of WT and PV-KCC2 KO mice. KO mice showed a significant elevation of serum CORT levels at resting state (WT = 1748.1 pg/ml ± 286.4; KO = 4806.5 pg/ml ±1037.0; n=8/9; Students t-test p = 0.016).

MORPHOLOGY OF PARVALBUMINERGIC INTERNEURONS

KCC2 has been reported to interact with the cortical actin cytoskeleton and thus contributes to the cellular architecture (Chamma et al., 2012). Therefore, we addressed whether the structure of PV^+ interneurons is affected by the knockout of KCC2. tdTomato expressing PV^+ interneurons of the hippocampal CA1 region were analysed. There was no obvious difference in the shape or size of the soma (WT = 16.43 ± 0.68 µm, KO = 16.06 ± 0.70 µm, n = 22/22, students t-test p = 0.7) of PV^+ interneurons between WT and KO. The number of basal dendrites - the dendrites emerging from the soma of the cell - was analysed in the CA1. KO animals did not display an alteration of the number of basal dendrites (figure 18; WT = 4.07 ±0.11; KO = 3.92 ± 0.12; students

t-test p = 0.2; n=4/4). Due to the excessive density of PV⁺ fibres in this region the analysis of dendritic branching was not possible since most of the time dendrites could not be clearly followed up to its soma. Patching and filling of PV⁺ neurons with Lucifer yellow did not improve the visibility of single fibres.

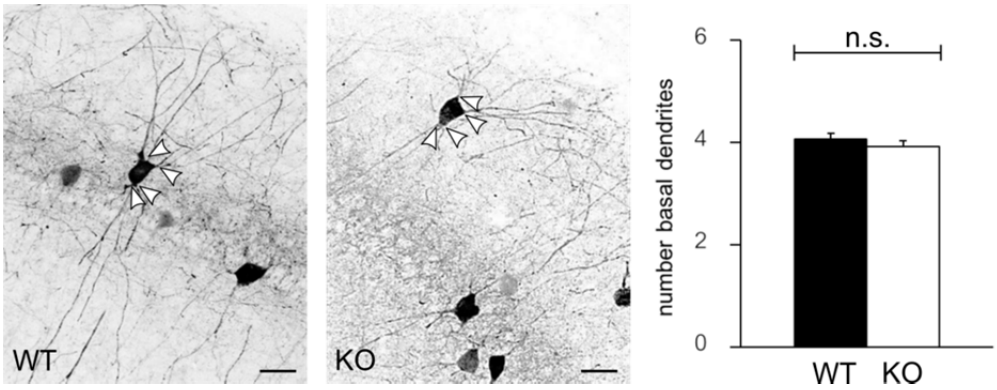

FIGURE 17: ANALYSIS OF THE MORPHOLOGY OF PV⁺ INTERNEURONS. Representative images of PV⁺ interneurons in the CA1 of hippocampus, PV⁺ interneurons of PV-KCC2 KO do not show differences in shape or size of the soma or alterations in the number of basal dendrites, shown by the white arrowheads. Bar diagram represents the number of basal dendrites per interneuron, n = 62/53, N = 4/4. Scale bar 20 µm.

LOSS OF PV⁺ INTERNEURONS

To assess whether there is a reduction in the number of the PV⁺ interneurons, brain slices were analysed at three different time points. Mice at 4 weeks of age were analysed because at this time point PV Cre expression was fully established (Lecea et al., 1995, Hippenmeyer et al., 2005) and motor deficits were not observed. At 8 weeks of age, the phenotype was fully established and most electrophysiological recordings were done at this age. At the age of 23 weeks, most of the PV-KCC2 KO mice show a very severe phenotype. Therefore, those two time points were analysed additionally.

At the age of 4 weeks no significant difference was observed in the number of PV^+ hippocampal interneurons (figure 18A; WT = 82.3 ± 4.2; HET = 79.3 ± 2.8; KO = 79.5 ± 4.5; one-way ANOVA $F = 1.32$; $p = 0.28$; n = 19/17/20, N = 4/3/4). At the age of 6 to 8 weeks, when the phenotype is fully established, a significant loss of 10-15 % of PV^+ interneurons in the hippocampus was observed for KO (WT = 87.5 ± 3.6; HET = 84.1 ± 2.9; KO = 70.8 ± 2.8; one-way ANOVA $F = 9.11$; $p = 0.0004$; n = 19/18/18; N = 4/3/3). Tukey's multiple comparison test revealed a difference between both WT and KO ($p < 0.001$) and HET and KO ($p < 0.01$), but not for HET compared to WT ($p > 0.05$). With 23 weeks of age there was a reduction of 13 % in HET and even 28 % in KO (WT = 85.4 ± 4.9; HET = 74.7 ± 3.0; KO = 60.6 ± 3.4; one-way ANOVA $F = 9.91$; $p = 0.0002$; n = 21/23/18; N = 4/4/3). Post-tests showed significant differences between WT and KO ($p < 0.001$) and HET and KO ($p < 0.05$), but not for HET compared to WT ($p > 0.05$). Statistical analysis was also performed for each genotype separately (figure 18B). The number of PV^+ interneurons did not differ between the 3 time points in WT (WT_{4weeks} = 82.3 ± 4.2; WT_{8weeks} = 87.5 ± 3.6; $WT_{23weeks}$ = 85.4 ± 4.9; ANOVA $F = 1.417$; $p = 0.25$; N = 4/4/4) and one-way ANOVA also showed no significant loss of PV^+ interneurons in HET mice over time (HET_{4weeks} = 79.3 ± 2.8; HET_{8weeks} = 84.1 ± 2.9; $HET_{23weeks}$ = 74.7; $F = 2.073$; $p = 0.14$; N = 3/3/4). For KO animals the decrease in the number of hippocampal PV^+ interneurons was confirmed (KO_{4weeks} = 79.5 ± 4.5; KO_{8weeks} 70.8± 2.8; $KO_{23weeks}$ = 60.6 ± 3.4; one-way ANOVA $F = 5.59$; $p = 0.006$: N = 4/3/3).

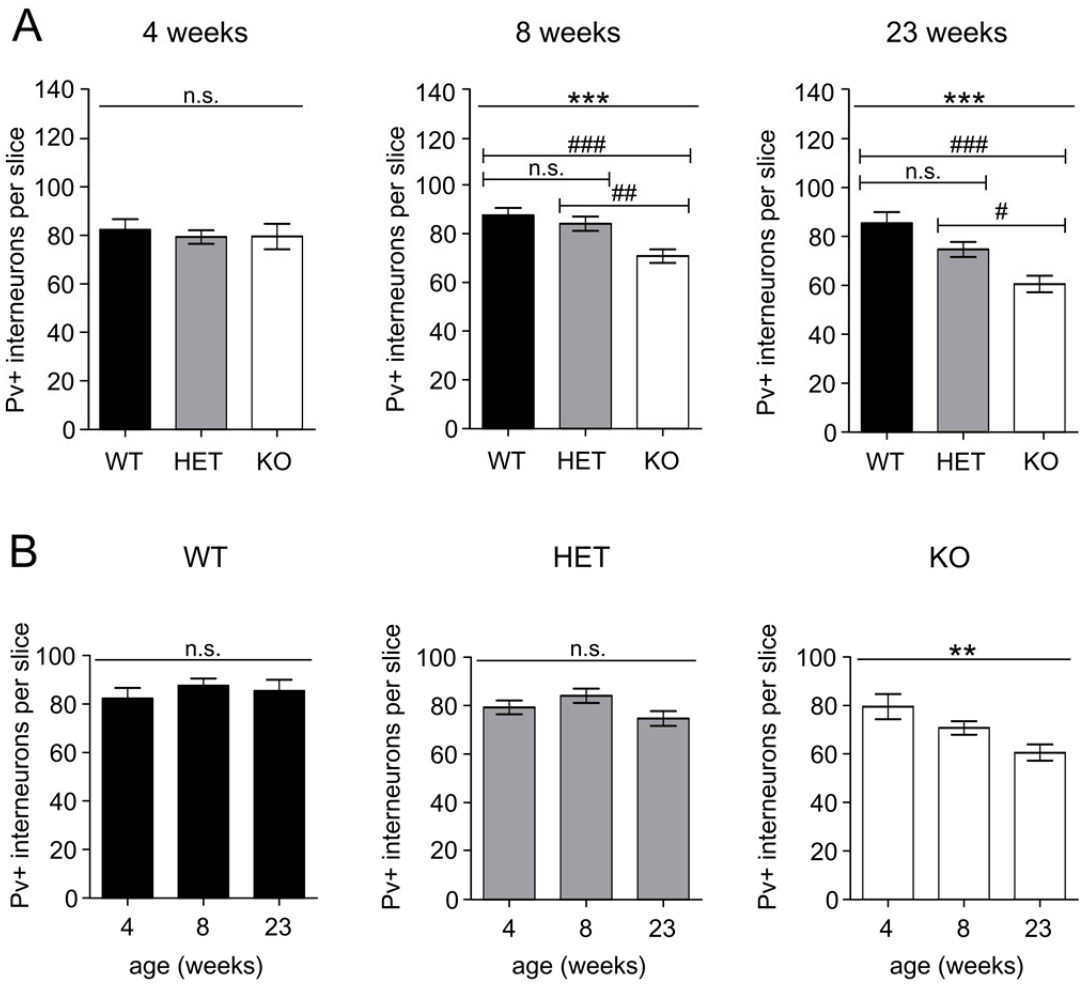

FIGURE 18: QUANTIFICATION OF PV⁺ INTERNEURONS IN THE HIPPOCAMPUS. **A|** Analysis according to age. Number of PV⁺ interneurons per slice did not differ at 4 weeks but decreased at 8 weeks of age (one-way ANOVA F = 9.11; p =0.0004). In KO mice the loss was even more pronounced at 23 weeks (one-way ANOVA F = 9.909; p = 0.0002) **B|** Analysis of the number of PV⁺ interneurons over time per genotype. WT and HET mice showed no change, a progressive reduction was detected only in KO animals (one-way ANOVA F = 5.59; p = 0.006). *one-way ANOVA, # Tukey's multiple comparison test.

The cortex was additionally analysed. However, no significant differences could be observed in the total number of PV⁺ interneurons at all 3 time points (figure 19A; 4 weeks n = 16/15/16, N = 4/3/3; 8 weeks n = 19/22/18, N = 4/4/3; 23 weeks n =

20/21/18; N = 4/4/3). Therefore, the number was analysed for different cortical layers that were defined by staining with DAPI (figure 19B). At all investigated time points the number of PV^+ interneurons did not differ in all cortical layers of WT slices. As seen in figure 20C there is no difference between genotypes in layer II-III, neither at 4 weeks (one-way ANOVA F = 0.336; p = 0.72), 8 weeks (F = 1.087; p = 0.34) nor 23 weeks (F = 1.567; p = 0.22). In layer IV the numbers of PV^+ interneurons did not change at all time points analysed (4 weeks: F = 0.4125; p = 0.66; 8 weeks: F = 0.8083; p = 0.45; 23 weeks: F = 0.1776; p = 0.84). A decrease in PV^+ interneurons was only detected in layers V-VI (figure 19C): at the age of 4 weeks the number was similar (F = 0.6073; p = 0.55), but at 8 week KO animals showed reduced numbers in layers V-VI (WT = 13.1 ± 0.6; HET = 12.2 ± 0.6; KO = 9.9 ± 0.6; one-way ANOVA F = 7.198; p = 0.002). This reduction was also present at 23 weeks (WT = 14.6 ± 1.9; HET = 13.9 ± 0.9; KO = 10.7 ± 0.5; one-way ANOVA F = 3.205; p = 0.04) but in contrast to the hippocampus there was no progression.

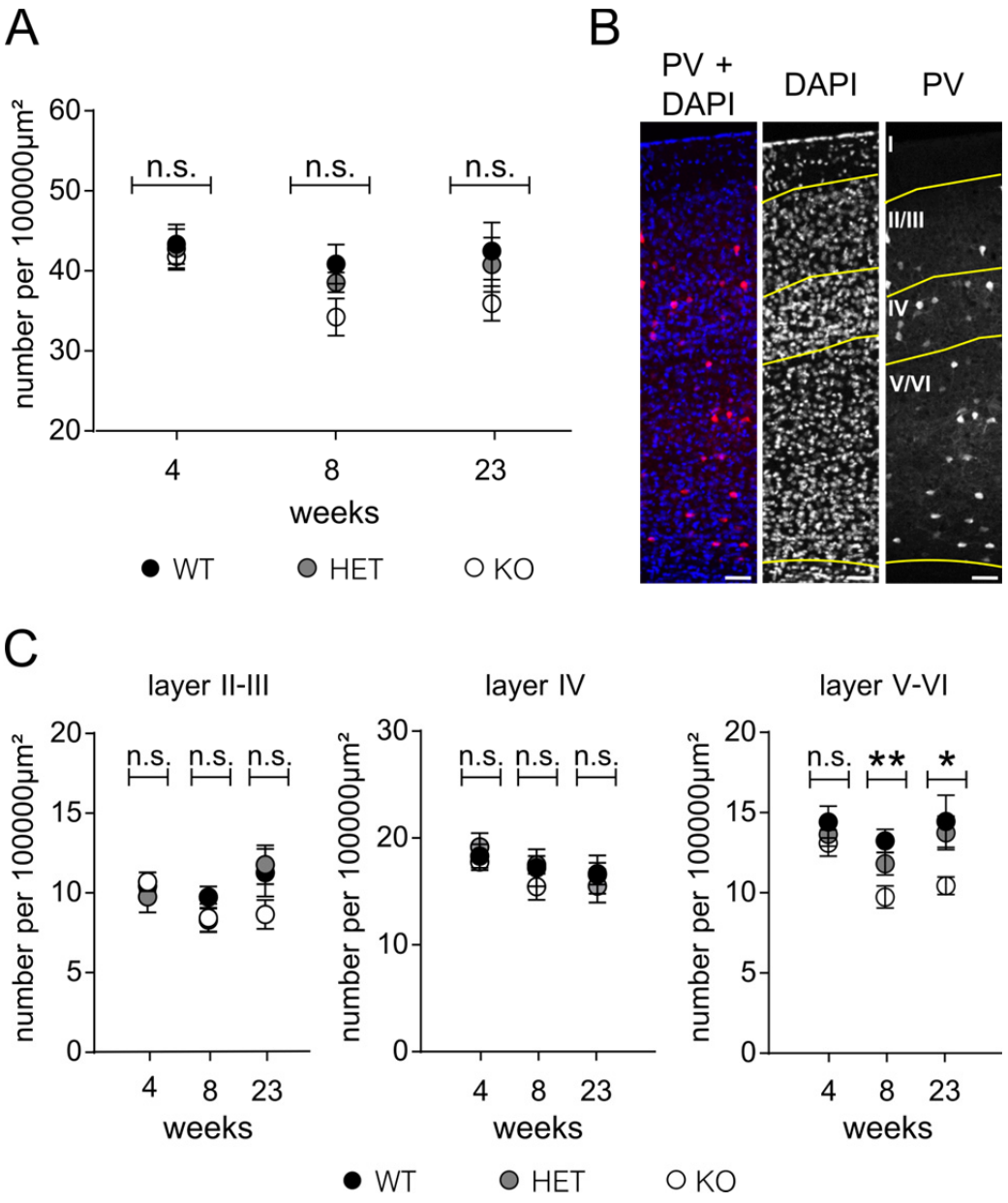

FIGURE 19: QUANTIFICATION OF PV⁺ INTERNEURONS IN THE SOMATOSENSORY CORTEX. **A|** Total number of PV⁺ interneurons per 100000 µm² was not different at all investigated time points. **B|** Representative pictures of quantification. For the layer specific analysis the channels of the pictures were split, maps of single layers were defined in the DAPI channel and transferred to the PV channel. Scale bar 50 µm. **C|** Numbers of PV⁺ interneurons in layers II-III, IV and V-VI. A reduction was detected only in layers V-VI in KO animals of 8 and 23 weeks of age; (one-way ANOVA 8weeks p = 0.0018; 23weeks p = 0.0487). In WT and HET animals, a decrease of the number of PV⁺ interneurons was not detected in all cortical layers at every time point.

EXCITABILITY

EPSP – TO – SPIKE COUPLING

To investigate the changes in excitability over time E-S coupling was recorded in acute brain slices of WT, HET and KO mice at either 8 or 23 weeks of age. The slope of the fEPSP recorded in the stratum radiatum and the amplitude of the PS recorded in the stratum pyramidale were analysed. Exemplary traces of all genotypes are shown below (figure 20A, B). In 8 week old mice (n = 14/17/17; N=4/4/4) slopes of fEPSPs increased with rising stimulus intensities and no significant differences were seen between genotypes (figure 20C; two-way ANOVA $F = 1.196$; $p = 0.31$). The amplitudes of WT and HET PS also rose similarly with ascending intensities; however, KO animals presented with smaller amplitudes than HET and WT mice (figure 20D; two way-ANOVA $F = 4.633$; $p = 0.01$). Spike generation from the EPSP was analysed by plotting the amplitudes of the population spikes in the pyramidal cell layer against the EPSP slope at the stratum radiatum of CA1. KO mice showed a decreased E-S coupling compared to WT and HET animals. In KO samples, small fEPSPs (slope 0.5 mV*ms) already lead to PS amplitudes of only half of the size of WT mice (WT = 1.8 ± 0.27 mV; HET = 1.4 ± 0.16 mV; KO = 0.97 ± 0.09 mV) and with increasing slopes of fEPSPs the reduction in PS amplitude accelerated (figure 20E; $F = 20.44$; $p < 0.0001$).

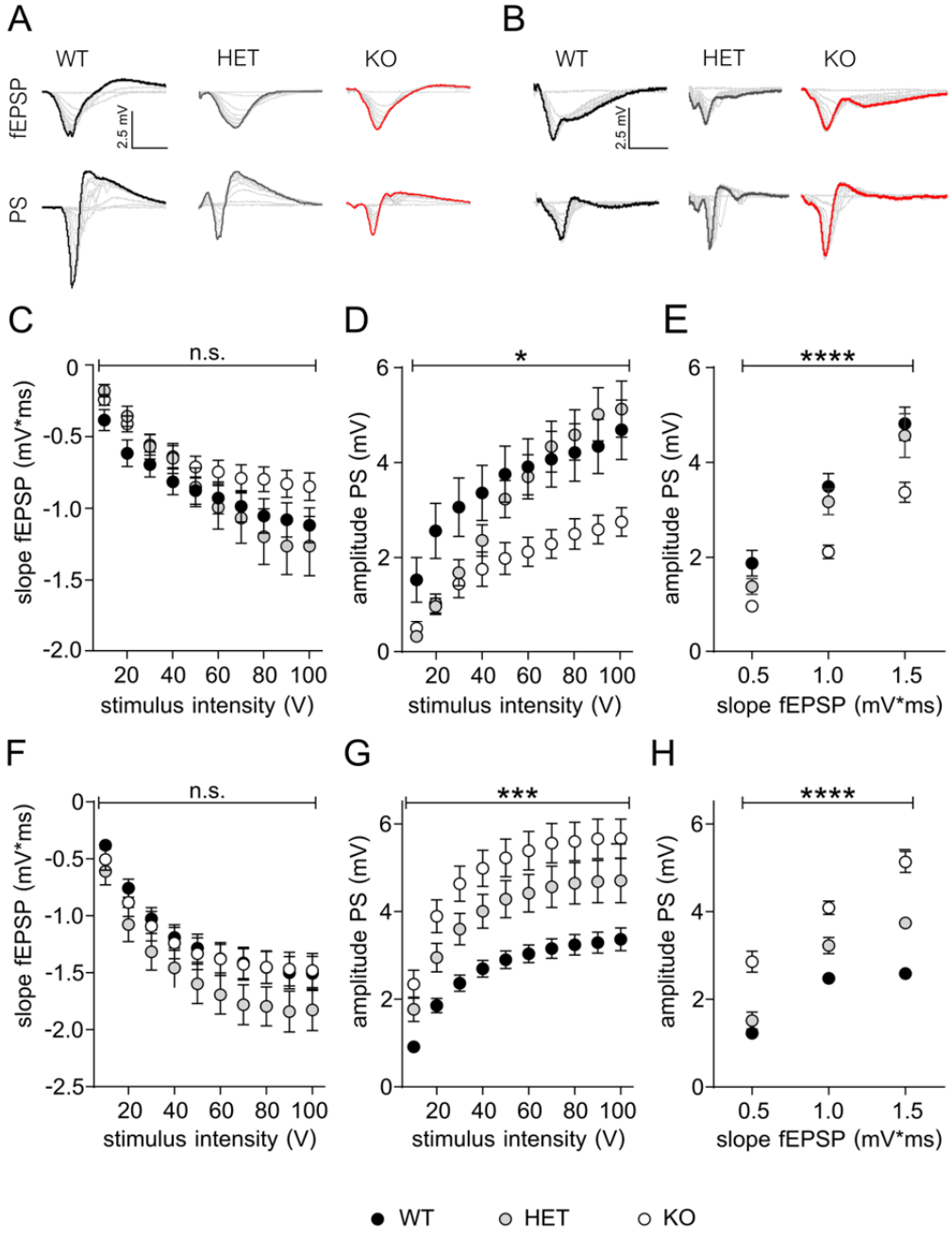

FIGURE 20: FEPSP - TO - SPIKE COUPLING (E-S COUPLING). **A|** Exemplary traces of fEPSPs and PS recorded from WT, HET and KO slices from 8 weeks old mice. **B|** Exemplary traces of fEPSPs and PS of slices from 23 weeks old mice. **C|** fEPSP slopes of slices from 8 weeks old mice **D|** PS amplitudes of 8 weeks old WT, HET and KO mice. Knockout mice showed a decrease in PS amplitude, p= 0.0002. **E|** E-S coupling at 8 weeks of age. KO animals show decreased amplitudes, $p < 0.0001$. **F|** fEPSP slopes slices from 23 weeks old mice. **G|** PS amplitudes were increased in HET and KO animals at 23 weeks of age, $p = 0.0002$. **H|** E-S coupling of 23 weeks old mice revealed an increase of PS amplitudes in HET and KO, $p < 0.0001$.

At the age of 23 weeks (n = 24/24/34, N=5/5/5) the same experimental procedure lead to a very different result. Slopes of extracellular fEPSPs were still similar in all genotypes (figure 20F; two-way ANOVA F = 1.470; p = 0.24) and comparable to fEPSPs recorded from young animals. At all stimulus intensities analysed, the PS amplitudes of 23 weeks old KO mice were increased compared to WT and HET (figure 20G; two-way ANOVA F = 9.604; p = 0.0002) in contrast to the recordings in 8 weeks old mice. If PS amplitudes were plotted against fEPSP slopes the upward shift of PS–EPSP curve in both HET and KO group was striking demonstrating an enhanced EPSP to spike (E–S) coupling. The increase of E-S coupling in HET and KO could be statistically confirmed (figure 20H; two-way ANOVA F = 66.43; p < 0.0001).

SEIZURE SUSCEPTIBILITY

To assess the *in vivo* consequences of KCC2 loss in PV^+ neurons on seizure susceptibility seizures were induced with pentylenetetrazole (PTZ) in 23 weeks old mice (N = 4/4/4). After injection, the mice were videotaped. Analysis of the time from the injection until start of the different seizure states revealed a significant difference between genotypes (figure 21).

Myoclonic jerks of KO mice started 93.0 ± 12.2 s after PTZ injection and therefore the latency was more than doubled compared to WT animals (WT = 38.3 ± 3.8 s; HET = 48.3 ± 6.4 s). PV-KCC2 KO animals displayed a delay not only in the onset of myoclonic jerks, but also a significant delay for clonic and tonic-clonic phases of seizures could be observed (two way ANOVA F = 12.21; p = 0.005).

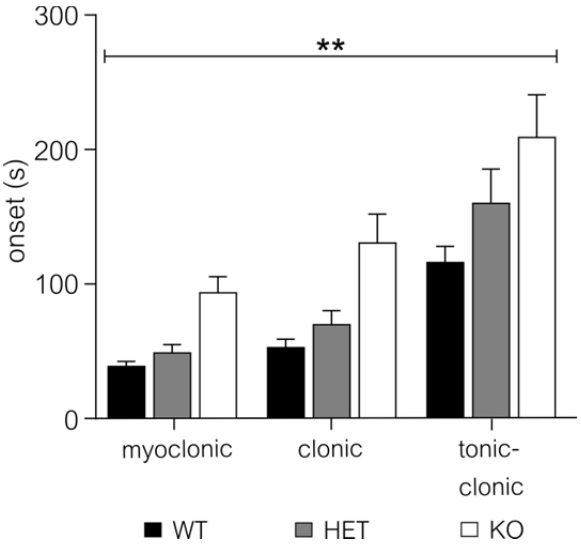

FIGURE 21: SEIZURE SUSCEPTIBILITY.

PTZ injections induced epileptic seizures in all mice, but PV-KCC2 knockout animals displayed a significant delay in onset of all seizure phases (two-way ANOVA $F = 12.21$; $p = 0.005$; N = 4/4/4).

DISCUSSION

Brain activity is a functional interplay of excitatory and inhibitory neurons and neuroglial cells. One prerequisite for a proper neuronal function is the homeostasis of intra- and extracellular ion concentrations. To establish a fine tuned inhibition and information processing, Cl^- homeostasis is essential (Blaesse et al., 2009, Buzsaki et al., 2007, Kaila et al., 2014a, Kaila et al., 2014b, Payne et al., 2003). In this study, the effects of KCC2-loss in a specific subset of neurons - namely PV^+-interneurons - were characterised. The discussion of the results consists of three parts, one part deals with general observations, learning and memory, the second section focusses on electrophysiological changes and the third part addresses the epileptic phenotype of the conditional knockout mice.

PHENOTYPICAL CHARACTERISATION

In the investigated mouse model, the KCC2 protein was deleted in PV^+ cells only. These GABAergic neurons account for 10-20 % of the neuron population (Freund and Buzsaki, 1996) and represent the largest interneuron subpopulation (Desiderato et al., 1966, Riccio et al., 1992). In the hippocampal area CA1 11 % of neurons are GABAergic, and 24 % of those are PV^+; thus, PV^+ interneurons represent only 2.6% of the total neuronal population (MacKenzie and Maguire, 2015).

Homozygous PV-KCC2 KO mice present with a decreased life span and an impaired motor function, which was not observed in HET animals. This suggests that 50 % of the KCC2 protein does not severely interfere with the function of inhibitory neurons.

Because of the widespread distribution of PV^+ neurons in nearly all areas of the brain (Lissek, 2012), the specific cause for the general phenotype like shortened life span, reduced body weight and motor impairment is difficult to assess.

Functional alterations or a change in the number of PV^+ interneurons were reported to be associated with a broad spectrum of both psychiatric and movement disorders (Cheah et al., 2012, Marín, 2012, Kalanithi et al., 2005, Gernert et al., 2000). Since GABA is the major inhibitory neurotransmitter in basal ganglia, where GABAergic pathways mostly dominate information processing, abnormalities of GABAergic transmission are key elements in pathophysiologic models of movement disorders (Kelso et al., 1986). Basal ganglia include the striatum, globus pallidus, substantia nigra and subthalamic nucleus. The most abundant neuronal cell type in the striatum are GABAergic medium spiny neurons. These striatal neurons receive inputs from the cerebral cortex, thalamus and several classes of local interneurons (Malinow and Miller, 1986). A reduction of PV^+ interneurons in the striatum leads to a reduced activity of basal ganglia – by reduced inhibition and the consequent activation of striatal GABAergic projection neurons - and thereby causes idiopathic dyskinesia with paroxysmal dystonia (Fanselow, 1980).

The loss of PV^+ striatal interneurons in the striatum was also reported to contribute to dystonia in patients with Huntington's disease (HD) (Bliss and Collingridge, 1993). Mice expressing human mutant superoxide dismutase (SOD)1, representing a widely investigated model of the familial form of the neurodegenerative disease amyotrophic lateral sclerosis (ALS), show an increase of PV^+ cortical interneurons in the motor and

somatosensory areas of the cortex compared to wild-type littermates (Lissek et al., 2013).

The motor phenotype of our KO mice could also arise from disturbed inhibition of motor neurons that establish the information transfer from the motor cortex via the spinal cord to the skeletal muscles. In motor neurons, located in the primary motor cortex or anterior grey column of the spinal cord, less inhibition can lead to a rapid series of action potentials and therefore tetanic contractions of downstream muscle fibres.

Proprioceptive afferents of type Ia also express PV (Celio, 1990, Sonner et al., 2017). These primary sensory fibres are sensitive to muscle length and speed of muscle lengthening (Tresilian, 2012), and are possibly affected by the KCC2 knockout in our mouse model. Type Ia afferents from the muscle spindle terminate on proximal dendrites of α-motor neurons (Jones, 2011) and can thereby stimulate the contraction of innervated muscles. If the inhibition is disturbed in type Ia fibres due to an increased Cl^- concentration, the targeted α-motor neurons may get hyper-activated, which may lead to spasticity of the downstream muscle fibres. This was already discussed for K^+-Cl^--cotransporter 3 (KCC3) knockout in PV^+ neurons, a mouse model with a similar motor phenotype. Ding and Delpire deleted KCC3 in different neuronal populations with subtype specific Cre lines and identified the PV^+ cells as phenotype causing neuron subtype (Ding and Delpire, 2014).

Mice with depletion or loss of Ia axons have been reported to develop abnormal, athetotic movements when walking (Brandalise et al., 2016, Kim et al., 2015). Therefore, the motor phenotype observed in our mice probably may result from

disruption of KCC2 in proprioceptive DRG neurons, which should be confirmed in further studies. A cerebellar contribution to the locomotor phenotype is less likely since specific KCC2 knockout in granule cells (GCs) or PV^+ Purkinje cells (PCs), the two main target cell types of synaptic inhibition in the cerebellum, did not elicit motoric deficits (Seja et al., 2012).

A possible explanation for the smaller statue of KO mice might be linked to the pituitary gland and its role in growth hormone regulation. The pituitary gland is part of the hypothalamic pituitary adrenal (HPA) axis, the major mediator of endocrine responses to stress (Aguilera, 2012). Stimulation of a specific group of neurons located in the dorsomedial parvocellular subdivision of the paraventricular nucleus (PVN) of the hypothalamus induces secretion of the hypothalamic peptide corticotropin-releasing hormone (CRH) and, to a lesser extent, vasopressin (VP). CRH and VP are released into the pituitary portal circulation and stimulate corticotropic cells in the anterior pituitary gland. These cells then release adrenocorticotropic hormone (ACTH) into the peripheral circulation. The release of ACTH stimulates cells of the adrenal cortex to produce and secrete glucocorticoids, which are essential for the metabolic adaptation to stress (Aguilera, 1994, Antoni, 1986, Aguilera, 2012).

As discussed previously the HPA axis is subject to GABAergic inhibitory control from the prefrontal cortex and ventral hippocampus (Luscher et al., 2011). Prolonged activation of the HPA axis leads to suppression of growth hormone (GH) and inhibition of insulin-like growth factor-1 (IGF-1) effects on target tissues (Bailey et al., 2013). The impairment of normal growth and weight development in KO animals is obvious. Weight differs significantly around two months after birth, when Cre expression has

reached a plateau and the knockout of KCC2 in PV^+ interneurons is fully established. This suggests that the altered chloride levels in affected interneurons and the consequently disturbed GABAergic inhibition may lead to malfunction of the HPA axis and thus results in disturbed levels of GH and growth retardation.

It has already been reported that extreme stress can affect growth in humans e.g. suffering from Kaspar Hauser syndrome. This syndrome is also called psychosocial dwarfism (PD) and associated with severe childhood or adolescent short stature and/or delayed puberty due to emotional deprivation or stress. They present with apparent idiopathic hypopituitarism, unusual behaviour and a stressful home environment (Skuse et al., 1996). The underlying mechanism for the growth retardation in these patients seems to be an altered hypothalamic growth hormone-releasing hormone (GHRH) secretion that is controlled by CRH neurons via direct synaptic mechanisms (Peroski et al., 2016). This circuitry additionally plays a major role in anxiety and affective behaviour. A comparable mechanism could lead to the reduced weight and size of PV-KCC2 KO mice.

To address the HPA axis function in our mouse model, corticosterone levels were determined from plasma of WT and KO mice. KO mice had increased serum corticosterone levels compared to WT animals (figure 17), suggesting an activation of the HPA axis.

The fear conditioning data (figure 13 and 14) are consistent with increased stress levels in KO mice. During the acquisition at day one, animals of all genotypes showed a similar behaviour in the first 60 s, moving around to explore the new environment.

The mice had in total 3 min prior to tone administration to adapt to the experimental setup. During the second and third minute KO animals already showed an increased freezing time although there were no cues presented. In all following trials KO mice presented with higher freezing levels compared to WT and HET. Key players in the generation of fear and the so called fight-or-flight response are the amygdaloid complex and the associated pathways like the superior colliculus (SC) – parabigeminal nucleus (PBGN) pathway that triggers fear response (Shang et al., 2015, Steimer, 2002). Since PV^+ interneurons display one of the biggest interneuron populations in the basolateral amygdaloid nucleus (BLA) (McDonald and Mascagni, 2001, Bocchio et al., 2015), they play an important role in controlling emotional behaviour by regulating the activity of principal neurons (Wolff et al., 2014, Povysheva et al., 2006). They are thought to be involved in the control of fear by targeting the perisomatic region of principal neurons (Bienvenu et al., 2012), inhibiting and synchronizing their firing (Popescu and Paré, 2011, Wolff et al., 2014). Although PV^+ interneurons are rare in the central nucleus of amygdala (CeA) (Zahm et al., 2003), their function in the central nucleus of amygdala has been shown to be related to anxiety-like behaviour (Wang et al., 2016, Ravenelle et al., 2014).

This susceptibility to fear induction might result from the overactivation of excitatory PV^+ projection neurons of the superior colliculus (SC) which are essential for detecting looming objects and triggering fear responses (Shang et al., 2015). These glutamatergic PV^+ projection neurons of the superficial SC project to different brain areas, including the parabigeminal nucleus (PBGN), an area connected to the amygdala. Activation of the PV^+ SC-PBGN pathway triggers fear responses, induces

conditioned aversion, and causes depression-related behaviours. Approximately 20% of mice subjected to the fear-conditioning paradigm during the studies of Shang et al. developed a generalised fear memory. Immunohistochemistry confirmed that the PV^+ neurons of the superficial SC are indeed affected by cell-specific KCC2 knock out (figure 15). This observation suggests a role of these glutamatergic PV^+ neurons in the formation of the anxiety phenotype, in addition to the alterations of the GABAergic system and the disturbed HPA axis.

During fear conditioning proper function of two major brain areas is essential, the amygdala for regulation of fear (Phillips and LeDoux, 1992, Phillips and LeDoux, 1994) and the hippocampus for the learning of the context in which a fearful event takes place (Phillips and LeDoux, 1992, Phillips and LeDoux, 1994). The hippocampus processes the context (shape, smell, colour, light of the box) and connects it to the aversive foot shock. The information of the foot shock is transmitted via the somatosensory cortex and thalamus to the lateral (LA) and central nucleus (CeA) of the amygdala. The information about the tone passes the auditory thalamus and the auditory cortex and is further relayed to the LA and is then integrated. A simultaneous interaction of both shock and tone induces neuronal plasticity in the LA and forms a link between tone and shock. The information is transmitted to the CeA which initiates vegetative processes like alterations in blood pressure and heart rate or the release of stress hormones (Medina et al., 2002).

Neither the memory of the cue nor the memory of the context lead to an altered freezing reaction, hence the memory assessed by fear conditioning did not appear to be affected in KO mice. In figure 14 the increase in freezing time (Δt_f) after tone

administration in a new environment illustrated a similar behaviour in all genotypes. Twenty-four hours after training, when placed in a novel testing context, KO mice exhibited higher freezing rates than WT and HET mice (Pre-CS in testing, Figure 14). In other words, in KO mice the foot shock additionally induced conditioned fear to stimuli not associated with the aversive event, in this case a new environment. This generalisation phenomenon is defined by freezing when no acoustic CS is presented and outside of the conditioning context (Riccio et al., 1992, Desiderato et al., 1966, Fanselow, 1980). Fear generalisation engages similar neurocircuitries than implicated in the acquisition, expression and regulation of conditioned fear like the hippocampus and the amygdala (Lissek, 2012, Lissek et al., 2013, Dymond et al., 2015), but the precise role of the amygdala, hippocampal complex, medial prefrontal cortex, and other regions in mediating fear generalisation versus inhibition in humans requires further investigation.

Other studies that focussed on the impact of KCC2 loss on learning, memory consolidation or mobility support this hypothesis. No difference could be observed between WT and HET in the Open field test with our mouse model. KO mice were excluded from the study because of the strong motor phenotype (Herrmann, 2015). In another study, Tornberg et al estimated exploratory activity and working memory of hypomorphic KCC2 mice by open field and Y-maze test. Such hypomorphic mice express 15–20 % of normal KCC2 protein levels in the CNS and show no impairment in working memory or exploration behaviour. Rearing activity of the $KCC2^{hy/null}$ mice did not habituate in contrast to WT mice, consistent with an increased anxiety. They confirmed the enhanced anxiety-like behaviour in the elevated plus-maze, where the

KCC2$^{hy/null}$ mice avoided entering the open arms almost completely (Tornberg et al., 2005). Spatial learning and memory were tested for both of these mouse models and consistently found impairments during that learning task using the water maze. Since spatial navigation and consolidation of memory requires the function of the hippocampus, the performance of hypomorphic KCC2 or PV$^+$-KCC2 knock out mice suggests a possible role for KCC2 in hippocampal learning. That hippocampal learning is affected in PV$^+$-KCC2 mice seems reasonable, since the affected PV$^+$ interneurons display around 20 % of GABAergic neurons and thereby represent the biggest subpopulation of inhibitory neurons of the hippocampus. The increased Cl^- concentration in PV$^+$ interneurons might result in depolarising GABA action and thereby to increased GABA release and inhibition of downstream pyramidal cells. This could cause deficits in the synchronisation of the neurons that are required for a proper consolidation or storage of a new memory.

ELECTROPHYSIOLOGICAL CHARACTERISATION

Because of the observed differences in spatial memory, LTP was recorded in the hippocampus. After brief tetanic stimulation of Schaffer collaterals a sustained increase in synaptic transmission can be observed, which is referred to as long-term potentiation (LTP), representing the most widely studied correlate of memory (Bliss and Collingridge, 1993). The potentiation created in the dendritic layer represents the mostly excitatory answer of the pyramidal dendrites to the stimulus applied to the Schaffer collaterals. The interneurons, especially the PV$^+$ interneurons, mainly project to the somata of pyramidal neurons located in the str. pyramidale. Therefore, it is not

surprising that the potentiation is not affected in the str. radiatum but decreased in the str. pyramidale of KO mice (figure 13).

In our mouse model, only PV^+ interneurons are affected by targeted KCC2 deletion and hence possibly changes in intracellular Cl^- concentration (Pellegrino et al., 2011, Rivera et al., 1999, Rivera et al., 2004). The measurement of intracellular Cl^- concentration is still ongoing. Previous experiments by perforated patch clamp recordings with gramicidin did not show a difference of the Cl^- reversal potentials (data not shown). Since gramicidin patch clamp recordings do not allow an efficient control over opening of the patch under the pipette, these results are uncertain. Recordings of the somato-dendritic Cl^- gradient are planned and the experimental settings of the uncaging setup are currently established.

An altered Cl^- concentration can lead to a weaker efflux or even influx of Cl^- and thereby change the answer of neurons to GABA from inhibitory to excitatory (Hübner et al., 2001a, Jentsch et al., 2004, Stein et al., 2004, Rivera et al., 1999, Nardou et al., 2011). In PV^+ neurons this would lead to an increase of GABA release onto downstream pyramidal cells and increased inhibition. The elevated GABA release can enhance the hyperpolarising current in the postsynaptic pyramidal cell during the conditioning high frequency stimulus, which can block LTP induction (Malinow and Miller, 1986, Kelso et al., 1986).

After tetanic stimulation the normal increase in the postsynaptic response is related to (i) presynaptic modifications that increase the amount of L-glutamate released per stimulus (ii) postsynaptic modifications like alterations in number or functional

characteristics of receptors, (iii) an extrasynaptic change, such as neurotransmitter uptake of glia cells, and (iiii) morphological modifications (Bliss and Collingridge, 1993). In our mouse model, KCC2 is only disrupted in PV^+ neurons, so the excitatory presynaptic function of principal neurons should be intact. Still the increased GABA release by PV^+ interneurons could affect the postsynaptic pyramidal neuron. The increased amount of GABA at the postsynapse might result in a smaller depolarisation and consequently missing reduction of the Mg^{2+} block from NMDA receptors, whose activation and NMDA receptor-dependent rise in postsynaptic Ca^{2+} are critical in LTP induction (Davies et al., 1991, Collingridge et al., 1988, Brandalise et al., 2016, Mulkey and Malenka, 1992). Since the GABAergic PV^+ neurons mainly target the somata and axon initial segments of pyramidal cells (Cobb et al., 1995), the differences are restricted to the str. pyramidale. The dendritic signal transduction seems to work properly, since no differences could be detected in the str. radiatum.

For memory formation and consolidation, a proper integration of spatial, contextual, and emotional information is necessary. In the hippocampus, this is done by the pyramidal cells that transmit the hippocampal output to various targets throughout the brain. The recorded signals in the str. pyramidale define the ouput of the hippocampal formation. Pyramidal cells in the CA1 and subiculum regions convey this output by firing action potentials after summation of all excitatory and inhibitory inputs. This summation takes place in the cell body of pyramidal neurons. Hence, the decrease of recorded amplitudes in the stratum pyramidale of KO slices might be a hint for an impaired memory function in PV^+-KCC2 KO mice. The impaired spatial learning in HET

KCC2 knockout mice during water maze is in agreement with this result (Herrmann, 2015).

To further characterise the impact of the modulation of PV^+ neurons several electrophysiological recordings were performed. Field potential and patch clamp recordings all point to an increased inhibition in PV^+-KCC2 KO mice. As mentioned in the introduction the field potential recordings of Ralf Dittmann showed a decreased *Paired-Pulse* Ratio (PPR) in the hippocampus and the cortex of KO mice. These results indicate a reduced transmitter release and therefore an increased inhibition of presynaptic neurons in KO mice (O'Donovan and Rinzel, 1997). The so-called paired-pulse depression (PPR<1) depends on both previous release and the residual Ca^{2+} concentration in the presynaptic terminal and can further be influenced by postsynaptic modifications of AMPA receptors. The altered Cl^- concentration in the PV^+ interneurons leads to a switch from an inhibitory to an excitatory GABA response in these interneurons (Rivera et al., 1999, Hübner et al., 2001b, Stein et al., 2004, Nardou et al., 2011) and consequently to an enhanced GABA release onto downstream pyramidal cells. This suggests an increased inhibition of pyramidal cells and could explain the smaller field potential amplitudes of the second pulse. The frequency of the network dependent inhibitory postsynaptic currents (sIPSCs) of pyramidal cells was shown to be increased in cortex and hippocampus in previous experiments in our lab (data not published), which is in agreement with the hypothesis of hyperactive PV^+ interneurons and increased inhibition.

To verify these results field potentials were recorded simultaneously from the str. radiatum and pyramidale and the fEPSP-to-spike coupling calculated. This allows a

statement on the information integration process. The conversion of EPSPs into action potentials is a fundamental property determining the coding of information in pyramidal cells (Konig et al., 1996). The recordings in the hippocampus of 8-10 weeks old mice showed no differences in fEPSP slope between genotypes but decreased population spike amplitudes in KO slices (figure 20C, D). When the simultaneously recorded values of fEPSP slope and PS amplitude were grouped and plotted against each other, the recordings from KO slices revealed an impaired EPSP-to-spike coupling (figure 20E). In KO animals, the same amount of EPSPs - generated in the dendrites of hippocampal pyramidal cells - created smaller population spike amplitudes, suggesting that enhanced inhibition occurs at perisomatic regions of pyramidal cells.

As mentioned before, the investigated mouse model shows spontaneous seizures and premature death at around 23 weeks of age. To identify the underlying cause for the disturbed excitation/inhibition balance, the numbers of PV^+ interneurons in hippocampus and cortex were quantified and their morphology examined. The quantification showed a progressive loss of PV^+ interneurons in the hippocampus and a small reduction in layer V-VI in the cortex of KO mice (figure 19). The result, which will be discussed in detail later, lead to the recording of EPSP-to-spike coupling in 21 weeks old mice. The fEPSP slopes recorded in str. radiatum displayed no significant differences between genotypes (20F), like already seen in the young cohort. The associated population spike amplitudes increased in HET and KO mice and the correlation showed an amplified EPSP-to-spike coupling (figure 20G, H). Therefore, in HET and KO animals the same amount of EPSPs generated in the dendrites of hippocampal pyramidal cells creates bigger spike amplitudes. This suggests that the

former enhanced inhibition at perisomatic regions of pyramidal cells is diminished at the age of 23 weeks. The reduction of inhibition in the hippocampus can be explained by the smaller amount of PV^+ interneurons at that age but it is also possible that the spontaneous seizures observed in KO mice lead to a progressive loss of interneurons. To date it is not clear, whether the reduction in the number of PV^+ interneurons is the cause or the consequence of the seizure phenotype. The decrease could be caused by the enhanced activity which can lead to excitotoxicity, a type of neurotoxicity mediated by NMDARs and calcium ions, well studied for excitatory cells (Choi, 1985, Choi, 1987, Rubio-Casillas and Fernandez-Guasti, 2016, Lehmann and Jacobson, 1990).

It has been proposed that excitotoxicity is caused by an excessive stimulation of neuronal excitation and that any source of excitation is potentially harmful (Lai et al., 2014). Moreover, the initial calcium influx mediated by NMDARs following excitotoxic glutamate stimulation is known to trigger a secondary intracellular calcium overload, which correlates with neuronal death (Randall and Thayer, 1992, Tymianski et al., 1993). Since the increased activation of PV^+ interneurons likely relies on the Cl^- accumulation by deletion of KCC2 in these interneurons, the involvement of NMDARs is not likely in our mouse model.

Conditions like acute (Yuen et al., 2009, Yuen et al., 2011) or chronic stress (Popoli et al., 2012) or seizure activity can lead to enhanced glutamate levels. This may trigger excitotoxicity in PV^+ interneurons by activating NMDARs. The already ‘overactive state’ could contribute to an intracellular calcium overload resulting in neuronal death. Alternatively, the loss of PV^+ interneurons could result from recurrent seizures. Many publications in rodents (Kobayashi and Buckmaster, 2003, Dinocourt et al., 2003, Sayin

et al., 2003, Huusko et al., 2015) and humans (de Lanerolle et al., 1989, Tóth et al., 2010, Arellano et al., 2004, Zhu et al., 1997, Maglóczky and Freund, 2005, Maglóczky et al., 2000) have shown a reduction of GABAergic interneurons after epileptic seizures. This may result in insufficient GABA release and consequently a disinhibition of principal cells, which could promote the spread of seizure activity.

Previous studies reported that a decreased number of GABAergic neurons reduces functional inhibition and increases excitability of principal neurons in the hippocampus of aged mice and that PV^+ interneurons are more vulnerable to acute seizure activity than other interneuron subtypes (Weiss et al., 1990, Kuruba et al., 2011). This increased susceptibility might be explained by the extraordinary high energy expenditure of this neuronal subtype, which is able to generate fast series of action potentials and thus gamma oscillations (30–100 Hz) (Kann et al., 2014). Increased spiking rates during seizures can enhance oxygen and nutrient consumption and could lead to depletion of cellular energy substrates and ATP. Energy consuming processes include the release and metabolism of GABA, the restoration of membrane ion gradients and Ca^{2+}-removal. As Kann et al discussed in detail, fast-spiking interneurons have unique electrophysiological and neuroenergetical properties that are different from principal cells or other interneuron subtypes and utilize much more energy than other cortical neurons. This might render them highly vulnerable to conditions of metabolic stress (Kann, 2016, Kann et al., 2014). In our mouse model a selective loss of PV^+ neurons was found only in infragranular layer V and VI of the somatosensory cortex. These layers are composed predominantly of larger pyramidal cells that give rise to the major output pathways of the cortex, projecting to other cortical areas and to

subcortical structures (Kandel and Mack, 2014). The local PV^+ interneurons are mostly basket cells, whose axons densely target the perisomatic compartments of principle neurons (Xiang et al., 2002). They regulate the information processing of these major output pathways of cortical layers V and VI (Naka and Adesnik, 2016, Briggs, 2010), which might require a higher activity compared to other cortical layers and therefore increases their sensitivity to stress.

During recurrent seizures, increased activation of PV^+ interneurons might result in cytosolic and mitochondrial Ca^{2+}-overload that would also enhance the generation of ROS and NO (Eyles et al., Kovacs et al., 2005, Kovacs et al., 2002, Malinska et al., 2010). Enhanced ROS generation combined with alterations of anti-oxidative mechanisms may cause higher levels of oxidative stress in fast-spiking interneurons as compared to other neuron subtypes, which might lead to damage of DNA and functional proteins, such as enzymes and ion channels (Behrens et al., 2007, Kann and Kovacs, 2007, Steullet et al., 2010). In our mouse model PV^+, interneurons are hyper-activated as effect of the GABA mediated excitation. Therefore, the described mechanism of Ca^{2+}-overload and increased oxidative stress may aplly to this interneuron subtype prior to occurrence of seizures. This could explain the progressive reduction of PV+ interneurons in the hippocampus and the cortex.

Another possibility that has to be considered is, that reduction of PV^+ neurons cannot only be a result of neuron loss but also due to a reduction of the PV protein expression. Several publications indicate that seizure activity causes loss of PV immunoreactivity but not neuron loss (Sloviter, 1989, Scotti et al., 1997, Wittner et al., 2005, Wittner et al., 2001). Results from studies on PV-deficient mice show that low levels of

parvalbumin in the axon terminals correlate with increased GABA release indicating that PV modulates Ca^{2+}-dependent GABA neurotransmission (Vreugdenhil et al., 2003). A reason for the loss of PV-like immunoreactivity from some of these cells could be the transient stop of PV synthesis, or a conformational change induced by Ca^{2+}-overload of PV (Johansen et al., 1990, Scotti et al., 1997). To rule out this possibility, further studies should include the quantification of the total number of GABA immunoreactive neurons. More importantly, the quantification should be repeated with the PV-tomato-KCC2 mouse strain. The PV^+ neurons remain tdTomato labelled even when PV expression is reduced and quantification of tomato positive cells should allow a reliable statement if there is indeed a reduction of PV^+ interneurons in PV-KCC2 KO mice.

EPILEPSY

The spontaneous seizures and the early death of KO animals are the most striking phenotype of this mouse model. So far, three influencing factors have to be considered (figure 22): (I) stress, (II) loss of PV^+ interneurons and (III) depolarising GABA actions.

The enhanced corticosterone levels and anxiety-like behaviour are reported to fuel epileptic seizures (Joëls, 2009, MacKenzie and Maguire, 2015, Maguire and Salpekar, 2013, O'Toole et al., 2014). Stress has been associated with altered GABAergic inhibition (Holm et al., 2011, Serra et al., 2008), decreased neurosteroid modulation (Dong et al., 2001) and induction of hippocampal damage/remodelling (McEwen, 1999, Mirescu and Gould, 2006, Fuchs et al., 2006) which may contribute to network hyperexcitability. Furthermore corticosterone, which was elevated in PV^+-KCC2

knockout mice (figure15), has been reported to increase seizure susceptibility to kainate-induced seizures and kindling (Kling et al., 1993, Karst et al., 1999, Roberts and Keith, 1994, Kumar et al., 2007). Another interesting effect of long-term glucocorticoid exposure is the reduction of cell number in the hippocampus by suppression of adult neurogenesis or loss of cells (Mizoguchi et al., 1992, Sapolsky et al., 1985, Stein-Behrens et al., 1994, Paizanis et al., 2007).

Moreover, PV^+ interneurons can be affected by stress induced cell death (Czeh et al., 2005, Hu et al., 2010), what might contribute to network dysfunction and hyperexcitability (figure 22).

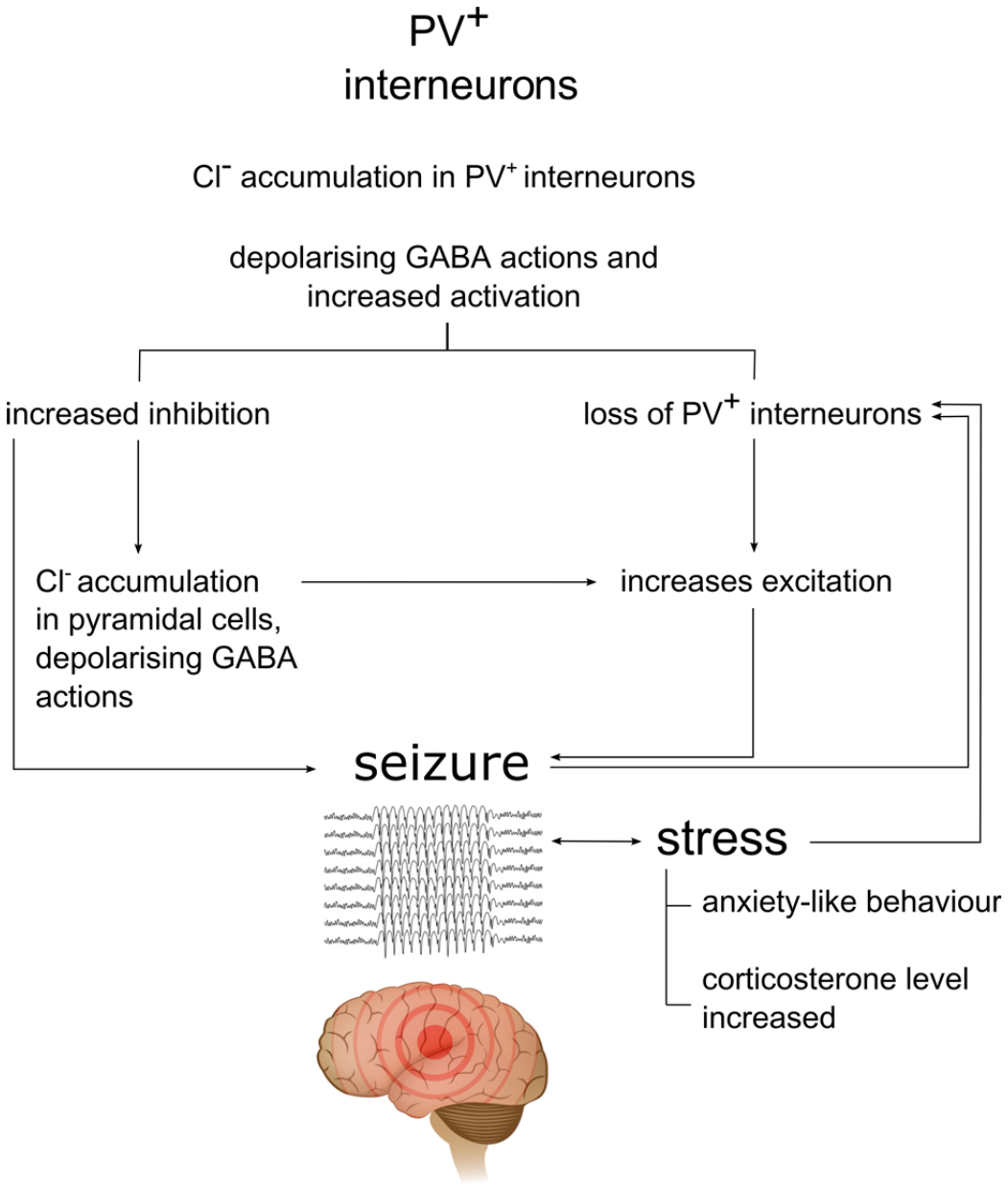

FIGURE 22: FACTORS INVOLVED IN SEIZURE GENERATION.

KCC2 knock out in PV^+ interneurons causes Cl^- accumulation and depolarising GABA actions in PV^+ interneurons. Therefore, inhibition onto pyramidal cells increases and the permanent increased activity could lead to the death of PV^+ neurons. Loss of PV^+ interneurons could increase excitation and seizure susceptibility. Increased inhibition could synchronise many brain areas or lead to Cl^- accumulation in downstream pyramidal cells and thereby trigger seizures. Moreover, the increased anxiety/stress could fuel seizure generation or induce hippocampal cell loss, promoting epilepsy.

Loss of PV^+ interneurons or loss of PV expression are associated with seizure activity (Schwaller et al., 2004, Andrioli et al., 2007, Sessolo et al., 2015, Yekhlef et al., 2015, Assaf and Schiller, 2016). One possible link is the importance of PV^+ interneurons in the generation of oscillations and synchronisation of network activity. Oscillatory activity in the hippocampus is well studied and it arises from feedback connections between neurons, resulting in synchronisation of their firing pattern with different frequencies. PV^+ interneurons have been associated with rhythmogenesis (Buzsaki and Eidelberg, 1983, Cardin et al., 2009, Fuchs et al., 2001, Sohal et al., 2009) and hippocampal theta or gamma oscillations (Wulff et al., 2009, Amilhon et al., 2015). Our collaboration partner Dr. Dirk Isbrand from the University of Cologne recorded EEGs in anesthetised WT and KO mice, which reflect the activity of a large number of neurons and found a difference in the amplitude of theta waves and in theta-gamma coupling between genotypes (data unpublished). Theta waves - associated with active movements, interactions with the environment and REM sleep (Vanderwolf, 1969, Buzsáki, 2002) - showed a decrease in amplitudes in KO animals compared to WT, confirming the importance of PV^+ related inhibition in theta rhythm generation (Amilhon et al., 2015, Klausberger et al., 2005). Gamma oscillations were not affected by KCC2-knock out in PV^+ interneurons. Theta/gamma coordination, which is proposed to be important for encoding and preserving serial order of inputs, thus providing a way of representing items in short-term and working memory (Burle and Bonnet, 2000, Lisman, 2005, Lisman and Buzsaki, 2008, Lisman and Idiart, 1995), were also disturbed in the hippocampus of HET and KO mice. Hence, deficits in the coupling of the oscillations could lead to alterations in the hippocampal information processing, which may explain

the deficits observed during water maze in our mouse model. The KCC2 loss in PV^+ interneurons and the resulting loss of inhibition could disturb the generation of the fine-tuned theta oscillations and consequently alter network synchronisation. Wulff et al. already showed that fast inhibition of PV^+ interneurons is critical for the generation of theta but not gamma oscillations and in the coupling of hippocampal rhythms across different frequency bands (Wulff et al., 2009). It would be interesting to know, if this leads to an altered synchrony between different brain areas, which is one mechanism proposed for seizure generation (Broggini et al., 2016, Warren et al., 2010).

Furthermore, the increased inhibition in young animals could affect synchrony of network oscillations and consequently proper coordination of network activity. During the last decades, more and more reports were published on how altered GABAergic signalling participates in the generation of human epileptiform discharges (Schwartzkroin and Haglund, 1986, Cohen et al., 2002, Avoli et al., 2005) and how increased inhibition can promote the induction of seizures. Special attention was paid to the role of PV^+ interneurons.

PV^+ interneurons, which are highly interconnected by both chemical and electrical synapses (Tamas et al., 2000, Gibson et al., 1999, Galarreta and Hestrin, 1999b), project to a large number of target cells and can synchronise large cell populations. In our mouse model only these interneurons are affected by cell-type specific KCC2 knock out and alterations in the firing pattern or activity could influence synchrony of the innervated pyramidal cell populations.

Depending on the resting membrane potential and transmembrane gradient of Cl^-, GABA can either hyperpolarise or depolarise a postsynaptic neuron (Farrant and Kaila, 2007, Kaila, 1994). Disinhibition of KCC2 deficient PV^+ interneurons and subsequent increase in GABA release onto the downstream pyramidal neurons can stress Cl^- extrusion mechanisms in postsynaptic neurons (Payne et al., 2003, Blaesse et al., 2009) leading to intracellular Cl^- accumulation and a consequent depolarising shift of E_{GABA}. Additionally, prolonged activity of $GABA_A$Rs results in increased extracellular K^+ levels via KCC2, thereby initiating a prolonged non-synaptic depolarisation (Viitanen et al., 2010). Both mechanisms could lead to excitation of a big cell population throughout different brain areas, starting an epileptic seizure. Interestingly, seizure induction with PTZ at the age of 23 weeks, when KO mice showed an electrophysiological increase in excitation, demonstrated elevated seizure thresholds (figure 21). This rather confusing result may suggest that in 23 weeks old KO mice disinhibition and consequently hyperactivation of PV^+ interneurons causes Cl^- accumulation in downstream pyramidal cells and therefore a depolarising GABA action on excitatory cells. This may lead to increased excitation and seizure generation. The mode of action of PTZ is not clear, complicating the interpretation of the results. To get more insights, this experiment should be repeated in younger animals, when inhibition is increased, and, for both ages, with another convulsive compound. To get a better idea of the involved processes experiments with a younger cohort are pending on the permission from the Thüringer Landesamt für Lebensmittelsicherheit und Verbraucherschutz.

CONCLUSION AND OUTLOOK

Many previous studies have underlined the importance of PV^+ neurons for proper brain function. Most focussed on their role in a specific brain area. In our mouse model, however, all PV^+ neurons are targeted. Therefore, alterations in different brain regions may contribute to the phenotype.

We could show that changes in KCC2 levels in PV^+ interneurons affect the excitability of this interneuron subtype with consequences for neuronal function. We observed a shortened life span, spontaneous epilepsy and a reduction of PV positive interneurons with 23 weeks. Unfortunately, we were not able to show the role of KCC2 for the regulation of the electrochemical chloride gradient in parvalbuminergic interneurons.

In future studies, one should assess GABA-evoked chloride currents and evoked IPSCs (eIPSCs) of PV^+ interneurons to confirm Cl^- accumulation. The somato-dendritic E_{GABA} gradients may give a more reliable estimate of KCC2 extrusion capacity than static E_{GABA} on the soma. The combination of perforated patch recordings of the latter with whole cell recordings of ΔGABA between soma and dendrites may provide important information regarding the consequences of KCC2 ablation in PV^+ neurons.

To verify, whether Cl^- accumulation in pyramidal cells are the cause of increased excitation at the age of 23 weeks, perforated patch recordings of pyramidal cells have to be conducted additionally. These results would allow a better understanding of GABA actions and the physiological synergy of excitatory and inhibitory neurons.

Since the inhibition is increased in 8 weeks old KO animals, a closer look into extrasynaptic $GABA_A$ receptors might be interesting. When more GABA is released due to enhanced PV^+ interneuron activity, this 'spillover' from the synaptic cleft could activate extrasynaptic or perisynaptic $GABA_ARs$ to generate a persistent or tonic inhibition (Belelli et al., 2009).

To better characterise the molecular mechanisms of epileptogenesis the BDNF-TrKB-KCC2 pathway and KCC2 phosphorylation patterns should be examined after controlled seizure induction in WT and KO animals.

Further in vivo studies could elicit the impact of stress to seizure generation and susceptibility. Therefore, an accurate determination of corticosterone levels over time and an analysis of additional stress hormones like adrenalin are possible.

The seizure threshold studies with PTZ should be repeated with mice of the age of 8 weeks, and, additionally, with another compound that is not acting via the $GABA_A$ receptor. These experiments would allow a better interpretation of the observations.

Future experiments will lead to a deeper insight into Cl^- homeostasis and epileptogenesis.

REFERENCES

AGUILERA, G. 1994. Regulation of pituitary ACTH secretion during chronic stress. *Front Neuroendocrinol,* 15**,** 321-50.

AGUILERA, G. 2012. The hypothalamic-pituitary-adrenal axis and neuroendocrine responses to stress. *Handbook of Neuroendocrinology.* Elsevier Inc.

AMILHON, B., HUH, C. Y., MANSEAU, F., DUCHARME, G., NICHOL, H., ADAMANTIDIS, A. & WILLIAMS, S. 2015. Parvalbumin Interneurons of Hippocampus Tune Population Activity at Theta Frequency. *Neuron,* 86**,** 1277-89.

ANDRIOLI, A., ALONSO-NANCLARES, L., ARELLANO, J. I. & DEFELIPE, J. 2007. Quantitative analysis of parvalbumin-immunoreactive cells in the human epileptic hippocampus. *Neuroscience,* 149**,** 131-43.

ANTONI, F. A. 1986. Hypothalamic control of adrenocorticotropin secretion: advances since the discovery of 41-residue corticotropin-releasing factor. *Endocr Rev,* 7**,** 351-78.

ARELLANO, J. I., MUÑOZ, A., BALLESTEROS-YÁÑEZ, I., SOLA, R. G. & DEFELIPE, J. 2004. Histopathology and reorganization of chandelier cells in the human epileptic sclerotic hippocampus. *Brain,* 127**,** 45-64.

ASCOLI, G. A., ALONSO-NANCLARES, L., ANDERSON, S. A., BARRIONUEVO, G., BENAVIDES-PICCIONE, R., BURKHALTER, A., BUZSAKI, G., CAULI, B., DEFELIPE, J., FAIREN, A., FELDMEYER, D., FISHELL, G., FREGNAC, Y., FREUND, T. F., GARDNER, D., GARDNER, E. P., GOLDBERG, J. H., HELMSTAEDTER, M., HESTRIN, S., KARUBE, F., KISVARDAY, Z. F., LAMBOLEZ, B., LEWIS, D. A., MARIN, O., MARKRAM, H., MUNOZ, A., PACKER, A., PETERSEN, C. C. H., ROCKLAND, K. S., ROSSIER, J., RUDY, B., SOMOGYI, P., STAIGER, J. F., TAMAS, G., THOMSON, A. M., TOLEDO-RODRIGUEZ, M., WANG, Y., WEST, D. C., YUSTE, R. & G, P. I. N. 2008. Petilla terminology: nomenclature of features of GABAergic interneurons of the cerebral cortex. *Nature Reviews Neuroscience,* 9**,** 557-568.

ASSAF, F. & SCHILLER, Y. 2016. The antiepileptic and ictogenic effects of optogenetic neurostimulation of PV-expressing interneurons. *Journal of Neurophysiology,* 116**,** 1694.

ATKINSON, H. C. & WADDELL, B. J. 1997. Circadian Variation in Basal Plasma Corticosterone and Adrenocorticotropin in the Rat: Sexual Dimorphism and Changes across the Estrous Cycle*. *Endocrinology,* 138**,** 3842-3848.

AVOLI, M. & DE CURTIS, M. 2011. GABAergic synchronization in the limbic system and its role in the generation of epileptiform activity. *Prog Neurobiol,* 95**,** 104-32.

AVOLI, M., DE CURTIS, M., GNATKOVSKY, V., GOTMAN, J., KOHLING, R., LEVESQUE, M., MANSEAU, F., SHIRI, Z. & WILLIAMS, S. 2016. Specific imbalance of excitatory/inhibitory signaling establishes seizure onset pattern in temporal lobe epilepsy. *J Neurophysiol,* 115**,** 3229-37.

AVOLI, M., LOUVEL, J., PUMAIN, R. & KOHLING, R. 2005. Cellular and molecular mechanisms of epilepsy in the human brain. *Prog Neurobiol,* 77**,** 166-200.

BAILEY, C. R., CORDELL, E., SOBIN, S. M. & NEUMEISTER, A. 2013. Recent Progress in Understanding the Pathophysiology of Post-Traumatic Stress Disorder. *CNS Drugs,* 27**,** 221-232.

BAINES, A. J., BENNETT, P. M., CARTER, E. W. & TERRACCIANO, C. 2009. Protein 4.1 and the control of ion channels. *Blood Cells Mol Dis,* 42**,** 211-5.

BARTOS, M., VIDA, I., FROTSCHER, M., GEIGER, J. R. P. & JONAS, P. 2001. Rapid Signaling at Inhibitory Synapses in a Dentate Gyrus Interneuron Network. *The Journal of Neuroscience,* 21**,** 2687-2698.

BAZHENOV, M., TIMOFEEV, I., STERIADE, M. & SEJNOWSKI, T. J. 1999. Self-sustained rhythmic activity in the thalamic reticular nucleus mediated by depolarizing GABAA receptor potentials. *Nat Neurosci,* 2**,** 168-174.

BEHRENS, M. M., ALI, S. S., DAO, D. N., LUCERO, J., SHEKHTMAN, G., QUICK, K. L. & DUGAN, L. L. 2007. Ketamine-induced loss of phenotype of fast-spiking interneurons is mediated by NADPH-oxidase. *Science,* 318**,** 1645-7.

BELELLI, D., HARRISON, N. L., MAGUIRE, J., MACDONALD, R. L., WALKER, M. C. & COPE, D. W. 2009. Extrasynaptic GABA_A Receptors: Form, Pharmacology, and Function. *The Journal of Neuroscience,* 29**,** 12757-12763.

BEN-ARI, Y. 2002. Excitatory actions of gaba during development: the nature of the nurture. *Nat Rev Neurosci,* 3**,** 728-39.

BEN-ARI, Y., KHALILOV, I., KAHLE, K. T. & CHERUBINI, E. 2012. The GABA excitatory/inhibitory shift in brain maturation and neurological disorders. *Neuroscientist,* 18**,** 467-86.

BERG, A. T., BERKOVIC, S. F., BRODIE, M. J., BUCHHALTER, J., CROSS, J. H., VAN EMDE BOAS, W., ENGEL, J., FRENCH, J., GLAUSER, T. A., MATHERN,

G. W., MOSHÉ, S. L., NORDLI, D., PLOUIN, P. & SCHEFFER, I. E. 2010. Revised terminology and concepts for organization of seizures and epilepsies: Report of the ILAE Commission on Classification and Terminology, 2005–2009. *Epilepsia,* 51**,** 676-685.

BIENVENU, T. C., BUSTI, D., MAGILL, P. J., FERRAGUTI, F. & CAPOGNA, M. 2012. Cell-type-specific recruitment of amygdala interneurons to hippocampal theta rhythm and noxious stimuli in vivo. *Neuron,* 74**,** 1059-74.

BLAESSE, P., AIRAKSINEN, M. S., RIVERA, C. & KAILA, K. 2009. Cation-chloride cotransporters and neuronal function. *Neuron,* 61**,** 820-38.

BLISS, T. V. P. & COLLINGRIDGE, G. L. 1993. A synaptic model of memory: long-term potentiation in the hippocampus. *Nature,* 361**,** 31-39.

BOCCHIO, M., FUCSINA, G., OIKONOMIDIS, L., MCHUGH, S. B., BANNERMAN, D. M., SHARP, T. & CAPOGNA, M. 2015. Increased Serotonin Transporter Expression Reduces Fear and Recruitment of Parvalbumin Interneurons of the Amygdala. *Neuropsychopharmacology,* 40**,** 3015-3026.

BORMANN, J. & FEIGENSPAN, A. 1995. GABAc receptors. *Trends in Neurosciences,* 18**,** 515-519.

BORMANN, J., HAMILL, O. P. & SAKMANN, B. 1987. Mechanism of anion permeation through channels gated by glycine and gamma-aminobutyric acid in mouse cultured spinal neurones. *The Journal of Physiology,* 385**,** 243-286.

BRANDALISE, F., CARTA, S., HELMCHEN, F., LISMAN, J. & GERBER, U. 2016. Dendritic NMDA spikes are necessary for timing-dependent associative LTP in CA3 pyramidal cells. *Nat Commun,* 7**,** 13480.

BRIGGS, F. 2010. Organizing Principles of Cortical Layer 6. *Frontiers in Neural Circuits,* 4**,** 3.

BROGGINI, A. C., ESTEVES, I. M., ROMCY-PEREIRA, R. N., LEITE, J. P. & LEAO, R. N. 2016. Pre-ictal increase in theta synchrony between the hippocampus and prefrontal cortex in a rat model of temporal lobe epilepsy. *Exp Neurol,* 279**,** 232-42.

BURLE, B. & BONNET, M. 2000. High-speed memory scanning: a behavioral argument for a serial oscillatory model. *Brain Res Cogn Brain Res,* 9**,** 327-37.

BUZSÁKI, G. 2002. Theta Oscillations in the Hippocampus. *Neuron,* 33**,** 325-340.

BUZSAKI, G. & EIDELBERG, E. 1983. Phase relations of hippocampal projection cells and interneurons to theta activity in the anesthetized rat. *Brain Research,* 266**,** 334-339.

BUZSÀKI, G. & EIDELBERG, E. 1981. Commissural projection to the dentate gyrus of the rat: evidence for feed-forward inhibition. *Brain Research,* 230**,** 346-350.

BUZSAKI, G. & JONAS, P. 2007. Neural inhibition. *Scholarpedia,* 2**,** 3286.

BUZSAKI, G., KAILA, K. & RAICHLE, M. 2007. Inhibition and brain work. *Neuron,* 56**,** 771-83.

CAMPAGNA-SLATER, V. & WEAVER, D. F. 2007. Molecular modelling of the GABAA ion channel protein. *Journal of Molecular Graphics and Modelling,* 25**,** 721-730.

CAMPBELL, S. L., ROBEL, S., CUDDAPAH, V. A., ROBERT, S., BUCKINGHAM, S. C., KAHLE, K. T. & SONTHEIMER, H. 2015. GABAergic disinhibition and impaired KCC2 cotransporter activity underlie tumor-associated epilepsy. *Glia,* 63**,** 23-36.

CANCEDDA, L., FIUMELLI, H., CHEN, K. & POO, M. M. 2007. Excitatory GABA action is essential for morphological maturation of cortical neurons in vivo. *J Neurosci,* 27**,** 5224-35.

CARDIN, J. A., CARLEN, M., MELETIS, K., KNOBLICH, U., ZHANG, F., DEISSEROTH, K., TSAI, L. H. & MOORE, C. I. 2009. Driving fast-spiking cells induces gamma rhythm and controls sensory responses. *Nature,* 459**,** 663-7.

CELIO, M. R. 1990. Calbindin D-28k and parvalbumin in the rat nervous system. *Neuroscience,* 35**,** 375-475.

CELIO, M. R. & HEIZMANN, C. W. 1981. Calcium-binding protein parvalbumin as a neuronal marker. *Nature,* 293**,** 300-2.

CHAMMA, I., CHEVY, Q., PONCER, J. C. & LEVI, S. 2012. Role of the neuronal K-Cl co-transporter KCC2 in inhibitory and excitatory neurotransmission. *Front Cell Neurosci,* 6**,** 5.

CHAVAS, J. & MARTY, A. 2003. Coexistence of Excitatory and Inhibitory GABA Synapses in the Cerebellar Interneuron Network. *The Journal of Neuroscience,* 23**,** 2019-2031.

CHEAH, C. S., YU, F. H., WESTENBROEK, R. E., KALUME, F. K., OAKLEY, J. C., POTTER, G. B., RUBENSTEIN, J. L. & CATTERALL, W. A. 2012. Specific deletion of NaV1.1 sodium channels in inhibitory interneurons causes seizures and premature death in a mouse model of Dravet syndrome. *Proc Natl Acad Sci U S A,* 109**,** 14646-51.

CHERUBINI, E. 2012. Phasic GABAA-Mediated Inhibition. *In:* NOEBELS, J. L., AVOLI, M., ROGAWSKI, M. A., OLSEN, R. W. & DELGADO-ESCUETA, A. V. (eds.) *Jasper's Basic Mechanisms of the Epilepsies.* Bethesda MD: Michael A

Rogawski, Antonio V Delgado-Escueta, Jeffrey L Noebels, Massimo Avoli and Richard W Olsen.

CHERUBINI, E. & CONTI, F. 2001. Generating diversity at GAB Aergic synapses. *Trends in Neurosciences,* 24**,** 155-162.

CHOI, D. W. 1985. Glutamate neurotoxicity in cortical cell culture is calcium dependent. *Neuroscience Letters,* 58**,** 293-297.

CHOI, D. W. 1987. Ionic dependence of glutamate neurotoxicity. *J Neurosci,* 7**,** 369-79.

CHOW, A., ERISIR, A., FARB, C., NADAL, M. S., OZAITA, A., LAU, D., WELKER, E. & RUDY, B. 1999. K(+) channel expression distinguishes subpopulations of parvalbumin- and somatostatin-containing neocortical interneurons. *J Neurosci,* 19**,** 9332-45.

COBB, S. R., BUHL, E. H., HALASY, K., PAULSEN, O. & SOMOGYI, P. 1995. Synchronization of neuronal activity in hippocampus by individual GABAergic interneurons. *Nature,* 378**,** 75-78.

COHEN, I., NAVARRO, V., CLEMENCEAU, S., BAULAC, M. & MILES, R. 2002. On the origin of interictal activity in human temporal lobe epilepsy in vitro. *Science,* 298**,** 1418-21.

COLLINGRIDGE, G. L., HERRON, C. E. & LESTER, R. A. 1988. Synaptic activation of N-methyl-D-aspartate receptors in the Schaffer collateral-commissural pathway of rat hippocampus. *J Physiol,* 399**,** 283-300.

COSSART, R., BERNARD, C. & BEN-ARI, Y. 2005. Multiple facets of GABAergic neurons and synapses: multiple fates of GABA signalling in epilepsies. *Trends in Neurosciences,* 28**,** 108-115.

CZEH, B., SIMON, M., VAN DER HART, M. G., SCHMELTING, B., HESSELINK, M. B. & FUCHS, E. 2005. Chronic stress decreases the number of parvalbumin-immunoreactive interneurons in the hippocampus: prevention by treatment with a substance P receptor (NK1) antagonist. *Neuropsychopharmacology,* 30**,** 67-79.

DAVIES, C. H., STARKEY, S. J., POZZA, M. F. & COLLINGRIDGE, G. L. 1991. GABA autoreceptors regulate the induction of LTP. *Nature,* 349**,** 609-11.

DE ALMEIDA, L., IDIART, M. & LISMAN, J. E. 2009a. The Input–Output Transformation of the Hippocampal Granule Cells: From Grid Cells to Place Fields. *The Journal of Neuroscience,* 29**,** 7504-7512.

DE ALMEIDA, L., IDIART, M. & LISMAN, J. E. 2009b. A second function of gamma frequency oscillations: an E%-max winner-take-all mechanism selects which cells fire. *J Neurosci,* 29**,** 7497-503.

DE CURTIS, M. & AVOLI, M. 2016. GABAergic networks jump-start focal seizures. *Epilepsia,* 57**,** 679-87.

DE LANEROLLE, N. C., KIM, J. H., ROBBINS, R. J. & SPENCER, D. D. 1989. Hippocampal interneuron loss and plasticity in human temporal lobe epilepsy. *Brain Res,* 495**,** 387-95.

DEFELIPE, J. 1999. Chandelier cells and epilepsy. *Brain,* 122**,** 1807-1822.

DESIDERATO, O., BUTLER, B. & MEYER, C. 1966. Changes in fear generalization gradients as a function of delayed testing. *J Exp Psychol,* 72**,** 678-82.

DING, J. & DELPIRE, E. 2014. Deletion of KCC3 in parvalbumin neurons leads to locomotor deficit in a conditional mouse model of peripheral neuropathy associated with agenesis of the corpus callosum. *Behav Brain Res,* 274**,** 128-36.

DINOCOURT, C., PETANJEK, Z., FREUND, T. F., BEN-ARI, Y. & ESCLAPEZ, M. 2003. Loss of interneurons innervating pyramidal cell dendrites and axon initial segments in the CA1 region of the hippocampus following pilocarpine-induced seizures. *J Comp Neurol,* 459**,** 407-25.

DONG, E., MATSUMOTO, K., UZUNOVA, V., SUGAYA, I., TAKAHATA, H., NOMURA, H., WATANABE, H., COSTA, E. & GUIDOTTI, A. 2001. Brain 5alpha-dihydroprogesterone and allopregnanolone synthesis in a mouse model of protracted social isolation. *Proc Natl Acad Sci U S A,* 98**,** 2849-54.

DYMOND, S., DUNSMOOR, J. E., VERVLIET, B., ROCHE, B. & HERMANS, D. 2015. Fear Generalization in Humans: Systematic Review and Implications for Anxiety Disorder Research. *Behavior Therapy,* 46**,** 561-582.

DZHALA, V. I., TALOS, D. M., SDRULLA, D. A., BRUMBACK, A. C., MATHEWS, G. C., BENKE, T. A., DELPIRE, E., JENSEN, F. E. & STALEY, K. J. 2005. NKCC1 transporter facilitates seizures in the developing brain. *Nat Med,* 11**,** 1205-13.

ELLENDER, T. J., RAIMONDO, J. V., IRKLE, A., LAMSA, K. P. & AKERMAN, C. J. 2014. Excitatory effects of parvalbumin-expressing interneurons maintain hippocampal epileptiform activity via synchronous afterdischarges. *J Neurosci,* 34**,** 15208-22.

ENGLAND, M. J., LIVERMAN, C. T., SCHULTZ, A. M. & STRAWBRIDGE, L. M. 2012. *Epilepsy Across the Spectrum,* THE NATIONAL ACADEMIES PRESS Committee on the Public Health Dimensions of the Epilepsies.

EYLES, D. W., MCGRATH, J. J. & REYNOLDS, G. P. Neuronal calcium-binding proteins and schizophrenia. *Schizophrenia Research,* 57**,** 27-34.

FANSELOW, M. S. 1980. Conditioned and unconditional components of post-shock freezing. *Pavlov J Biol Sci,* 15**,** 177-82.

FANSELOW, M. S. 1990. Factors Governing One-Trial Contextual Conditioning. *Animal Learning & Behavior,* 18**,** 264-270.

FANSELOW, M. S. & POULOS, A. M. 2005. The neuroscience of mammalian associative learning. *Annu Rev Psychol,* 56**,** 207-34.

FARRANT, M. & KAILA, K. 2007. The cellular, molecular and ionic basis of GABA(A) receptor signalling. *Prog Brain Res,* 160**,** 59-87.

FARRANT, M. & NUSSER, Z. 2005. Variations on an inhibitory theme: phasic and tonic activation of GABAA receptors. *Nat Rev Neurosci,* 6**,** 215-229.

FEREZOU, I., CAULI, B., HILL, E. L., ROSSIER, J., HAMEL, E. & LAMBOLEZ, B. 2002. 5-HT3 receptors mediate serotonergic fast synaptic excitation of neocortical vasoactive intestinal peptide/cholecystokinin interneurons. *J Neurosci,* 22**,** 7389-97.

FREUND, T. F. & BUZSAKI, G. 1996. Interneurons of the hippocampus. *Hippocampus,* 6**,** 347-470.

FRIEDEL, P., KAHLE, K. T., ZHANG, J., HERTZ, N., PISELLA, L. I., BUHLER, E., SCHALLER, F., DUAN, J., KHANNA, A. R., BISHOP, P. N., SHOKAT, K. M. & MEDINA, I. 2015. WNK1-regulated inhibitory phosphorylation of the KCC2 cotransporter maintains the depolarizing action of GABA in immature neurons. *Sci Signal,* 8**,** ra65.

FUCHS, E., FLUGGE, G. & CZEH, B. 2006. Remodeling of neuronal networks by stress. *Front Biosci,* 11**,** 2746-58.

FUCHS, E. C., DOHENY, H., FAULKNER, H., CAPUTI, A., TRAUB, R. D., BIBBIG, A., KOPELL, N., WHITTINGTON, M. A. & MONYER, H. 2001. Genetically altered AMPA-type glutamate receptor kinetics in interneurons disrupt long-range synchrony of gamma oscillation. *Proc Natl Acad Sci U S A,* 98**,** 3571-6.

FUCHS, E. C., ZIVKOVIC, A. R., CUNNINGHAM, M. O., MIDDLETON, S., LEBEAU, F. E., BANNERMAN, D. M., ROZOV, A., WHITTINGTON, M. A., TRAUB, R. D., RAWLINS, J. N. & MONYER, H. 2007. Recruitment of parvalbumin-positive

interneurons determines hippocampal function and associated behavior. *Neuron,* 53**,** 591-604.

FUJIWARA-TSUKAMOTO, Y., ISOMURA, Y., NAMBU, A. & TAKADA, M. 2003. Excitatory gaba input directly drives seizure-like rhythmic synchronization in mature hippocampal CA1 pyramidal cells. *Neuroscience,* 119**,** 265-275.

FURMAN, G. G. 1965. Comparison of models for subtractive and shunting lateral-inhibition in receptor-neuron fields. *Kybernetik,* 2**,** 257-74.

GAGNON, K. B. & DELPIRE, E. 2013. Physiology of SLC12 transporters: lessons from inherited human genetic mutations and genetically engineered mouse knockouts. *American Journal of Physiology - Cell Physiology,* 304**,** C693-C714.

GAGNON, M., BERGERON, M. J., LAVERTU, G., CASTONGUAY, A., TRIPATHY, S., BONIN, R. P., PEREZ-SANCHEZ, J., BOUDREAU, D., WANG, B., DUMAS, L., VALADE, I., BACHAND, K., JACOB-WAGNER, M., TARDIF, C., KIANICKA, I., ISENRING, P., ATTARDO, G., COULL, J. A. & DE KONINCK, Y. 2013. Chloride extrusion enhancers as novel therapeutics for neurological diseases. *Nat Med,* 19**,** 1524-8.

GALANOPOULOU, A. S. 2008. Sexually dimorphic expression of KCC2 and GABA function. *Epilepsy Res,* 80**,** 99-113.

GALARRETA, M. & HESTRIN, S. 1999a. A network of fast-spiking cells in the neocortex connected by electrical synapses. *Nature,* 402**,** 72-75.

GALARRETA, M. & HESTRIN, S. 1999b. A network of fast-spiking cells in the neocortex connected by electrical synapses. *Nature,* 402**,** 72-5.

GAUVAIN, G., CHAMMA, I., CHEVY, Q., CABEZAS, C., IRINOPOULOU, T., BODRUG, N., CARNAUD, M., LEVI, S. & PONCER, J. C. 2011. The neuronal K-Cl cotransporter KCC2 influences postsynaptic AMPA receptor content and lateral diffusion in dendritic spines. *Proc Natl Acad Sci U S A,* 108**,** 15474-9.

GERNERT, M., HAMANN, M., BENNAY, M., LÖSCHER, W. & RICHTER, A. 2000. Deficit of Striatal Parvalbumin-Reactive GABAergic Interneurons and Decreased Basal Ganglia Output in a Genetic Rodent Model of Idiopathic Paroxysmal Dystonia. *The Journal of Neuroscience,* 20**,** 7052-7058.

GERSTMANN, K., PENSOLD, D., SYMMANK, J., KHUNDADZE, M., HUBNER, C. A., BOLZ, J. & ZIMMER, G. 2015. Thalamic afferents influence cortical progenitors via ephrin A5-EphA4 interactions. *Development,* 142**,** 140-50.

GIBSON, J. R., BEIERLEIN, M. & CONNORS, B. W. 1999. Two networks of electrically coupled inhibitory neurons in neocortex. *Nature,* 402**,** 75-79.

GLYKYS, J. & MODY, I. 2007. Activation of GABAA receptors: views from outside the synaptic cleft. *Neuron,* 56**,** 763-70.

HAUSER, W. A. 1995. Recent developments in the epidemiology of epilepsy. *Acta Neurol Scand Suppl,* 162**,** 17-21.

HELBIG, I. & LOWENSTEIN, D. H. 2013. Genetics of the epilepsies: where are we and where are we going? *Curr Opin Neurol,* 26**,** 179-85.

HENDRY, S. H., JONES, E. G., EMSON, P. C., LAWSON, D. E., HEIZMANN, C. W. & STREIT, P. 1989. Two classes of cortical GABA neurons defined by differential calcium binding protein immunoreactivities. *Exp Brain Res,* 76**,** 467-72.

HERRMANN, T. 2015. The role of cation-chloride cotransporters KCC2 and NKCC1 in GABAergic signaling and cognitive functions in mice*. Master Thesis*, Friedrich-Schiller-Universität Jena.

HILDEBRAND, M. S., DAHL, H. H., DAMIANO, J. A., SMITH, R. J., SCHEFFER, I. E. & BERKOVIC, S. F. 2013. Recent advances in the molecular genetics of epilepsy. *J Med Genet,* 50**,** 271-9.

HIPPENMEYER, S., VRIESELING, E., SIGRIST, M., PORTMANN, T., LAENGLE, C., LADLE, D. R. & ARBER, S. 2005. A developmental switch in the response of DRG neurons to ETS transcription factor signaling. *PLoS Biol,* 3**,** e159.

HOLM, M. M., NIETO-GONZALEZ, J. L., VARDYA, I., HENNINGSEN, K., JAYATISSA, M. N., WIBORG, O. & JENSEN, K. 2011. Hippocampal GABAergic dysfunction in a rat chronic mild stress model of depression. *Hippocampus,* 21**,** 422-33.

HU, W., ZHANG, M., CZEH, B., FLUGGE, G. & ZHANG, W. 2010. Stress impairs GABAergic network function in the hippocampus by activating nongenomic glucocorticoid receptors and affecting the integrity of the parvalbumin-expressing neuronal network. *Neuropsychopharmacology,* 35**,** 1693-707.

HÜBNER, C. A., LORKE, D. E. & HERMANS-BORGMEYER, I. 2001a. Expression of the Na-K-2Cl-cotransporter NKCC1 during mouse development. *Mech Dev,* 102**,** 267-9.

HÜBNER, C. A., STEIN, V., HERMANS-BORGMEYER, I., MEYER, T., BALLANYI, K. & JENTSCH, T. J. 2001b. Disruption of KCC2 reveals an essential role of K-Cl cotransport already in early synaptic inhibition. *Neuron,* 30**,** 515-24.

HUUSKO, N., ROMER, C., NDODE-EKANE, X. E., LUKASIUK, K. & PITKANEN, A. 2015. Loss of hippocampal interneurons and epileptogenesis: a comparison of two animal models of acquired epilepsy. *Brain Struct Funct,* 220**,** 153-91.

HYDE, T. M., LIPSKA, B. K., ALI, T., MATHEW, S. V., LAW, A. J., METITIRI, O. E., STRAUB, R. E., YE, T., COLANTUONI, C., HERMAN, M. M., BIGELOW, L. B., WEINBERGER, D. R. & KLEINMAN, J. E. 2011. Expression of GABA signaling molecules KCC2, NKCC1, and GAD1 in cortical development and schizophrenia. *J Neurosci,* 31**,** 11088-95.

ILAE 1993. Guidelines for epidemiologic studies on epilepsy. Commission on Epidemiology and Prognosis, International League Against Epilepsy. *Epilepsia,* 34**,** 592-6.

INOUE, K., FURUKAWA, T., KUMADA, T., YAMADA, J., WANG, T., INOUE, R. & FUKUDA, A. 2012. Taurine inhibits K+-Cl- cotransporter KCC2 to regulate embryonic Cl- homeostasis via with-no-lysine (WNK) protein kinase signaling pathway. *J Biol Chem,* 287**,** 20839-50.

JACOB, T. C., MOSS, S. J. & JURD, R. 2008. GABA(A) receptor trafficking and its role in the dynamic modulation of neuronal inhibition. *Nat Rev Neurosci,* 9**,** 331-43.

JACOBS, S., RUUSUVUORI, E., SIPILA, S. T., HAAPANEN, A., DAMKIER, H. H., KURTH, I., HENTSCHKE, M., SCHWEIZER, M., RUDHARD, Y., LAATIKAINEN, L. M., TYYNELA, J., PRAETORIUS, J., VOIPIO, J. & HUBNER, C. A. 2008. Mice with targeted Slc4a10 gene disruption have small brain ventricles and show reduced neuronal excitability. *Proc Natl Acad Sci U S A,* 105**,** 311-6.

JENTSCH, T. J., HUBNER, C. A. & FUHRMANN, J. C. 2004. Ion channels: function unravelled by dysfunction. *Nat Cell Biol,* 6**,** 1039-47.

JINNO, S. & KOSAKA, T. 2004. Parvalbumin is expressed in glutamatergic and GABAergic corticostriatal pathway in mice. *J Comp Neurol,* 477**,** 188-201.

JOËLS, M. 2009. Stress, the hippocampus, and epilepsy. *Epilepsia,* 50**,** 586-597.

JOHANSEN, F. F., TONDER, N., ZIMMER, J., BAIMBRIDGE, K. G. & DIEMER, N. H. 1990. Short-term changes of parvalbumin and calbindin immunoreactivity in the rat hippocampus following cerebral ischemia. *Neurosci Lett,* 120**,** 171-4.

JONES, E. G. & HENDRY, S. H. C. 1986. Co-localization of GABA and neuropeptides in neocortical neurons. *Trends in Neurosciences,* 9**,** 71-76.

JONES, K. 2011. *Neurological Assessment: A Clinician's Guide*, Elsevier Health Sciences UK.

KAHLE, K. T., KHANNA, A. R., DUAN, J., STALEY, K. J., DELPIRE, E. & PODURI, A. 2016. The KCC2 Cotransporter and Human Epilepsy: Getting Excited About Inhibition. *Neuroscientist*.

KAILA, K. 1994. Ionic basis of GABAA receptor channel function in the nervous system. *Prog Neurobiol,* 42**,** 489-537.

KAILA, K., LAMSA, K., SMIRNOV, S., TAIRA, T. & VOIPIO, J. 1997. Long-lasting GABA-mediated depolarization evoked by high-frequency stimulation in pyramidal neurons of rat hippocampal slice is attributable to a network-driven, bicarbonate-dependent K+ transient. *J Neurosci,* 17**,** 7662-72.

KAILA, K., PRICE, T. J., PAYNE, J. A., PUSKARJOV, M. & VOIPIO, J. 2014a. Cation-chloride cotransporters in neuronal development, plasticity and disease. *Nat Rev Neurosci,* 15**,** 637-54.

KAILA, K., RUUSUVUORI, E., SEJA, P., VOIPIO, J. & PUSKARJOV, M. 2014b. GABA actions and ionic plasticity in epilepsy. *Curr Opin Neurobiol,* 26**,** 34-41.

KALANITHI, P. S. A., ZHENG, W., KATAOKA, Y., DIFIGLIA, M., GRANTZ, H., SAPER, C. B., SCHWARTZ, M. L., LECKMAN, J. F. & VACCARINO, F. M. 2005. Altered parvalbumin-positive neuron distribution in basal ganglia of individuals with Tourette syndrome. *Proceedings of the National Academy of Sciences of the United States of America,* 102**,** 13307-13312.

KAMPRATH, K. & WOTJAK, C. T. 2004. Nonassociative learning processes determine expression and extinction of conditioned fear in mice. *Learn Mem,* 11**,** 770-86.

KANAKA, C., OHNO, K., OKABE, A., KURIYAMA, K., ITOH, T., FUKUDA, A. & SATO, K. 2001. The differential expression patterns of messenger RNAs encoding K-Cl cotransporters (KCC1,2) and Na-K-2Cl cotransporter (NKCC1) in the rat nervous system. *Neuroscience,* 104**,** 933-46.

KANDEL, E. R. & MACK, S. 2014. *Principles of neural science*.

KANN, O. 2016. The interneuron energy hypothesis: Implications for brain disease. *Neurobiol Dis,* 90**,** 75-85.

KANN, O. & KOVACS, R. 2007. Mitochondria and neuronal activity. *Am J Physiol Cell Physiol,* 292**,** C641-57.

KANN, O., PAPAGEORGIOU, I. E. & DRAGUHN, A. 2014. Highly energized inhibitory interneurons are a central element for information processing in cortical networks. *J Cereb Blood Flow Metab,* 34**,** 1270-82.

KARST, H., DE KLOET, E. R. & JOELS, M. 1999. Episodic corticosterone treatment accelerates kindling epileptogenesis and triggers long-term changes in hippocampal CA1 cells, in the fully kindled state. *Eur J Neurosci,* 11**,** 889-98.

KASH, T. L., TRUDELL, J. R. & HARRISON, N. L. 2004. Structural elements involved in activation of the γ-aminobutyric acid type A (GABAA) receptor. *Biochemical Society Transactions,* 32**,** 540-546.

KAWAGUCHI, Y. & KUBOTA, Y. 1993. Correlation of physiological subgroupings of nonpyramidal cells with parvalbumin- and calbindinD28k-immunoreactive neurons in layer V of rat frontal cortex. *J Neurophysiol,* 70**,** 387-96.

KELSO, S. R., GANONG, A. H. & BROWN, T. H. 1986. Hebbian synapses in hippocampus. *Proc Natl Acad Sci U S A,* 83**,** 5326-30.

KIGHT, K. E. & MCCARTHY, M. M. 2014. Using sex differences in the developing brain to identify nodes of influence for seizure susceptibility and epileptogenesis. *Neurobiol Dis,* 72 Pt B**,** 136-43.

KIM, Y., HSU, C. L., CEMBROWSKI, M. S., MENSH, B. D. & SPRUSTON, N. 2015. Dendritic sodium spikes are required for long-term potentiation at distal synapses on hippocampal pyramidal neurons. *Elife,* 4.

KLAUSBERGER, T., MARTON, L. F., O'NEILL, J., HUCK, J. H., DALEZIOS, Y., FUENTEALBA, P., SUEN, W. Y., PAPP, E., KANEKO, T., WATANABE, M., CSICSVARI, J. & SOMOGYI, P. 2005. Complementary roles of cholecystokinin- and parvalbumin-expressing GABAergic neurons in hippocampal network oscillations. *J Neurosci,* 25**,** 9782-93.

KLING, M. A., SMITH, M. A., GLOWA, J. R., PLUZNIK, D., DEMAS, J., DEBELLIS, M. D., GOLD, P. W. & SCHULKIN, J. 1993. Facilitation of cocaine kindling by glucocorticoids in rats. *Brain Research,* 629**,** 163-166.

KNOFLACH, F., HERNANDEZ, M. C. & BERTRAND, D. 2016. GABAA receptor-mediated neurotransmission: Not so simple after all. *Biochem Pharmacol,* 115**,** 10-7.

KOBAYASHI, M. & BUCKMASTER, P. S. 2003. Reduced inhibition of dentate granule cells in a model of temporal lobe epilepsy. *J Neurosci,* 23**,** 2440-52.

KONIG, P., ENGEL, A. K. & SINGER, W. 1996. Integrator or coincidence detector? The role of the cortical neuron revisited. *Trends Neurosci,* 19**,** 130-7.

KOROTKOVA, T., FUCHS, E. C., PONOMARENKO, A., VON ENGELHARDT, J. & MONYER, H. 2010. NMDA receptor ablation on parvalbumin-positive interneurons impairs hippocampal synchrony, spatial representations, and working memory. *Neuron,* 68**,** 557-69.

KORPI, E. R., GRUNDER, G. & LUDDENS, H. 2002. Drug interactions at GABA(A) receptors. *Prog Neurobiol,* 67**,** 113-59.

KOVACS, R., KARDOS, J., HEINEMANN, U. & KANN, O. 2005. Mitochondrial calcium ion and membrane potential transients follow the pattern of epileptiform discharges in hippocampal slice cultures. *J Neurosci,* 25**,** 4260-9.

KOVACS, R., SCHUCHMANN, S., GABRIEL, S., KANN, O., KARDOS, J. & HEINEMANN, U. 2002. Free radical-mediated cell damage after experimental status epilepticus in hippocampal slice cultures. *J Neurophysiol,* 88**,** 2909-18.

KUMAR, G., COUPER, A., O'BRIEN, T. J., SALZBERG, M. R., JONES, N. C., REES, S. M. & MORRIS, M. J. 2007. The acceleration of amygdala kindling epileptogenesis by chronic low-dose corticosterone involves both mineralocorticoid and glucocorticoid receptors. *Psychoneuroendocrinology,* 32**,** 834-842.

KURUBA, R., HATTIANGADY, B., PARIHAR, V. K., SHUAI, B. & SHETTY, A. K. 2011. Differential Susceptibility of Interneurons Expressing Neuropeptide Y or Parvalbumin in the Aged Hippocampus to Acute Seizure Activity. *PLoS ONE,* 6**,** e24493.

LAI, T. W., ZHANG, S. & WANG, Y. T. 2014. Excitotoxicity and stroke: Identifying novel targets for neuroprotection. *Progress in Neurobiology,* 115**,** 157-188.

LANGWIESER, N., CHRISTEL, C. J., KLEPPISCH, T., HOFMANN, F., WOTJAK, C. T. & MOOSMANG, S. 2010. Homeostatic switch in hebbian plasticity and fear learning after sustained loss of Cav1.2 calcium channels. *J Neurosci,* 30**,** 8367-75.

LECEA, L. D., DEL RI´O, J. A. & SORIANO, E. 1995. Developmental expression of parvalbumin mRNA in the cerebral cortex and hippocampus of the rat. *Molecular Brain Research,* 32**,** 1-13.

LEHMANN, A. & JACOBSON, I. 1990. Ion Dependence and Receptor Mediation of Glutamate Toxicity in the Immature Rat Hippocampal Slice. *Eur J Neurosci,* 2**,** 620-628.

LEWIS, D. A., CRUZ, D. A., MELCHITZKY, D. S. & PIERRI, J. N. 2001. Lamina-specific deficits in parvalbumin-immunoreactive varicosities in the prefrontal cortex of subjects with schizophrenia: evidence for fewer projections from the thalamus. *Am J Psychiatry,* 158**,** 1411-22.

LEWIS, D. A., HASHIMOTO, T. & VOLK, D. W. 2005. Cortical inhibitory neurons and schizophrenia. *Nat Rev Neurosci,* 6**,** 312-324.

LEWIS, D. A. & LUND, J. S. 1990. Heterogeneity of chandelier neurons in monkey neocortex: Corticotropin-releasing factor-and parvalbumin-immunoreactive populations. *The Journal of Comparative Neurology,* 293**,** 599-615.

LI, H., KHIRUG, S., CAI, C., LUDWIG, A., BLAESSE, P., KOLIKOVA, J., AFZALOV, R., COLEMAN, S. K., LAURI, S., AIRAKSINEN, M. S., KEINANEN, K., KHIROUG, L., SAARMA, M., KAILA, K. & RIVERA, C. 2007. KCC2 interacts with the dendritic cytoskeleton to promote spine development. *Neuron,* 56**,** 1019-33.

LIEBMANN, L., KARST, H. & JOELS, M. 2009. Effects of corticosterone and the beta-agonist isoproterenol on glutamate receptor-mediated synaptic currents in the rat basolateral amygdala. *Eur J Neurosci,* 30**,** 800-7.

LISMAN, J. 2005. The theta/gamma discrete phase code occuring during the hippocampal phase precession may be a more general brain coding scheme. *Hippocampus,* 15**,** 913-22.

LISMAN, J. & BUZSAKI, G. 2008. A neural coding scheme formed by the combined function of gamma and theta oscillations. *Schizophr Bull,* 34**,** 974-80.

LISMAN, J. E. & IDIART, M. A. 1995. Storage of 7 +/- 2 short-term memories in oscillatory subcycles. *Science,* 267**,** 1512-5.

LISSEK, S. 2012. TOWARD AN ACCOUNT OF CLINICAL ANXIETY PREDICATED ON BASIC, NEURALLY MAPPED MECHANISMS OF PAVLOVIAN FEAR-LEARNING: THE CASE FOR CONDITIONED OVERGENERALIZATION. *Depression and Anxiety,* 29**,** 257-263.

LISSEK, S., BRADFORD, D. E., ALVAREZ, R. P., BURTON, P., ESPENSEN-STURGES, T., REYNOLDS, R. C. & GRILLON, C. 2013. Neural substrates of classically conditioned fear-generalization in humans: a parametric fMRI study. *Social Cognitive and Affective Neuroscience,* 9**,** 1134-1142.

LIU, Q. & WONG-RILEY, M. T. 2012. Postnatal development of Na(+)-K(+)-2Cl(-) co-transporter 1 and K(+)-Cl(-) co-transporter 2 immunoreactivity in multiple brain stem respiratory nuclei of the rat. *Neuroscience,* 210**,** 1-20.

LUSCHER, B., SHEN, Q. & SAHIR, N. 2011. The GABAergic deficit hypothesis of major depressive disorder. *Mol Psychiatry,* 16**,** 383-406.

MACDONALD, R. L. & OLSEN, R. W. 1994. GABAA receptor channels. *Annu Rev Neurosci,* 17**,** 569-602.

MACKENZIE, G. & MAGUIRE, J. 2015. Chronic stress shifts the GABA reversal potential in the hippocampus and increases seizure susceptibility. *Epilepsy Research,* 109**,** 13-27.

MADISEN, L., ZWINGMAN, T. A., SUNKIN, S. M., OH, S. W., ZARIWALA, H. A., GU, H., NG, L. L., PALMITER, R. D., HAWRYLYCZ, M. J., JONES, A. R., LEIN, E. S. & ZENG, H. 2010. A robust and high-throughput Cre reporting and characterization system for the whole mouse brain. *Nat Neurosci,* 13**,** 133-40.

MAGLÓCZKY, Z. & FREUND, T. F. 2005. Impaired and repaired inhibitory circuits in the epileptic human hippocampus. *Trends in Neurosciences,* 28**,** 334-340.

MAGLÓCZKY, Z., WITTNER, L., BORHEGYI, Z., HALÁSZ, P., VAJDA, J., CZIRJÁK, S. & FREUND, T. F. 2000. Changes in the distribution and connectivity of interneurons in the epileptic human dentate gyrus. *Neuroscience,* 96**,** 7-25.

MAGUIRE, J. & SALPEKAR, J. A. 2013. Stress, seizures, and hypothalamic–pituitary–adrenal axis targets for the treatment of epilepsy. *Epilepsy & Behavior,* 26**,** 352-362.

MALINOW, R. & MILLER, J. P. 1986. Postsynaptic hyperpolarization during conditioning reversibly blocks induction of long-term potentiation. *Nature,* 320**,** 529-30.

MALINSKA, D., KULAWIAK, B., KUDIN, A. P., KOVACS, R., HUCHZERMEYER, C., KANN, O., SZEWCZYK, A. & KUNZ, W. S. 2010. Complex III-dependent superoxide production of brain mitochondria contributes to seizure-related ROS formation. *Biochim Biophys Acta,* 1797**,** 1163-70.

MARÍN, O. 2012. Interneuron dysfunction in psychiatric disorders. *Nature Reviews Neuroscience*.

MARKKANEN, M., UVAROV, P. & AIRAKSINEN, M. S. 2008. Role of upstream stimulating factors in the transcriptional regulation of the neuron-specific K-Cl cotransporter KCC2. *Brain Res,* 1236**,** 8-15.

MARKRAM, H., TOLEDO-RODRIGUEZ, M., WANG, Y., GUPTA, A., SILBERBERG, G. & WU, C. 2004. Interneurons of the neocortical inhibitory system. *Nat Rev Neurosci,* 5**,** 793-807.

MCDONALD, A. J. & MASCAGNI, F. 2001. Colocalization of calcium-binding proteins and GABA in neurons of the rat basolateral amygdala. *Neuroscience,* 105**,** 681-693.

MCEWEN, B. S. 1999. Stress and hippocampal plasticity. *Annu Rev Neurosci,* 22**,** 105-22.

MCKERNAN, R. M. & WHITING, P. J. 1996. Which GABAA-receptor subtypes really occur in the brain? *Trends in Neurosciences,* 19**,** 139-143.

MCTAGUE, A., HOWELL, K. B., CROSS, J. H., KURIAN, M. A. & SCHEFFER, I. E. 2016. The genetic landscape of the epileptic encephalopathies of infancy and childhood. *The Lancet Neurology,* 15**,** 304-316.

MEDINA, J. F., REPA, J. C., MAUK, M. D. & LEDOUX, J. E. 2002. Parallels between cerebellum- and amygdala-dependent conditioning. *Nat Rev Neurosci,* 3**,** 122-31.

MIKAWA, S., WANG, C., SHU, F., WANG, T., FUKUDA, A. & SATO, K. 2002. Developmental changes in KCC1, KCC2 and NKCC1 mRNAs in the rat cerebellum. *Brain Res Dev Brain Res,* 136**,** 93-100.

MILLS, J. W., SCHWIEBERT, E. M. & STANTON, B. A. 1994. Evidence for the role of actin filaments in regulating cell swelling. *J Exp Zool,* 268**,** 111-20.

MIRESCU, C. & GOULD, E. 2006. Stress and adult neurogenesis. *Hippocampus,* 16**,** 233-8.

MITCHELL, S. J. & SILVER, R. A. 2003. Shunting inhibition modulates neuronal gain during synaptic excitation. *Neuron,* 38**,** 433-45.

MIZOGUCHI, K., KUNISHITA, T., CHUI, D. H. & TABIRA, T. 1992. Stress induces neuronal death in the hippocampus of castrated rats. *Neurosci Lett,* 138**,** 157-60.

MOHANDAS, N., WINARDI, R., KNOWLES, D., LEUNG, A., PARRA, M., GEORGE, E., CONBOY, J. & CHASIS, J. 1992. Molecular basis for membrane rigidity of hereditary ovalocytosis. A novel mechanism involving the cytoplasmic domain of band 3. *J Clin Invest,* 89**,** 686-92.

MORALES, M. & BLOOM, F. E. 1997. The 5-HT3 receptor is present in different subpopulations of GABAergic neurons in the rat telencephalon. *J Neurosci,* 17**,** 3157-67.

MORITA, Y., CALLICOTT, J. H., TESTA, L. R., MIGHDOLL, M. I., DICKINSON, D., CHEN, Q., TAO, R., LIPSKA, B. K., KOLACHANA, B., LAW, A. J., YE, T., STRAUB, R. E., WEINBERGER, D. R., KLEINMAN, J. E. & HYDE, T. M. 2014. Characteristics of the cation cotransporter NKCC1 in human brain: alternate transcripts, expression in development, and potential relationships to brain function and schizophrenia. *J Neurosci,* 34**,** 4929-40.

MULKEY, R. M. & MALENKA, R. C. 1992. Mechanisms underlying induction of homosynaptic long-term depression in area CA1 of the hippocampus. *Neuron,* 9**,** 967-975.

MURRAY, A. J., SAUER, J. F., RIEDEL, G., MCCLURE, C., ANSEL, L., CHEYNE, L., BARTOS, M., WISDEN, W. & WULFF, P. 2011. Parvalbumin-positive CA1 interneurons are required for spatial working but not for reference memory. *Nat Neurosci,* 14**,** 297-9.

MYERS, C. T. & MEFFORD, H. C. 2015. Advancing epilepsy genetics in the genomic era. *Genome Med,* 7**,** 91.

NABEKURA, J., UENO, T., OKABE, A., FURUTA, A., IWAKI, T., SHIMIZU-OKABE, C., FUKUDA, A. & AKAIKE, N. 2002. Reduction of KCC2 expression and GABAA receptor-mediated excitation after in vivo axonal injury. *J Neurosci,* 22**,** 4412-7.

NAKA, A. & ADESNIK, H. 2016. Inhibitory Circuits in Cortical Layer 5. *Frontiers in Neural Circuits,* 10.

NARDOU, R., YAMAMOTO, S., CHAZAL, G., BHAR, A., FERRAND, N., DULAC, O., BEN-ARI, Y. & KHALILOV, I. 2011. Neuronal chloride accumulation and excitatory GABA underlie aggravation of neonatal epileptiform activities by phenobarbital. *Brain,* 134**,** 987-1002.

NOEBELS, J. 2015. Pathway-driven discovery of epilepsy genes. *Nat Neurosci,* 18**,** 344-50.

O'DONOVAN, M. J. & RINZEL, J. 1997. Synaptic depression: a dynamic regulator of synaptic communication with varied functional roles. *Trends Neurosci,* 20**,** 431-3.

O'TOOLE, K. K., HOOPER, A., WAKEFIELD, S. & MAGUIRE, J. 2014. Seizure-induced disinhibition of the HPA axis increases seizure susceptibility. *Epilepsy Research,* 108**,** 29-43.

OLBRICH, H.-G. & BRAAK, H. 1985. Ratio of pyramidal cells versus non-pyramidal cells in sector CA1 of the human Ammon's horn. *Anatomy and Embryology,* 173**,** 105-110.

OLIVER, K. L., LUKIC, V., THORNE, N. P., BERKOVIC, S. F., SCHEFFER, I. E. & BAHLO, M. 2014. Harnessing Gene Expression Networks to Prioritize Candidate Epileptic Encephalopathy Genes. *PLoS ONE,* 9**,** e102079.

PAIZANIS, E., KELAÏ, S., RENOIR, T., HAMON, M. & LANFUMEY, L. 2007. Life-Long Hippocampal Neurogenesis: Environmental, Pharmacological and Neurochemical Modulations. *Neurochemical Research,* 32**,** 1762-1771.

PAULUS, W. & ROTHWELL, J. C. 2016. Membrane resistance and shunting inhibition: where biophysics meets state-dependent human neurophysiology. *The Journal of Physiology,* 594**,** 2719-2728.

PAXINOS, G. & FRANKLIN, K. B. J. 2004. *The Mouse Brain in Stereotaxic Coordinates*, Elsevier Academic Press.

PAYNE, J. A., RIVERA, C., VOIPIO, J. & KAILA, K. 2003. Cation-chloride co-transporters in neuronal communication, development and trauma. *Trends in Neurosciences,* 26**,** 199-206.

PAYNE, J. A., STEVENSON, T. J. & DONALDSON, L. F. 1996. Molecular characterization of a putative K-Cl cotransporter in rat brain. A neuronal-specific isoform. *J Biol Chem,* 271**,** 16245-52.

PELLEGRINO, C., GUBKINA, O., SCHAEFER, M., BECQ, H., LUDWIG, A., MUKHTAROV, M., CHUDOTVOROVA, I., CORBY, S., SALYHA, Y., SALOZHIN, S., BREGESTOVSKI, P. & MEDINA, I. 2011. Knocking down of the KCC2 in rat hippocampal neurons increases intracellular chloride concentration and compromises neuronal survival. *J Physiol,* 589**,** 2475-96.

PEROSKI, M., PROUDAN, N., GRIGNOL, G., MERCHENTHALER, I. & DUDAS, B. 2016. Corticotropin-releasing hormone (CRH)-immunoreactive (IR) axon varicosities target a subset of growth hormone-releasing hormone (GHRH)-IR neurons in the human hypothalamus. *Journal of Chemical Neuroanatomy,* 78**,** 119-124.

PFEFFER, C. K., XUE, M., HE, M., HUANG, Z. J. & SCANZIANI, M. 2013. Inhibition of inhibition in visual cortex: the logic of connections between molecularly distinct interneurons. *Nat Neurosci,* 16**,** 1068-76.

PHILLIPS, R. G. & LEDOUX, J. E. 1992. Differential contribution of amygdala and hippocampus to cued and contextual fear conditioning. *Behav Neurosci,* 106**,** 274-85.

PHILLIPS, R. G. & LEDOUX, J. E. 1994. Lesions of the dorsal hippocampal formation interfere with background but not foreground contextual fear conditioning. *Learn Mem,* 1**,** 34-44.

POPESCU, A. T. & PARÉ, D. 2011. Synaptic Interactions Underlying Synchronized Inhibition in the Basal Amygdala: Evidence for Existence of Two Types of Projection Cells. *Journal of Neurophysiology,* 105**,** 687-696.

POPOLI, M., YAN, Z., MCEWEN, B. S. & SANACORA, G. 2012. The stressed synapse: the impact of stress and glucocorticoids on glutamate transmission. *Nat Rev Neurosci,* 13**,** 22-37.

PORTER, J. T., CAULI, B., STAIGER, J. F., LAMBOLEZ, B., ROSSIER, J. & AUDINAT, E. 1998. Properties of bipolar VIPergic interneurons and their excitation by pyramidal neurons in the rat neocortex. *Eur J Neurosci,* 10**,** 3617-28.

POUILLE, F., MARIN-BURGIN, A., ADESNIK, H., ATALLAH, B. V. & SCANZIANI, M. 2009. Input normalization by global feedforward inhibition expands cortical dynamic range. *Nat Neurosci,* 12**,** 1577-1585.

POUILLE, F. & SCANZIANI, M. 2001. Enforcement of Temporal Fidelity in Pyramidal Cells by Somatic Feed-Forward Inhibition. *Science,* 293**,** 1159-1163.

POUILLE, F. & SCANZIANI, M. 2004. Routing of spike series by dynamic circuits in the hippocampus. *Nature,* 429**,** 717-723.

POVYSHEVA, N. V., GONZALEZ-BURGOS, G., ZAITSEV, A. V., KRONER, S., BARRIONUEVO, G., LEWIS, D. A. & KRIMER, L. S. 2006. Properties of excitatory synaptic responses in fast-spiking interneurons and pyramidal cells from monkey and rat prefrontal cortex. *Cereb Cortex,* 16**,** 541-52.

PUIG, M. V., SANTANA, N., CELADA, P., MENGOD, G. & ARTIGAS, F. 2004. In vivo excitation of GABA interneurons in the medial prefrontal cortex through 5-HT3 receptors. *Cereb Cortex,* 14**,** 1365-75.

PUSKARJOV, M., AHMAD, F., KAILA, K. & BLAESSE, P. 2012. Activity-Dependent Cleavage of the K-Cl Cotransporter KCC2 Mediated by Calcium-Activated Protease Calpain. *The Journal of Neuroscience,* 32**,** 11356-11364.

RANDALL, R. D. & THAYER, S. A. 1992. Glutamate-induced calcium transient triggers delayed calcium overload and neurotoxicity in rat hippocampal neurons. *J Neurosci,* 12**,** 1882-95.

RAVENELLE, R., NEUGEBAUER, N. M., NIEDZIELAK, T. & DONALDSON, S. T. 2014. Sex differences in diazepam effects and parvalbumin-positive GABA neurons in trait anxiety Long Evans rats. *Behav Brain Res,* 270**,** 68-74.

RICCIO, D. C., ACKIL, J. & BURCH-VERNON, A. 1992. Forgetting of stimulus attributes: methodological implications for assessing associative phenomena. *Psychol Bull,* 112**,** 433-45.

RIVERA, C., VOIPIO, J., PAYNE, J. A., RUUSUVUORI, E., LAHTINEN, H., LAMSA, K., PIRVOLA, U., SAARMA, M. & KAILA, K. 1999. The K+/Cl- co-transporter

KCC2 renders GABA hyperpolarizing during neuronal maturation. *Nature,* 397**,** 251-5.

RIVERA, C., VOIPIO, J., THOMAS-CRUSELLS, J., LI, H., EMRI, Z., SIPILA, S., PAYNE, J. A., MINICHIELLO, L., SAARMA, M. & KAILA, K. 2004. Mechanism of activity-dependent downregulation of the neuron-specific K-Cl cotransporter KCC2. *J Neurosci,* 24**,** 4683-91.

ROBERTS, A. J. & KEITH, L. D. 1994. Sensitivity of the circadian rhythm of kainic acid-induced convulsion susceptibility to manipulations of corticosterone levels and mineralocorticoid receptor binding. *Neuropharmacology,* 33**,** 1087-1093.

ROBINSON, S., MIKOLAENKO, I., THOMPSON, I., COHEN, M. L. & GOYAL, M. 2010. Loss of cation-chloride cotransporter expression in preterm infants with white matter lesions: implications for the pathogenesis of epilepsy. *J Neuropathol Exp Neurol,* 69**,** 565-72.

RUBIO-CASILLAS, A. & FERNANDEZ-GUASTI, A. 2016. The dose makes the poison: from glutamate-mediated neurogenesis to neuronal atrophy and depression. *Rev Neurosci,* 27**,** 599-622.

RUDOLPH, U. & MOHLER, H. 2004. Analysis of GABAA receptor function and dissection of the pharmacology of benzodiazepines and general anesthetics through mouse genetics. *Annu Rev Pharmacol Toxicol,* 44**,** 475-98.

RUDY, B., FISHELL, G., LEE, S. & HJERLING-LEFFLER, J. 2011. Three groups of interneurons account for nearly 100% of neocortical GABAergic neurons. *Dev Neurobiol,* 71**,** 45-61.

SAPOLSKY, R. M., KREY, L. C. & MCEWEN, B. S. 1985. Prolonged glucocorticoid exposure reduces hippocampal neuron number: implications for aging. *J Neurosci,* 5**,** 1222-7.

SAYIN, U., OSTING, S., HAGEN, J., RUTECKI, P. & SUTULA, T. 2003. Spontaneous seizures and loss of axo-axonic and axo-somatic inhibition induced by repeated brief seizures in kindled rats. *J Neurosci,* 23**,** 2759-68.

SCHWALLER, B., TETKO, I. V., TANDON, P., SILVEIRA, D. C., VREUGDENHIL, M., HENZI, T., POTIER, M. C., CELIO, M. R. & VILLA, A. E. 2004. Parvalbumin deficiency affects network properties resulting in increased susceptibility to epileptic seizures. *Mol Cell Neurosci,* 25**,** 650-63.

SCHWARTZKROIN, P. A. & HAGLUND, M. M. 1986. Spontaneous rhythmic synchronous activity in epileptic human and normal monkey temporal lobe. *Epilepsia,* 27**,** 523-33.

SCOTTI, A. L., KALT, G., BOLLAG, O. & NITSCH, C. 1997. Parvalbumin disappears from GABAergic CA1 neurons of the gerbil hippocampus with seizure onset while its presence persists in the perforant path. *Brain Research,* 760**,** 109-117.

SEDMAK, G., JOVANOV-MILOSEVIC, N., PUSKARJOV, M., ULAMEC, M., KRUSLIN, B., KAILA, K. & JUDAS, M. 2015. Developmental Expression Patterns of KCC2 and Functionally Associated Molecules in the Human Brain. *Cereb Cortex*.

SEJA, P., SCHONEWILLE, M., SPITZMAUL, G., BADURA, A., KLEIN, I., RUDHARD, Y., WISDEN, W., HUBNER, C. A., DE ZEEUW, C. I. & JENTSCH, T. J. 2012. Raising cytosolic Cl- in cerebellar granule cells affects their excitability and vestibulo-ocular learning. *EMBO J,* 31**,** 1217-30.

SERRA, M., PISU, M. G., MOSTALLINO, M. C., SANNA, E. & BIGGIO, G. 2008. Changes in neuroactive steroid content during social isolation stress modulate GABAA receptor plasticity and function. *Brain Res Rev,* 57**,** 520-30.

SESSOLO, M., MARCON, I., BOVETTI, S., LOSI, G., CAMMAROTA, M., RATTO, G. M., FELLIN, T. & CARMIGNOTO, G. 2015. Parvalbumin-Positive Inhibitory Interneurons Oppose Propagation But Favor Generation of Focal Epileptiform Activity. *J Neurosci,* 35**,** 9544-57.

SHANG, C., LIU, Z., CHEN, Z., SHI, Y., WANG, Q., LIU, S., LI, D. & CAO, P. 2015. BRAIN CIRCUITS. A parvalbumin-positive excitatory visual pathway to trigger fear responses in mice. *Science,* 348**,** 1472-7.

SKUSE, D., ALBANESE, A., STANHOPE, R., GILMOUR, J. & VOSS, L. 1996. A new stress-related syndrome of growth failure and hyperphagia in children, associated with reversibility of growth-hormone insufficiency. *The Lancet,* 348**,** 353-358.

SLOVITER, R. S. 1989. Calcium-binding protein (calbindin-D28k) and parvalbumin immunocytochemistry: localization in the rat hippocampus with specific reference to the selective vulnerability of hippocampal neurons to seizure activity. *J Comp Neurol,* 280**,** 183-96.

SMIRNOV, S., PAALASMAA, P., UUSISAARI, M., VOIPIO, J. & KAILA, K. 1999. Pharmacological isolation of the synaptic and nonsynaptic components of the GABA-mediated biphasic response in rat CA1 hippocampal pyramidal cells. *J Neurosci,* 19**,** 9252-60.

SMITH, D. R., GALLAGHER, M. & STANTON, M. E. 2007. Genetic background differences and nonassociative effects in mouse trace fear conditioning. *Learn Mem,* 14**,** 597-605.

SOHAL, V. S., ZHANG, F., YIZHAR, O. & DEISSEROTH, K. 2009. Parvalbumin neurons and gamma rhythms enhance cortical circuit performance. *Nature,* 459**,** 698-702.

SOMOGYI, P. & KLAUSBERGER, T. 2005. Defined types of cortical interneurone structure space and spike timing in the hippocampus. *J Physiol,* 562**,** 9-26.

SONNER, M. J., WALTERS, M. C. & LADLE, D. R. 2017. Analysis of Proprioceptive Sensory Innervation of the Mouse Soleus: A Whole-Mount Muscle Approach. *PLOS ONE,* 12**,** e0170751.

STALEY, K., SOLDO, B. & PROCTOR, W. 1995. Ionic mechanisms of neuronal excitation by inhibitory GABAA receptors. *Science,* 269**,** 977-981.

STALEY, K. J. & MODY, I. 1992. Shunting of excitatory input to dentate gyrus granule cells by a depolarizing GABAA receptor-mediated postsynaptic conductance. *J Neurophysiol,* 68**,** 197-212.

STARK, E., EICHLER, R., ROUX, L., FUJISAWA, S., ROTSTEIN, H. G. & BUZSAKI, G. 2013. Inhibition-induced theta resonance in cortical circuits. *Neuron,* 80**,** 1263-76.

STEIMER, T. 2002. The biology of fear- and anxiety-related behaviors. *Dialogues in Clinical Neuroscience,* 4**,** 231-249.

STEIN-BEHRENS, B., MATTSON, M. P., CHANG, I., YEH, M. & SAPOLSKY, R. 1994. Stress exacerbates neuron loss and cytoskeletal pathology in the hippocampus. *J Neurosci,* 14**,** 5373-80.

STEIN, V., HERMANS-BORGMEYER, I., JENTSCH, T. J. & HUBNER, C. A. 2004. Expression of the KCl cotransporter KCC2 parallels neuronal maturation and the emergence of low intracellular chloride. *J Comp Neurol,* 468**,** 57-64.

STEULLET, P., CABUNGCAL, J. H., KULAK, A., KRAFTSIK, R., CHEN, Y., DALTON, T. P., CUENOD, M. & DO, K. Q. 2010. Redox dysregulation affects the ventral but not dorsal hippocampus: impairment of parvalbumin neurons, gamma oscillations, and related behaviors. *J Neurosci,* 30**,** 2547-58.

TAMAS, G., BUHL, E. H., LORINCZ, A. & SOMOGYI, P. 2000. Proximally targeted GABAergic synapses and gap junctions synchronize cortical interneurons. *Nat Neurosci,* 3**,** 366-71.

TORNBERG, J., VOIKAR, V., SAVILAHTI, H., RAUVALA, H. & AIRAKSINEN, M. S. 2005. Behavioural phenotypes of hypomorphic KCC2-deficient mice. *Eur J Neurosci,* 21**,** 1327-37.

TÓTH, K., ERŐSS, L., VAJDA, J., HALÁSZ, P., FREUND, T. F. & MAGLÓCZKY, Z. 2010. Loss and reorganization of calretinin-containing interneurons in the epileptic human hippocampus. *Brain,* 133**,** 2763-2777.

TRESILIAN, J. 2012. *Sensorimotor Control and Learning: An Introduction to the Behavioral Neuroscience of Action*, Palgrave Macmillan.

TYMIANSKI, M., CHARLTON, M. P., CARLEN, P. L. & TATOR, C. H. 1993. Secondary Ca2+ overload indicates early neuronal injury which precedes staining with viability indicators. *Brain Res,* 607**,** 319-23.

UVAROV, P., LUDWIG, A., MARKKANEN, M., PRUUNSILD, P., KAILA, K., DELPIRE, E., TIMMUSK, T., RIVERA, C. & AIRAKSINEN, M. S. 2007. A novel N-terminal isoform of the neuron-specific K-Cl cotransporter KCC2. *J Biol Chem,* 282**,** 30570-6.

UVAROV, P., LUDWIG, A., MARKKANEN, M., RIVERA, C. & AIRAKSINEN, M. S. 2006. Upregulation of the neuron-specific K+/Cl- cotransporter expression by transcription factor early growth response 4. *J Neurosci,* 26**,** 13463-73.

UVAROV, P., PRUUNSILD, P., TIMMUSK, T. & AIRAKSINEN, M. S. 2005. Neuronal K+/Cl- co-transporter (KCC2) transgenes lacking neurone restrictive silencer element recapitulate CNS neurone-specific expression and developmental up-regulation of endogenous KCC2 gene. *J Neurochem,* 95**,** 1144-55.

VAN DEN POL, A. N., OBRIETAN, K. & CHEN, G. 1996. Excitatory actions of GABA after neuronal trauma. *J Neurosci,* 16**,** 4283-92.

VANDERWOLF, C. H. 1969. Hippocampal electrical activity and voluntary movement in the rat. *Electroencephalography and Clinical Neurophysiology,* 26**,** 407-418.

VIBAT, C. R., HOLLAND, M. J., KANG, J. J., PUTNEY, L. K. & O'DONNELL, M. E. 2001. Quantitation of Na+-K+-2Cl- cotransport splice variants in human tissues using kinetic polymerase chain reaction. *Anal Biochem,* 298**,** 218-30.

VIITANEN, T., RUUSUVUORI, E., KAILA, K. & VOIPIO, J. 2010. The K+-Cl cotransporter KCC2 promotes GABAergic excitation in the mature rat hippocampus. *J Physiol,* 588**,** 1527-40.

VOGELS, T. P. & ABBOTT, L. F. 2009. Gating multiple signals through detailed balance of excitation and inhibition in spiking networks. *Nat Neurosci,* 12**,** 483-491.

VREUGDENHIL, M., JEFFERYS, J. G., CELIO, M. R. & SCHWALLER, B. 2003. Parvalbumin-deficiency facilitates repetitive IPSCs and gamma oscillations in the hippocampus. *J Neurophysiol,* 89**,** 1414-22.

WAGNER, S., CASTEL, M., GAINER, H. & YAROM, Y. 1997. GABA in the mammalian suprachiasmatic nucleus and its role in diurnal rhythmicity. *Nature,* 387**,** 598-603.

WANG, L., SHEN, M., JIANG, C., MA, L. & WANG, F. 2016. Parvalbumin Interneurons of Central Amygdala Regulate the Negative Affective States and the Expression of Corticotrophin-Releasing Hormone During Morphine Withdrawal. *International Journal of Neuropsychopharmacology,* 19**,** pyw060.

WARREN, C. P., HU, S., STEAD, M., BRINKMANN, B. H., BOWER, M. R. & WORRELL, G. A. 2010. Synchrony in normal and focal epileptic brain: the seizure onset zone is functionally disconnected. *J Neurophysiol,* 104**,** 3530-9.

WEI, W. C., AKERMAN, C. J., NEWEY, S. E., PAN, J., CLINCH, N. W., JACOB, Y., SHEN, M. R., WILKINS, R. J. & ELLORY, J. C. 2011. The potassium-chloride cotransporter 2 promotes cervical cancer cell migration and invasion by an ion transport-independent mechanism. *J Physiol,* 589**,** 5349-59.

WEISS, J. H., KOH, J., BAIMBRIDGE, K. G. & CHOI, D. W. 1990. Cortical neurons containing somatostatin- or parvalbumin-like immunoreactivity are atypically vulnerable to excitotoxic injury in vitro. *Neurology,* 40**,** 1288-92.

WITTNER, L., EROSS, L., CZIRJAK, S., HALASZ, P., FREUND, T. F. & MAGLOCZKY, Z. 2005. Surviving CA1 pyramidal cells receive intact perisomatic inhibitory input in the human epileptic hippocampus. *Brain,* 128**,** 138-52.

WITTNER, L., MAGLOCZKY, Z., BORHEGYI, Z., HALASZ, P., TOTH, S., EROSS, L., SZABO, Z. & FREUND, T. F. 2001. Preservation of perisomatic inhibitory input of granule cells in the epileptic human dentate gyrus. *Neuroscience,* 108**,** 587-600.

WOLFF, S. B. E., GRUNDEMANN, J., TOVOTE, P., KRABBE, S., JACOBSON, G. A., MULLER, C., HERRY, C., EHRLICH, I., FRIEDRICH, R. W., LETZKUS, J. J. & LUTHI, A. 2014. Amygdala interneuron subtypes control fear learning through disinhibition. *Nature,* 509**,** 453-458.

WULFF, P., PONOMARENKO, A. A., BARTOS, M., KOROTKOVA, T. M., FUCHS, E. C., BAHNER, F., BOTH, M., TORT, A. B., KOPELL, N. J., WISDEN, W. & MONYER, H. 2009. Hippocampal theta rhythm and its coupling with gamma oscillations require fast inhibition onto parvalbumin-positive interneurons. *Proc Natl Acad Sci U S A,* 106**,** 3561-6.

XIANG, Z., HUGUENARD, J. R. & PRINCE, D. A. 2002. Synaptic inhibition of pyramidal cells evoked by different interneuronal subtypes in layer v of rat visual cortex. *J Neurophysiol,* 88**,** 740-50.

YEKHLEF, L., BRESCHI, G. L., LAGOSTENA, L., RUSSO, G. & TAVERNA, S. 2015. Selective activation of parvalbumin- or somatostatin-expressing interneurons triggers epileptic seizurelike activity in mouse medial entorhinal cortex. *J Neurophysiol,* 113**,** 1616-30.

YUEN, E. Y., LIU, W., KARATSOREOS, I. N., FENG, J., MCEWEN, B. S. & YAN, Z. 2009. Acute stress enhances glutamatergic transmission in prefrontal cortex and facilitates working memory. *Proc Natl Acad Sci U S A,* 106**,** 14075-9.

YUEN, E. Y., LIU, W., KARATSOREOS, I. N., REN, Y., FENG, J., MCEWEN, B. S. & YAN, Z. 2011. Mechanisms for acute stress-induced enhancement of glutamatergic transmission and working memory. *Mol Psychiatry,* 16**,** 156-170.

ZAHM, D. S., GROSU, S., IRVING, J. C. & WILLIAMS, E. A. 2003. Discrimination of striatopallidum and extended amygdala in the rat: a role for parvalbumin immunoreactive neurons? *Brain Research,* 978**,** 141-154.

ZHANG, L. L., DELPIRE, E. & VARDI, N. 2007. NKCC1 does not accumulate chloride in developing retinal neurons. *J Neurophysiol,* 98**,** 266-77.

ZHOU, H.-Y., CHEN, S.-R., BYUN, H.-S., CHEN, H., LI, L., HAN, H.-D., LOPEZ-BERESTEIN, G., SOOD, A. K. & PAN, H.-L. 2012. N-Methyl-d-aspartate Receptor- and Calpain-mediated Proteolytic Cleavage of K(+)-Cl(−) Cotransporter-2 Impairs Spinal Chloride Homeostasis in Neuropathic Pain. *The Journal of Biological Chemistry,* 287**,** 33853-33864.

ZHU, Z.-Q., ARMSTRONG, D. L., HAMILTON, W. J. & GROSSMAN, R. G. 1997. Disproportionate Loss of CA4 Parvalbumin-immunoreactive Interneurons in Patients with Ammon's Horn Sclerosis. *Journal of Neuropathology & Experimental Neurology,* 56**,** 988-998.

APPENDIX

LIST OF GENE NAMES FIGURE 1

Arx	aristaless related homeobox
Upar	Urokinase receptor, also called plasminogen activator, urokinase receptor (PLAUR)
Dlx1,2	distal-less homeobox 1,2
Cit-K	citron rho-interacting serine/threonine kinase
Sox6	SRY (sex determining region Y)-box 6
Cacnγ2	calcium voltage-gated channel auxiliary subunit gamma 2
Gria4	glutamate ionotropic receptor AMPA type subunit 4
Pick1	protein interacting with C kinase 1
Elfn1	extracellular leucine rich repeat and fibronectin type III domain containing 1
Bassoon	BSN, scaffolding protein
Tnap	official ALPL, alkaline phosphatase, liver/bone/kidney
Gad65	GAD2, glutamate decarboxylase 2
Aldh5a1	aldehyde dehydrogenase 5 family member A1
NHE1/SLC9A1	Na[+]/H[+] hydrogen exchanger 1
GLUT1/SLC2A1	glucose transporter 1
GAT1/SLC6A1	gamma-aminobutyric acid (GABA) transporter 1
Eaat1/SLC1A3	Excitatory amino acid transporter 1
Syn	Synapsin
Snap25	synaptosome associated protein 25

Sv2a	synaptic vesicle glycoprotein 2A
LGI1	leucine rich glioma inactivated 1
STXBP1	syntaxin binding protein 1
Nav	voltage gated sodium channel subunit
Kv	voltage gated potassium channel
KCNMA	potassium calcium-activated channel subfamily M alpha 1
Hcn	hyperpolarization-activated, cyclic nucleotide-gated K^+
GIRK2	KCNJ6, potassium voltage-gated channel subfamily J member 6
CACNA1A	calcium voltage-gated channel subunit alpha1 A
GabaR	gamma-aminobutyric acid (GABA) receptor
GabaRb1	gamma-aminobutyric acid type A receptor beta1 subunit
Kcc2	potassium-chloride cotransporter 2

RESULT TABLES FEAR CONDITIONING

ACQUISITION

time intervals (s)	WT	HET	KO
0-60	1.90 ± 0.99	0.32 ± 0.20	2.74 ± 0.70
61-120	3.45 ± 0.77	2.98 ± 0.91	7.75 ± 1.92
121-180	5.08 ± 1.92	4.60 ± 1.61	16.48 ± 3.39
181-240	14.67 ± 4.88	10.75 ± 1.85	31.44 ± 5.31

TABLE 4: FEAR CONDITIONING PV-KCC2 MICE; ACQUISITION. The table shows the time freezing (%) during the different stages of acquisition; tone started after 180s; foot shock was applied after 198s and lasted 2s.

CUED TEST

time intervals (s)	WT	HET	KO
0-60	26.70 ± 5.20	18.74 ± 3.15	27.76 ± 4.07
61-120	30.56 ± 3.83	33.38 ± 5.52	46.85 ± 5.87
121-180	22.58 ± 3.15	33.65 ± 5.40	47.59 ± 5.87
181-240	74.52 ± 3.73	74.29 ± 4.81	89.67 ± 1.71
241-300	61.22 ± 4.54	65.28 ± 6.85	84.41 ± 4.65
301-360	60.48 ± 6.11	51.76 ±6.64	79.17 ± 5.09
361-420	32.05 ± 4.90	38.08 ± 9.42	59.74 ± 7.81

TABLE 5: FEAR CONDITIONING; CUED TEST. The table shows the time freezing (%) during the different time intervals of the cued test; tone started after 180s and lasted 180s; no foot shock.

CONTEXT TEST

time intervals (s)	WT	HET	KO
0-60	38.07 ± 4.91	46.58 ± 8.32	54.58 ± 6.25
61-120	48.26 ± 6.51	55.69 ± 6.58	72.89 ± 7.46
121-180	37.18 ± 6.79	46.47 ± 7.71	66.86 ± 6.48

TABLE 6: FEAR CONDITIONING; CUED TEST. The table shows the time freezing (%) during the different time intervals of the cued test; tone started after 180s and lasted 180s; no foot shock.

EHRENWÖRTLICHE ERKLÄRUNG

Hiermit erkläre ich, dass mir die Promotionsordnung der Medizinischen Fakultät der Friedrich-Schiller-Universität bekannt ist,

ich die Dissertation selbst angefertigt habe und alle von mir benutzten Hilfsmittel, persönlichen Mitteilungen und Quellen in meiner Arbeit angegeben sind,

mich folgende Personen bei der Auswahl und Auswertung des Materials sowie bei der Herstellung des Manuskripts unterstützt haben: Prof. Dr. Christian Hübner, Dr. Lutz Liebmann und Tanja Herrmann,

die Hilfe eines Promotionsberaters nicht in Anspruch genommen wurde und dass Dritte weder unmittelbar noch mittelbar geldwerte Leistungen von mir für Arbeiten erhalten haben, die im Zusammenhang mit dem Inhalt der vorgelegten Dissertation stehen,

dass ich die Dissertation noch nicht als Prüfungsarbeit für eine staatliche oder andere wissenschaftliche Prüfung eingereicht habe und

dass ich die gleiche, eine in wesentlichen Teilen ähnliche oder eine andere Abhandlung nicht bei einer anderen Hochschule als Dissertation eingereicht habe.

Ort, Datum Unterschrift des Verfassers

DANKSAGUNG

An dieser Stelle möchte ich meinen besonderen Dank nachstehenden Personen entgegen bringen:

Mein Dank gilt zunächst Herrn Prof. Dr. Hübner, Leiter des Instituts für Humangenetik Jena für die Betreuung dieser Arbeit, der freundlichen Hilfe und der mannigfachen Ideengebung, die mir einen kritischen Zugang zu dieser Thematik eröffnete.

Besonders danken möchte ich Dr. Lutz Liebmann für die Unterstützung und unendliche Geduld bei der Diskussion verschiedenster Fragestellungen und Thesen. Die zahlreichen Gespräche auf intellektueller und persönlicher Ebene werden mir immer als bereichernder und konstruktiver Austausch in Erinnerung bleiben. Ich habe unsere Dialoge stets als Ermutigung und Motivation empfunden.

Prof. Dr. Baniahmad und Prof. Dr. Rivera danke ich für ihren wissenschaftlichen Beitrag und ihre Gutachtertätigkeit.

Ein ebenso großer Dank geht an alle meine Arbeitskollegen des Instituts für Humangenetik für die Unterstützung während der gesamten Promotion. Besonders bedanken möchte ich mich bei Theresa Heinrich, Tanja Herrmann, Hartmut Bocker und Patricia Franzka, sowohl für die konstruktiven wissenschaftlichen Diskussionen, die moralische Unterstützung als auch für die vielen Stunden lustigen Beisammenseins. Es hat mir in schwierigen Zeiten das Weitermachen erleichtert.

Besonderen Dank schulde ich Dr. Martin Ungelenk für allzeit ehrliche Kritik, die Motivation und die musikalische Untermalung in unserer gemeinsamen Bürozeit. Ich werde mich immer gern daran zurück erinnern.

Nicht minder dankbar bin ich meiner Familie, die dieses Werk in allen Phasen mit jeder möglichen Unterstützung bedacht hat. Ihnen gilt mein besonderer Dank.

Stephan Schacke bin ich für immer tief verbunden für seine unglaubliche Unterstützung, sein Verständnis und den Rückhalt bei der Anfertigung dieser Doktorarbeit. Darüber hinaus gilt mein Dank allen Verwandten, Freunden und Bekannten, die mich auf diesem Weg begleitet haben.